THE EWS/FLI FUSION PROTEIN DRIVES METABOLIC MISREGULATION IN EWING SARCOMA

by

Jason Michael Tanner

A dissertation submitted to the faculty of
The University of Utah
in partial fulfillment of the requirements for the degree of

Doctor of Philosophy

Department of Biochemistry

The University of Utah

August 2017

The University of Utah Graduate School

STATEMENT OF DISSERTATION APPROVAL

The dissertation of **Jason Michael Tanner**

has been approved by the following supervisory committee members:

Jared P. Rutter	, Chair	**May 30, 2017** Date Approved
Bradley R. Cairns	, Member	**May 30, 2017** Date Approved
Michael E. Engel	, Member	**May 30, 2017** Date Approved
Adam L. Hughes	, Member	**May 30, 2017** Date Approved
Janet E. Lindsley	, Member	**May 30, 2017** Date Approved

and by **Christopher P. Hill** , Chair/Dean of

the Department/College/School of **Biochemistry**

and by David B. Kieda, Dean of The Graduate School.

ABSTRACT

Ewing sarcoma is a malignant disease of young people that arises most frequently in bones of the femur and pelvis. The disease most often afflicts adolescents, creating physical, emotional, and developmental challenges during an individual's most formative years. Mainstays of therapy include surgery and chemotherapy, meaning that survival may come at very high costs – amputation and lifelong disability. Those who suffer metastasis or relapse must confront a poor prognosis. This is due in part to a lack of effective therapeutic options capable of destroying cancer at the cellular and molecular levels. To this end, molecular research continues to pursue greater understanding of the underlying biology of these tumors.

The principal genetic lesion in Ewing sarcoma is a translocation that fuses chromosomes 11 and 22, giving rise to an oncogenic fusion protein known as EWS/FLI. EWS/FLI causes massive transcriptional misregulation, generating a gene expression program that transforms cells into cancer. Studies of transcriptional consequences of EWS/FLI misregulation have identified numerous genes that are necessary – but not sufficient – for tumorigenesis of Ewing sarcoma. These efforts have produced several candidates for molecular therapies for this malignancy, but no new therapies have yet reached the clinic.

Research continues this pursuit, and hope persists. The work presented in this dissertation is some of the first efforts to investigate the metabolic

underpinnings of Ewing sarcoma. Specifically, these data provide preliminary insights into the effects that EWS/FLI has on misregulating metabolism, generating a program of biosynthesis that promotes and/or contributes to oncogenesis in these tumors. Numerous metabolic pathways are altered upon silencing of EWS/FLI, suggesting that EWS/FLI drives expression changes of key enzymes involved in metabolic processes. These data appear to indicate that generating a pro-oncogenic metabolic program is a key part of how EWS/FLI drives oncogenesis. Due to the fact that metabolic enzymes are generally amenable to pharmacological modulation, these findings offer new hope to the pursuit of a molecular therapy for Ewing sarcoma.

Dedicated to Charlotte and Kate,
who exemplify unbridled curiosity,
unquenchable thirst for knowledge,
and unconditional love for all.

“I do not know what I may appear to the world, but to myself I seem to have been only like a boy playing on the sea-shore, and diverting myself in now and then finding a smoother pebble or a prettier shell than ordinary, whilst the great ocean of truth lay all undiscovered before me.”

Sir Isaac Newton

TABLE OF CONTENTS

LIST OF FIGURES

ACKNOWLEDGMENTS

In the novel *Frankenstein*, Mary Shelley wrote, “None but those who have experienced them can conceive of the enticements of science” (1). It may have been meant ironically in the novel, but the sentiment rings true to me. My first experiences with “the enticements of science” occurred when I was a young boy. One year, I was given a microscope for my birthday, and I went about observing the various tiny creatures that lived in the creek that ran through my back yard. I also looked at blood, insects, textiles, and anything else I could think of. I became fascinated with the microscopic world. In later years, I was given toys of electronic circuits, Lego kits, toy rockets, airplanes, and others – all of which helped me to learn creativity and problem solving. I am thankful to my parents, grandparents, aunts, and uncles for the many ways that they encouraged my curiosity and creativity, and helped foster my appreciation of science.

Later, as I started college, I came to know Dr. J. David Symons, and received my first experiences in University-level scientific investigation. His mentorship and support kindled an interest in research that prompted me to pursue a dual degree program as an MD/PhD student. It was after joining the MD/PhD program at the University of Utah that I was introduced to mentors like Dr. Dean Li and Dr. Jerry Kaplan, and I began to appreciate and strive for scientific rigor.

As I began my graduate studies, I was privileged to work with and be taught

by Dr. Stephen Lessnick. As a member of his lab, I learned many unforgettable and formative lessons about science, as well as the intrigues of academic medicine. I am grateful to Dr. Lessnick for the opportunities he offered me, and for giving me the freedom and independence that set me on a path toward being an autonomous, self-directed scientist. I spent three years in the Lessnick Lab, and the training I received there laid the groundwork for my continuing development as a scientist.

I have been fortunate to have many other mentors, as well. They have each taught me foundation-forming lessons. I am particularly grateful to the members of my advisory committee, both past and present: Dr. Sheri Holmen, Dr. Sunil Sharma, Dr. Mike Engel, Dr. Brad Cairns, Dr. Janet Lindsley, and Dr. Adam Hughes. Without the support and guidance from these individuals I would not have been able to complete the work presented in this dissertation.

I am also exceedingly thankful for the support of Dr. Jared Rutter. After three years of studying in the Lessnick Lab, it was announced that the lab would be relocating. I was invited to move with the lab, and I am grateful for Dr. Lessnick's invitation and offers of continued support. Nevertheless, for many reasons, I decided that I would not move with the lab, and so I needed to join a different research group. Dr. Rutter offered to take me under his wing and continue my training, and he gave me the opportunity to join his lab. (It should be noted that Dr. Holmen also offered me a position in her lab, and I am also very grateful to her for that. These invitations meant very much to me during a personally difficult time of self doubt and shaken confidence.)

In Dr. Rutter's lab, I began studying cellular metabolism of stem cells and cancer. I was immersed in high-level scientific debate and discussion. The mentorship that I received from Dr. Rutter, and others in his lab, has enhanced my critical thinking skills, helping me to question my assumptions and seek out rigorous scientific evidence. I am especially grateful to Dr. Rutter for allowing me the freedom to explore projects beyond the primary focus of the lab, which provided many lessons on the challenges of pursuing a project independently.

I am particularly appreciative of the close personal support and mentorship given to me by my fellow MD/PhD students: Dr. John Schell, Dr. Kris Olson, and Claire Bensard (MD/PhD Candidate). I never cease to be impressed by them and their sharp aptitudes for science and medicine, as well as the core altruism that guides them. It is an honor to call them colleagues and friends, and I have been truly uplifted by working so closely with them.

Additionally, I must attempt to express the depths of my appreciation to my friends and family. My wife, Dr. Windy Tanner, has been an example of strength, tenacity, and dedication. Through all of my struggles, I am thankful for her enduring love and support. In spite of having gone through her own challenges, she has somehow found the time and energy to support me through mine. She has been my partner throughout, providing comfort, love, and kindness. My daughters, Charlotte and Kate, are my role models. They are so smart, so inquisitive, so kind, and so fun-loving that I strive to emulate them. They are a genuine reminder to me of the meaning of unfailing and unconditional love.

I also must acknowledge my good friend Ben Robertson (for occasionally

getting me out of the lab and into the mountains) and my many friends and colleagues at Salt Lake County Search & Rescue, who persistently demonstrate true integrity, heroism, and dedication. It has been an honor to serve alongside such selfless and devoted individuals.

Finally, I wish to acknowledge the many sources of funding without which this work would not have been possible, including the National Institutes of Health, the National Cancer Institute, the Huntsman Cancer Foundation, and the Howard Hughes Medical Institute. Special thanks to the core facilities of the University of Utah, particularly the High-Throughput Genomics core, the Bioinformatic Analysis core, and the Metabolomics core.

I have been truly fortunate to have interacted with so many amazing individuals, and I am better for having known all of them. I hope to live up to the principles instilled in me by having associated with all of these people during the past several years.

1. M. W. Shelley, *Frankenstein, or, The modern Prometheus* (Broadview Press, Peterborough, Ont, 2nd ed., 1999), *Broadview literary texts*.

CHAPTER 1

INTRODUCTION

1.1 The Roaring Twenties

The second decade of the twentieth century was an era of cultural, social, and scientific dynamism. Major advances in physics, chemistry, and biology – discoveries that would not merely change their field, but the entire world – burst forth during these years. Much of the foundation of modern science and medicine was being established, creating the platform upon which we could firmly build our current and future understanding.

In this single decade: insulin was discovered and first used to treat diabetes; hydrocodone was first synthesized; epidural anesthesia was invented; the existence of macromolecules was first proposed; vitamins D & E were discovered; vaccines against diphtheria and pertussis were invented; the Pauli exclusion principle and the Heisenberg uncertainty principle were first described; the first human electroencephalogram was performed; the “Big Bang” theory was first described; covalent bonding of atoms was first proposed; penicillin was discovered; and the existence of DNA was proven. Much of our current understanding of the realities of our universe began in the 1920s. And immersed in this lively atmosphere of scientific advancement, in 1921, a New York pathologist named James Ewing first described a cancer of bone that would later

come to bear his name.

1.2 Diffuse Endothelioma of Bone

James Ewing, the third son of a prominent Pittsburg judge, received an MD from the College of Physicians of New York, where he acquired an interest in histology and pathology. He later taught at Cornell University, and became the Medical College's first professor of pathology. His position at Cornell enabled him to pursue various avenues of research at the New York Memorial Hospital (now known as Memorial Sloan-Kettering Cancer Center) where he offered the first descriptions of a "diffuse endothelioma of bone" (1). He recognized that these cells exhibited morphological characteristics that distinguished them from other bone cancers and lymphomas. In 1921, he wrote:

> For some years I have been encountering in material curetted from bone tumors a structure which differed markedly from that of osteogenic sarcoma, was not identical with any known form of myeloma, and which had to be designated by the vague term 'round cell sarcoma' of unknown origin and nature (1).

These tumors quickly became known as "Ewing's" sarcoma, with case reports being published as early as 1927 (2). (While originally named using the possessive form "Ewing's" sarcoma, current World Health Organization guidelines avoid possessive nomenclature; hence, "Ewing" sarcoma is the term utilized herein.)

Ewing became well known and much respected as a cancer scientist. His portrait was printed on the cover of Time magazine in 1931 with the subtitle "Cancer Man Ewing" (3). He was a firm proponent of using radioactivity to treat cancers, and Ewing sarcoma was found to be exquisitely sensitive to radiation

therapy. Radiotherapy and surgery were the mainstays of treatment for much of the first half of the twentieth century, but the advent of chemotherapeutic agents would later supplant radiation therapy in the efforts to treat patients with these tumors (4,5). The therapeutic landscape continued to evolve, and the understanding of the true molecular roots of cancer continued to grow.

I was not until the late twentieth century (many years after Ewing's death in 1943) that other scientists discovered the cytogenetic abnormalities responsible for tumorigenesis in Ewing sarcoma. Their work would reveal that these tumors are driven by chromosomal translocations that generate fusion proteins with neomorphic functions and oncogenic consequences. These translocations and our current understanding of their role in producing Ewing sarcoma are discussed in Chapter 2 and Chapter 3 of this dissertation.

1.3 The Fermentation of Tumors

The scientific enlivenment of the 1920s was, of course, not confined to the United States. Six years after James Ewing first published his description of "diffuse endothelioma", a German scientist named Otto Warburg published a paper raising questions of cancer metabolism (6). Ewing and Warburg were contemporaries, and co-contributors to publications in cancer science. (It is perhaps interesting to note that Otto Warburg is also named in the 1931 Time Magazine article about James Ewing.) Warburg wrote in 1927, "The fermentation of tumors was first found with cut pieces of tumor *in vitro*," and asked "whether tumor cells in living animals can be killed off through lack of energy" (6). Warburg hypothesized that anaerobic fermentation of glucose was a crucial part of tumor

formation, and maybe even a cause of cancer. These were the first observations of a set of hallmark metabolic characteristics of cancer that have only recently begun to be understood, known today as the Warburg effect.

Based on his experiments assessing glucose consumption in rat tumors, Warburg theorized that tumor cells were incapable of effective respiration. However, as it became possible to isolate mitochondria from cancer cells and test their respiratory capacity, researchers discovered that respiratory proteins were not defective in cancer cells. As techniques in genetics gained momentum, and mutations in oncogenes and tumor suppressors were discovered, the study of the role of metabolic alterations in tumorigenesis fell out of favor.

Nevertheless, seminal findings leading into the twenty-first century have just recently reignited the field of cancer metabolism. Instead of altering metabolism for energetic purposes, it is now accepted that tumor cells shift metabolism into a more glycolytic state for the purpose of generating precursors for the biosynthetic processes that are necessary for rapid growth and proliferation (7). Techniques in biochemical analysis have become increasingly sophisticated, and it is now possible to assess the flux through metabolic pathways with great accuracy and resolution (8–10). One such study, tracing atoms from precursor molecules and assessing their contribution to cellular mass, is briefly discussed in Chapter 4.

1.4 Ewing and Warburg Converge

Although it is doubtful whether the two ever met, the work of James Ewing and Otto Warburg has begun to converge nearly 100 years after they first published their findings. Since Ewing sarcoma is driven by a chromosomal

rearrangement – a decidedly genetic event – little attention has been focused on metabolic derangements that may play a role in these tumors.

Considering that Ewing sarcoma behaves similarly to other cancers, it is not unreasonable to hypothesize that these tumors harbor metabolic aberrations similar to those seen in other cancers. However, since Ewing sarcoma is principally driven by a single genetic mutation (a chromosomal translocation that generates a fusion protein known as EWS/FLI) it provides a uniquely "clean" system in which metabolic processes of cancer can be studied without the potential confounding influence of numerous other genetic mutations. Determining what metabolic changes are induced by EWS/FLI could shed light on the oncogenic role that such metabolic changes may have in Ewing sarcoma, and perhaps in many other tumors as well. Our work on this front is presented in Chapter 5 of this dissertation.

1.5 A Continuing Crusade

Despite having distinct backgrounds and interests, Ewing and Warburg shared a common goal: to cure cancer. We continue to pursue this goal today. Ewing sarcoma remains a devastating disease of young people. It threatens their lives and takes their limbs. Survival often comes only at the severe cost of amputation and lifelong disability. Although some go on to live fulfilling lives, others are not so fortunate. The methods of scientific inquiry have seldom, if ever, been exercised in pursuit of a more laudable objective than curing childhood cancer.

While much remains to be done, and success is not guaranteed, we can build upon the foundations established during the past century by Ewing, Warburg

and others. Scientists with aggressive curiosity and tenacious enthusiasm will continue to make breakthroughs, and cancer will progressively become more manageable. It is hoped that the work presented herein will make some small contribution toward these efforts, or that they will – at minimum – provoke thought and reflection leading toward greater contributions by others.

1.6 References

1. Ewing J. Diffuse endothelioma of bone. Proc N Pathol Soc. 1921;21:17.

2. Pritchard JE. Ewing's sarcoma: a report of a case. Can Med Assoc J. 1927 Oct;17(10 Pt 1):1164–7.

3. TIME Magazine Cover: Professor James Ewing - Jan. 12, 1931 [Internet]. TIME.com. [cited 2017 May 15]. Available from: http://content.time.com/time/covers/0,16641,19310112,00.html

4. Lee ES. Treatment of bone sarcoma. Proc R Soc Med. 1971 Dec;64(12):1179–80.

5. Rosen G, Caparros B, Mosende C, McCormick B, Huvos AG, Marcove RC. Curability of Ewing's sarcoma and considerations for future therapeutic trials. Cancer. 1978 Mar;41(3):888–99.

6. Warburg O, Wind F, Negelein E. The metabolism of tumors in the body. J Gen Physiol. 1927 Mar 7;8(6):519–30.

7. Ward PS, Thompson CB. Metabolic reprogramming: a cancer hallmark even Warburg did not anticipate. Cancer Cell. 2012 Mar 20;21(3):297–308.

8. Niklas J, Schneider K, Heinzle E. Metabolic flux analysis in eukaryotes. Curr Opin Biotechnol. 2010 Feb;21(1):63–9.

9. Wiechert W. 13C metabolic flux analysis. Metab Eng. 2001 Jul;3(3):195–206.

10. Zamboni N. 13C metabolic flux analysis in complex systems. Curr Opin Biotechnol. 2011 Feb;22(1):103–8.

CHAPTER 2

TRANSLOCATIONS IN EWING SARCOMA

Chromosomal Translocations and Genomic Rearrangements in Cancer, p. 333-354

ISBN: 978-3-319-19983-2

Chapter 15
Translocations in Ewing Sarcoma

Jason M. Tanner and Stephen L. Lessnick

Contents

Abstract Ewing sarcoma is a bone-associated malignancy arising primarily in childhood and adolescence. It is an aggressive cancer harbouring a characteristic translocation, t(11;22)(q24.3;q12.2). This rearrangement fuses the genes *EWSR1* and *FLI1*, producing a fusion protein (EWS/FLI) that initiates an oncogenic transcription programme. Other rearrangements between similar genes have also been found to be drivers of Ewing sarcoma in a minority of cases. Understanding the

J.M. Tanner
Department of Oncological Sciences, Huntsman Cancer Institute, School of Medicine, University of Utah, Salt Lake City, UT 84112, USA

S.L. Lessnick, M.D., Ph.D. (✉)
Department of Pediatrics, The Ohio State University College of Medicine, Columbus, OH 43205, USA

Center for Childhood Cancer and Blood Disorders, The Research Institute at Nationwide Children's Hospital, 700 Children's Drive WA5011, Columbus, OH 43205, USA
e-mail: Stephen.Lessnick@nationwidechildrens.org

J.D. Rowley et al. (eds.), *Chromosomal Translocations and Genome Rearrangements in Cancer*, DOI 10.1007/978-3-319-19983-2_15

molecular processes governed by these rearrangements promises to generate immediately actionable therapeutic strategies. This chapter discusses the defining role that translocations and their after-effects play in Ewing sarcoma.

Keywords Translocation • EWS/FLI • Ewing sarcoma • Transcription factor • Oncogenesis

15.1 Introduction

Ewing sarcoma was first described by James Ewing (Fig. 15.1) in 1921 as a tumour composed of distinctive sheets of cells with "small hyperchromatic nuclei" [1]. He noted that these tumours were distinguishable from osteogenic sarcoma by their histopathological morphology. Indeed, Ewing sarcoma continues to be characterized by its appearance as a small, round blue cell tumour, and modern molecular biology techniques have enabled scientists to elucidate many mechanistic details important for development of this tumour [2]. One particularly important discovery – made roughly 60 years after Ewing's first description of the disease – was that Ewing sarcoma harbours a recurrent set of chromosomal translocations that drive oncogenesis [3–5]. Further study of this key translocation event and its consequences have led to greater understanding of the disease and promises to provide improved therapies for those who fall victim to this malignancy. In this chapter, we discuss the biology of Ewing sarcoma with a focus on its associated translocations, including the two most common rearrangements t(11;22)(q24.3;q12.2) and t(21;22)(q22.2;q12.2) (which generate the fusion proteins EWS/FLI and EWS/ERG, respectively) as well as other, less common translocations.

Fig. 15.1 James Ewing (ca. 1890; Source: Images from the History of Medicine, National Library of Medicine; record UI: 101414702)

15.2 Clinical Overview

Ewing sarcoma is a relatively broad term for a group of tumours collectively known as the Ewing sarcoma family of tumours. (Previously referred to as "Ewing's" sarcoma, the WHO has opted to avoid possessive nomenclature; hence, "Ewing" sarcoma is the current WHO-accepted term that will be utilized in this chapter.) This family is predominantly composed of classic Ewing sarcoma, which is a bone-associated tumour that harbours one of a set of oncogenic translocations (discussed hereafter), but also includes tumours such as Askin's tumour, primitive neuroectodermal tumours (PNETs), and Ewing tumours arising in soft-tissue, known as extraosseous Ewing sarcoma [6–9]. Despite the nuances distinguishing these different members of the Ewing sarcoma family of tumours, chromosomal rearrangements are a common feature of Ewing family tumours, and are the focus of this chapter [8–11].

Ewing sarcoma is a disease of young people, occurring most commonly in children and adolescents. The mean age at diagnosis is 15 years, and ~80 % of all cases occur in patients under the age of 25 [12, 13]. For reasons that are not understood, the disease occurs at a modestly higher rate in males than females (male-to-female ratio of 1.2) (Fig. 15.2) [13, 14]. Although the disease is relatively rare, with an incidence of ~3 per million per year in the United States, Ewing sarcoma is the second most common childhood bone tumour, after osteosarcoma [15, 16]. It is most commonly encountered in patients of European ancestry, and is exceedingly uncommon in populations of African or East Asian ancestry [17–21].

Ewing sarcoma is an aggressive cancer with a high propensity for metastasis. In fact, up to 25 % of patients already have metastatic disease at the time of diagnosis [22]. This may well be an underestimation, as it is thought that many patients have undetectable micrometastatic disease at diagnosis as well. Indeed, the relapse rate is

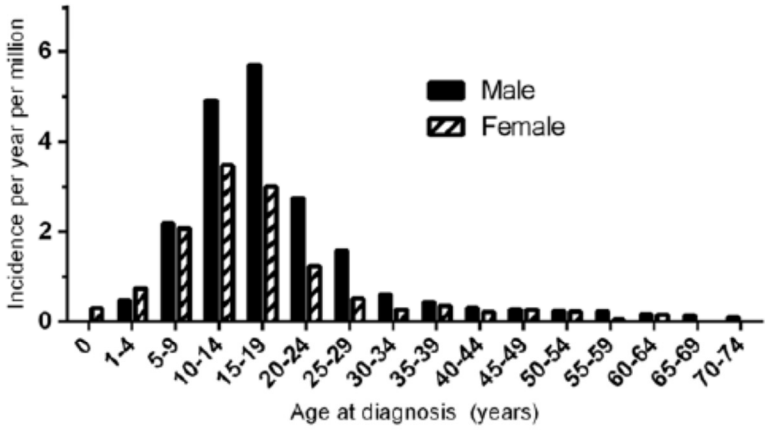

Fig. 15.2 Incidence of Ewing Sarcoma per year per million grouped by age at diagnosis (SEER data, 1973–2010) [13]

~90 % for patients who undergo surgical resection of their primary tumours without adjuvant chemotherapy [23–25]. As Ewing first observed, these tumours are often highly sensitive to radiation therapy, which was thus was a mainstay of treatment for much of the twentieth century [26, 27]. The refinement of chemotherapeutic strategies and improved surgical techniques have led to great improvements in patient survival, and current conventional treatment modalities have achieved 5-year disease-free survival rates of 60–70 % for non-metastatic disease. However, prognosis for metastatic disease remains dismal with a 5-year disease-free survival of only 10–30 % [28–30]. Moreover, survivors frequently must endure morbidities resulting from conventional anti-cancer therapy, such as severe deformities and amputations due to radical surgical resections of their tumour, and increased risk of future malignancy resulting from radiation and chemotherapy [31, 32]. Better treatments are clearly needed to provide greater survival and higher quality of life. To this end, studies continue to seek a better understanding of the molecular processes underlying Ewing sarcoma oncogenesis, including the molecular consequences of its associated chromosomal translocations.

15.3 Translocations in Ewing Sarcoma

In 1983, scientists at the Curie Institute in France identified a balanced reciprocal translocation between chromosomes 11 and 22 in patient samples and cell lines of Ewing sarcoma [3, 4, 33]. This rearrangement, t(11;22)(q24.3;q12.2), was successfully cloned several years later, and the translocation breakpoint was characterized [34]. It was revealed that this translocation resulted in an in-frame fusion of two genes: Ewing Sarcoma Breakpoint Region 1 (*EWSR1*) on chromosome 22 and Friend Leukaemia Virus Integration Site 1 (*FLI1*) on chromosome 11 [34]. The fusion protein encoded by the joining of these two genes is known as EWS/FLI. Approximately 85 % of Ewing sarcoma tumours carry this hallmark cytogenetic abnormality [9, 11, 28, 33]. The remaining 15 % of tumours carry other chromosomal rearrangements resulting in similar fusions of other genes in the same families as *EWSR1* and *FLI1* [35–39]. A list of these chromosomal rearrangements found in Ewing sarcoma is provided in Table 15.1. Details regarding each of these translocations will be discussed in the following sections.

Table 15.1 Chromosomal rearrangements found in Ewing sarcoma

Fusion	Translocation	References
EWSR1/FLI1	t (11;22)(q24;q12)	[3, 4, 33]
EWSR1/ERG	t(21;22)(q22;q12)	[38, 72]
EWSR1/ETV1	t(7;22)(p22;q12)	[35]
EWSR1/ETV4	t(7;22)(q21;q12)	[36]
EWSR1/FEV	t(2;22)(q35;q12)	[37]
FUS/ERG	t(16;21)(p11;q22)	[111]
FUS/FEV	t(2;16)(q35;p11)	[110]

15.4 EWS/FLI

15.4.1 Wild-Type EWS and the FET Family of Proteins

Prior to its cloning as part of *EWSR1/FLI1* in Ewing sarcoma, the *EWSR1* gene had not been identified and hence bears the name of the disease. *EWSR1* encodes a 656-amino acid protein called EWS. EWS is part of the FET (FUS, EWS, TAF15) family of proteins, which are involved in diverse cellular functions including gene expression and RNA processing (Fig. 15.3) [34, 40, 41].

It is ubiquitously expressed and is principally found in the nucleus, although it can be cytoplasmic or localized to the cell membrane [42–44]. The amino terminus of EWS contains a transcriptional activation region comprised of multiple pseudo-repeats rich in serine, tyrosine, glycine, and glutamine (SYGQ) (Fig. 15.3) [45–48]. This SYGQ transactivation domain is critical for interaction between EWS and RNA polymerase II; indeed, wild-type EWS has also been shown to interact with other members of the transcriptional machinery including TFIID and CREBBP/CBP/p300 [45, 46, 49]. The C-terminus of EWS contains arginine-glycine-glycine (RGG) motifs and an RNA recognition motif (RRM), possibly implicating full-length EWS in RNA binding, processing and transcription [41, 50]. The two other members of the FET family of proteins, FUS (also known as TLS) and TAF15, can also be involved in the development of other non-Ewing sarcoma cancers (Table 15.2) [51–58]. These proteins bear striking similarities to EWS, particularly with respect to the domain organization found in the N-termini of EWS and FUS [59–61].

As will be discussed in the following sections, translocations between FET genes and various partners can result in fusion proteins that alter transcriptional programmes and drive oncogenic transformation. Thus, the aforementioned interactions between FET proteins and members of the transcriptional machinery have important implications for molecular mechanisms underlying Ewing sarcoma tumourigenesis,

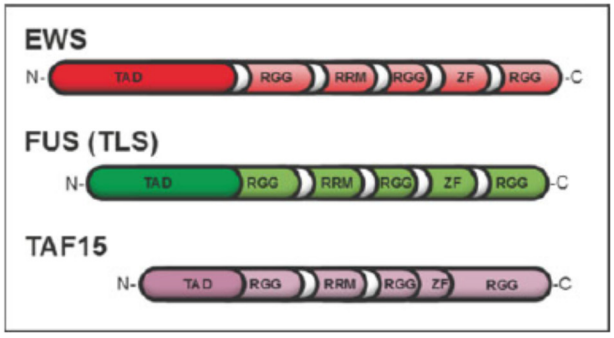

Fig. 15.3 Diagrammatic representation of FET-family proteins and their functional domains. *TAD* Transcriptional activation domain, *RGG* arginine-glycine-glycine motif, *RRM* RNA recognition motif, *ZF* zinc finger

Table 15.2 Representative non-Ewing sarcoma cancers involving translocations of FET-family proteins

	Fusion	Translocation	References
Clear cell sarcoma	EWSR1/ATF1	t(12;22)(q13;q12)	[53]
Desmoplastic small round cell tumour	EWSR1/WT1	t(11;22)(p13;q12)	[54]
Extraskeletal myxoid chondrosarcoma	EWSR1/NR4A3	t(9;22)(q22;q12)	[56]
Extraskeletal myxoid chondrosarcoma	TRF15/NR4A3	t(9;17)(q22;q11)	[52]
Myxoid liposarcoma	FUS/DDIT3	t(12;16)(q13;p11)	[51]
Myxoid liposarcoma	EWSR1/DDIT3	t(12;22)(q13;q12)	[58]
Small round cell sarcoma	EWSR1/ZNF278	t(1;22)(p36.1;q12)	[134]
Acute myelogenous leukaemia	FUS/ERG	t(16;21)(p11;q22)	[55]

as well as other cancers driven by translocations of FET genes. Recent experiments have elegantly demonstrated that FUS and EWS are able to form both homotypic and heterotypic "amyloid-like" polymers via interactions between disordered regions of polypeptides with little diversity in amino acid sequence, termed low complexity domains [49, 62]. Such aggregates could form a platform for intermolecular binding similar to molecular "velcro", leading to alteration of various cellular processes. Indeed, these polymers have been shown to bind to the C-terminal domain (CTD) of RNA polymerase II and induce transcription [49]. Accordingly, improper localization of FET proteins and their corresponding low complexity domains could disrupt gene expression at multiple loci, potentially contributing to an oncogenic phenotype. Such a model remains unproven, but is currently being actively tested.

15.4.2 Wild-Type FLI and the ETS Family of Transcription Factors

The *FLI1* gene encodes the 452 amino acid FLI protein, which is a member of the ETS (E26 transformation-specific) family of transcription factors. ETS transcription factors share a highly conserved DNA binding domain. This binding domain is known as the ETS domain, and is a winged helix-turn-helix that binds to DNA, most avidly at DNA motifs containing a core sequence of GGAA or GGAT [63, 64]. Full-length murine *Fli1* is capable of oncogenic function; indeed, the *Fli1* gene was first characterized as an integration site for the Friend murine leukaemia virus, a function from which the gene derives its name (Friend Leukaemia Virus Integration Site 1) [65]. Integration of the virus at the murine *Fli1* locus results in overexpression of *Fli1* and produces erythroleukaemia in mice [66]. Wild-type FLI appears to play important roles in haematopoiesis, particularly in megakaryocyte development [67]. Deletion of *Fli1* in mice results in dysfunctional megakaryocyte differentiation, and overexpression of *Fli1* in erythroleukaemia cells pushes them toward a megakaryocytic programme of differentiation [68, 69].

15.4.3 The EWS/FLI Fusion

To form EWS/FLI, the 5′ portion of the *EWSR1* gene and the 3′ region of the *FLI1* gene are joined together, allowing transcription of in-frame fusion transcripts and ultimately synthesis of the EWS/FLI fusion protein. The reciprocal fusion of the 5′ end of *FLI1* and the 3′ end of *EWSR1* is not expressed, and the reciprocal derivative chromosome is sometimes lost [9, 70]. Interestingly, the oncogenic *EWSR1/FLI1* fusion can result from several distinct translocation breakpoints occuring within introns of *EWSR1* and *FLI1* [71–73]. Classic splicing processes then generate fusion transcripts joining 5′ exons of *EWSR1* with 3′ exons of *FLI1*. EWS/FLI can thus be categorized into subtypes based upon the location of the translocation breakpoint and which exons are fused together [34]. For instance, the most commonly observed translocation in Ewing sarcoma joins exons 1–7 of *EWSR1* to exons 6–10 of *FLI1*. This rearrangement is sometimes termed a "Type I" fusion, but it is more commonly referred to simply as a "7/6" EWS/FLI fusion. Likewise, other fusions of EWS/FLI can be referred to by the exons that are fused, and a partial list of observed EWS/FLI fusions is illustrated in Fig. 15.4.

The functional significance of these subtly different EWS/FLI fusion products remains largely unknown. However, some data exist that suggest that the "7/6" EWS/FLI fusion ("Type I") is more weakly transactivating compared to other EWS/FLI fusion subtypes [74]. This distinction was thought to be potentially useful as a prognostic variable, and retrospective analyses of patient cohorts suggested that patients with "7/6" EWS/FLI fusions had better survival rates compared to patients whose tumours harboured EWS/FLI from other translocation breakpoints [75, 76]. However, recent studies have revealed that prognostic differences no longer exist within current treatment protocols [77, 78]. Hence, the functional significance of different breakpoints, if any exists at all, remains unknown.

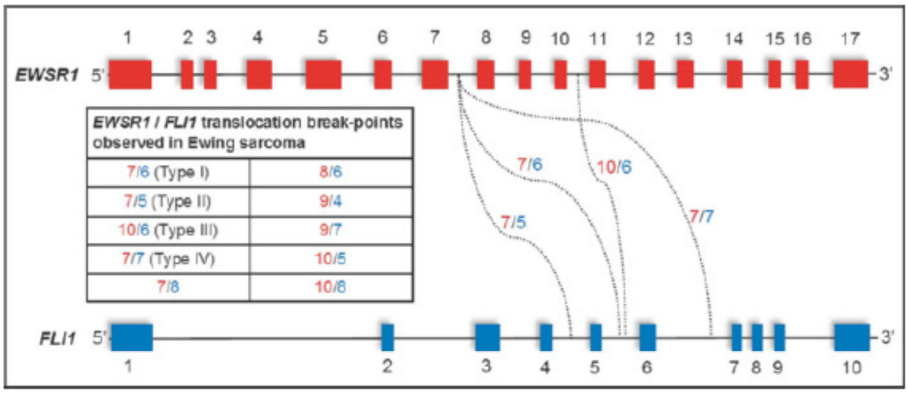

Fig. 15.4 Diagrammatic representation of *EWSR1* and *FLI1* exons. Known translocation breakpoints are indicated

15.4.4 Oncogenic Function of EWS/FLI

EWSR1 and *FLI1* genes are fused in-frame, encoding the EWS/FLI oncoprotein (Fig. 15.5). This translocation-derived oncoprotein contains the N-terminal transactivation domain of EWS fused with the DNA-binding domain of FLI, forming an oncogenic transcription factor that is indispensible for tumourigenesis [34, 42, 79–81]. The first studies implicating EWS/FLI as a driver in Ewing sarcoma observed that overexpression of EWS/FLI in NIH3T3 murine fibroblasts induced oncogenic transformation, measured by anchorage-independent growth in soft agar. This was later confirmed by experiments demonstrating the ability of EWS/FLI-expressing NIH3T3 cells to form tumours in mouse xenografts [80, 82, 83]. Furthermore, studies utilizing patient-derived Ewing sarcoma cell lines have shown that disruption of EWS/FLI expression by RNA interference (RNAi) and other means results in loss of transformation [70, 84–92]. Together, these findings clearly indicate that EWS/FLI is the driver mutation underlying Ewing sarcoma oncogenesis.

This loss of transformation is accompanied by changes in gene expression, including activation and repression of numerous EWS/FLI target genes [70, 89, 92–94]. Importantly, when EWS/FLI is reintroduced after being silenced by RNAi, the oncogenic expression profile and transformed phenotype of Ewing sarcoma are restored, indicating that EWS/FLI is at the head of an oncogenic programme of gene expression [70, 92, 94]. Studies show that thousands of genes are either

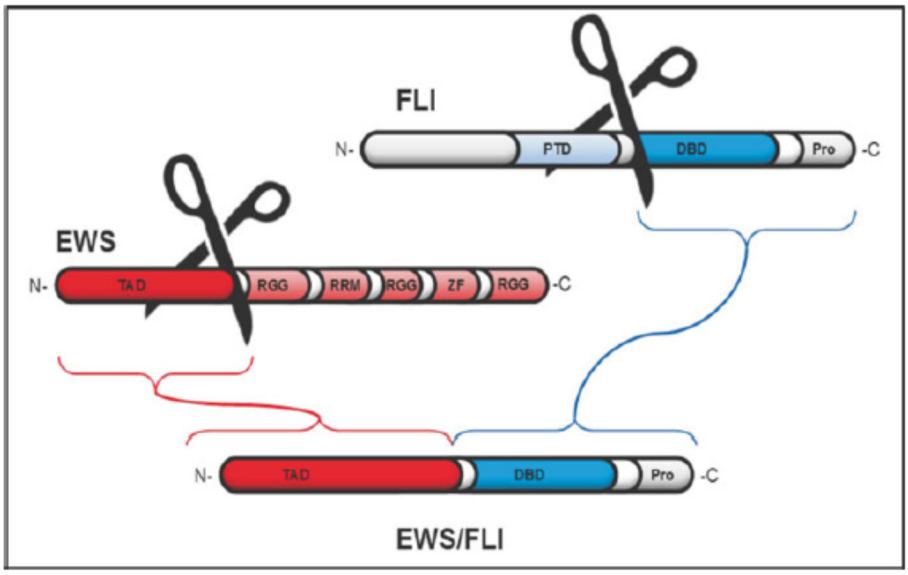

Fig. 15.5 Illustration of the EWS/FLI fusion protein, joining the N-terminal portion of EWS with the C-terminal portion of FLI. *PTD* pointed domain, *DBD* DNA binding domain, *Pro* proline-rich activation domain, *TAD* Transcriptional activation domain, *RGG* arginine-glycine-glycine motif, *RRM* RNA recognition motif, *ZF* zinc finger

upregulated or downregulated by EWS/FLI, leading to "transcriptional mayhem" [70, 81, 95]. This dysregulation of EWS/FLI target gene expression has been the focus of investigations into the mechanisms by which EWS/FLI drives tumourigenesis, and studies have revealed several EWS/FLI-regulated genes that are also required for tumourigenesis, including NR0B1, NKX2.2 and GLI1 [70, 92, 94, 96, 97].

The exact mechanisms by which EWS/FLI causes up-regulation of target genes is an area of active study. It is known that EWS/FLI alters expression of some genes in a direct manner, while it dysregulates other genes indirectly [98, 99]. Nevertheless, it has been definitively shown that the ability of EWS/FLI to bind DNA is essential for Ewing sarcoma oncogenesis [79]. Chromatin immunoprecipitation experiments followed by microarray analysis (ChIP-chip) and deep sequencing (ChIP-seq) have clearly demonstrated that EWS/FLI binds to high-affinity ETS sequences (ACCGGAAGTG) [63, 64, 100, 101]. Interestingly, it was also revealed that EWS/FLI binds to microsatellite repeats of the sequence GGAA [102, 103]. In fact, binding of EWS/FLI to microsatellites is required for upregulation of *NR0B1*, *CAV1*, and *GSTM4*; genes that are critical downstream effectors of EWS/FLI-driven tumourigenesis [102, 103].

Furthermore, as previously mentioned, it has been shown that wild-type EWS is capable of forming a molecular "velcro"-like polymer that facilitates protein-protein interactions between EWS and other proteins, including RNA polymerase II [49, 62]. The low complexity domain in the N-terminal region of wild-type EWS is retained in the EWS/FLI fusion protein, fused to the DNA-binding ETS domain of FLI. It is tempting to speculate, therefore, that the DNA-binding domain of FLI acts to re-direct the molecular "velcro" of EWS to different loci throughout the genome, leading to disruption of regulatory protein complexes and transcriptional activation of EWS/FLI target genes. For instance, GGAA microsatellite repeats could facilitate EWS/FLI polymerization as multiple DNA sequence repeats could permit EWS/FLI to bind in series, forming a scaffold of EWS low complexity domains to which coactivator complexes and transcriptional machinery (e.g., RNA polymerase II) could bind, thus upregulating that locus. Similarly, such a phenomenon could allow EWS/FLI to recruit repressive regulatory complexes to various loci, resulting in down-regulation of target genes. This model, while intriguing, remains unproven, and further testing will shed light on the true mechanisms underlying EWS/FLI-mediated transcriptional dysregulation.

EWS/FLI also down-regulates thousands of genes in Ewing sarcoma. This is particularly interesting considering the presence of the N-terminal transactivation domain of EWS in the EWS/FLI oncoprotein. The mechanisms by which such a transactivator-containing transcription factor causes direct repression of genes remains another active area of study, and several mechanistic insights have been revealed. For instance, it has been demonstrated that a corepressor complex called the Nucleosome Remodelling and Deacetylase (NuRD) complex plays an important role in repression of EWS/FLI targets. Interestingly, disruption of NuRD complex function by vorinostat treatment (a histone deacetylase inhibitor) or RNAi-mediated silencing of *CHD4* (a core NuRD component) resulted in de-repression of EWS/FLI-repressed target genes [104]. Additionally, inhibition of lysine-specific demethylase 1

(LSD1) resulted in de-repression of EWS/FLI-regulated target genes. This effect was lost upon silencing of EWS/FLI, implicating EWS/FLI-mediated disruption of associated epigenetic factors in Ewing sarcoma oncogenesis [104, 105]. Continued investigation of these phenomena is likely to generate a clearer mechanistic understanding of EWS/FLI-driven up- and down-regulation of target genes, potentially providing targets for new and better therapeutics.

15.5 EWS/ERG

In 1993 it was found that a distinct translocation event between the *EWSR1* gene and another ETS family member, *ERG* (ETS-Related Gene), also generated a fusion protein, termed EWS/ERG [38]. The t(21;22)(q22.2;q12.2) rearrangement producing this alternate fusion oncoprotein is present in approximately 10 % of Ewing tumours, making it the most common alternate translocation in Ewing sarcoma [38, 72]. Tumours carrying the EWS/ERG mutation do not carry the EWS/FLI fusion, indicating that EWS/ERG likely drives Ewing sarcoma oncogenesis in ways very similar to EWS/FLI. Indeed, the DNA-binding ETS domain of ERG is shares 98 % amino acid identity with the ETS domain of FLI, and the full-length proteins are 68 % similar [38, 106]. Furthermore, EWS/ERG-harbouring Ewing sarcoma tumours were no different compared to cases of EWS/FLI-containing tumours with respect to age at diagnosis, primary site, metastasis, as well as overall and event-free survival [107].

Like EWS/FLI, EWS/ERG induces oncogenic transformation when it is expressed in NIH3T3 cells [83]. Functionally, EWS/ERG is presumed to bind similar, if not identical, sets of loci as EWS/FLI, likely dysregulating expression of target genes in similar ways. This presumption is supported by evidence indicating that EWS/FLI and EWS/ERG dysregulate the same core subset of genes when introduced into NIH 3T3 cells, although these results must be interpreted cautiously considering the inaccuracies of this model [70, 108].

15.6 EWS/ETV1, EWS/ETV4, EWS/FEV

In addition to EWS/FLI and EWS/ERG, other EWS/ETS translocations have also been described in Ewing sarcoma. These alternate rearrangements result in the fusion of the *EWSR1* gene with *ETV1* (ETS variant gene 1), *ETV4* (ETS variant gene 4) and *FEV* (fifth Ewing sarcoma variant) (Table 15.1) [35–37, 39]. Each of these additional fusion proteins occurs in <1 % of all Ewing sarcoma cases, making them exceptionally rare. Being members of the same family of transcription factors, ERG, ETV1, ETV4 and FEV are all highly similar, particularly in their ETS DNA-binding domains. In fact, ETS domains of FLI, ERG and FEV are 98 % similar. ETV1 and ETV4 are also similar to other ETS proteins, but are more similar to each other because they have identical DNA-binding domains.

These rare alternate fusions have been less well studied than EWS/FLI. However, their structural similarities suggest that they share much of the same oncogenic functions required for Ewing sarcoma tumourigenesis. Indeed, the mutually exclusive nature of these different types of EWS/ETS fusions suggests that they may be largely interchangeable. Notwithstanding the relative paucity of data regarding these uncommon rearrangements, some functional differences have been observed in experiments utilizing NIH3T3 cells. Using this model, it was shown that EWS/FLI, EWS/ERG and EWS/FEV were capable of inducing anchorage-independent growth in soft agar assays, whereas EWS/ETV1 and EWS/ETV4 were incapable of inducing such transformation [108]. Interestingly, each fusion protein enabled tumour formation by NIH3T3 cells in murine xenografts. The mechanism and relevance of these differences remain unknown. It has also been suggested that EWS/FEV, EWS/ETV1 and EWS/ETV4 exist predominantly in extraosseous Ewing sarcoma [109]. However, insufficient data exists at the present time to draw any definitive conclusions about this potential correlation. It is also unknown whether these different fusion proteins have any significance with regard to outcome.

15.7 FUS/ERG and FUS/FEV

EWSR1 is the founding member of the FET (*FUS*, *EWSR1*, *TAF15*) family of RNA-binding proteins involved in Ewing sarcoma translocations. However, in rare instances, other members of the family are involved. Chromosomal rearrangements between *FUS* (also known as *TLS*) and *ERG* or *FEV*, both ETS family member genes, have been identified in rare cases of Ewing sarcoma [110, 111].

The FUS protein has a similar domain structure to that of EWS, containing an N-terminal transactivation domain with SYGQ repeats, and C-terminal RGG and RRM motifs (Fig. 15.5). Considering these shared structural features, it is likely that FUS/ETS fusions drive oncogenesis via mechanisms similar to those utilized by EWS/FLI. However, this hypothesis has not been thoroughly tested, in large part due to the relative scarcity of these alternate chromosomal rearrangements. Nevertheless, some functional similarities have been observed. For instance, both EWS/FLI and FUS/ERG have been shown to disrupt RNA splicing by similar mechanisms [112]. Expression of insulin-like growth factor 1 (*IGF1*) is also induced by several FET/ETS fusion proteins, including FUS/ERG [113]. However, these data must be interpreted with some caution as they are based largely on murine cells, which may lack some features important for EWS/FLI function [114].

Currently, only FUS/ERG and FUS/FEV fusions have been described, but it is possible that other FET/ETS fusions could exist in Ewing sarcoma. However, such instances would be exceedingly rare. The uncommon nature of such alternate fusions makes it difficult to elucidate whether specific rearrangements have important implications for prognosis, probability of relapse, or other factors. As mentioned before, these alternate translocations do pose a potential complication for molecular diagnosis of the disease, as a tumour that appears negative for all known

translocations may harbour an oncogenic FET/ETS rearrangement that has not yet been characterized and thus evades detection. These fusions are so scarce, however, that only a small minority of patients would be impacted by such a scenario.

15.8 "Ewing-Like Sarcomas" and Their Translocations

The existence of multiple alternate chromosomal rearrangements in Ewing sarcoma raises the question of how best to molecularly define the disease. In general, histopathological features and patient presentation give good pre-test probability for diagnosis, and definitive diagnosis commonly given by detection of CD99, a cell surface marker found on most Ewing sarcoma cells [115]. Biopsies are often subjected to molecular tests detecting the presence of the t(11;22)(q24.3;q12.2) translocation. Presence of EWS/FLI transcript are detected with RT-PCR, and translocations involving *EWSR1* are detected via breakapart FISH assays. These methods will detect almost all known FET/ETS chromosomal rearrangements in Ewing sarcoma. However, a family of tumours exists in which non-FET/ETS fusions are present (Table 15.3). These cancers are termed "Ewing-like sarcomas".

One such "Ewing-like" tumour was first reported in 2009 as a new t(20;22)(q13;q12) rearrangement between *EWSR1* and *NFATC2* (nuclear factor of activated T-cells, cytoplasmic, calcineurin-dependent 2) [116]. The wild-type NFATC2 protein is a member of the NFAT family of transcription factors and is a key player in T-cell and neuronal development. NFATC2 binds DNA cooperatively with Fos and Jun, members of the activator protein 1 (AP1) family of regulatory transcription factors [117–120]. Interestingly, ETS proteins and the EWS/FLI fusion protein are also capable of cooperative DNA binding with AP1 proteins [121–123]. Also, NFAT proteins, like ETS proteins, recognize DNA sequences with a core motif of GGAA/T [116]. Together these findings suggest possible shared mechanisms of oncogenesis between EWS/ETS and EWS/NFATC2 fusions.

EWSR1 can fuse to a number of other non-ETS proteins to drive formation of "Ewing-like" tumours. Another such fusion is EWS/POU5F1 [124]. POU5F1 (POU class 5 homeobox 1) is also known as OCT4 (octamer-binding transcription factor 4), and is a transcription factor important for regulating pluripotency of stem cells [125–127]. It is thought that this fusion protein functions as an aberrant transcription

Table 15.3 Non-FET/ETS chromosomal rearrangements found "Ewing-like sarcomas"

Fusion	Translocation	References
EWSR1/NFATC2	t(20;22)(q13;q12)	[116]
EWSR1/POU5F1	t(6;22)(p21;q12)	[124]
EWSR1/SMARCA5	t(4;22)(q31;q12)	[133]
EWSR1/PATZ1	t(22;22)(q12;q12)	[134]
EWSR1/SP3	t(2;22)(q31;q12)	[109]
CIC/DUX4	t(4;19)(q35;q13)	[136]
BCOR/CCNB3	inv(X)(p11.4p11.22)	[137]

factor in these tumours, transcriptionally reprogramming cells and generating an oncogenic phenotype.

Fusions between *EWSR1* and *PATZ1* (POZ (BTB) and AT Hook Containing Zinc Finger 1, also known as *ZSG*) or *SP3* are also found in some "Ewing-like" tumours [109, 128]. Both ZSG and SP3 are zinc finger-containing transcription factor proteins and, therefore, potentially function by binding DNA and allowing the EWS portion of the fusion to dysregulate gene expression profiles, similar to EWS/FLI and other Ewing sarcoma rearrangements [109, 129]. Wild-type SP3 also contains an inhibitory domain that is lost in the translocation event generating EWS/SP3, potentially contributing to its oncogenic function.

EWSR1 can also fuse with *SMARCA5* (SWI/SNF related, matrix associated, actin dependent regulator of chromatin, subfamily A, member 5), an ATPase found in various chromatin remodelling complexes [130–135]. While the EWS/SMARCA5 fusion protein does not directly bind DNA in a sequence-specific manner, it alters expression of key target genes perhaps by altering a chromatin remodelling function. Interestingly, SMARCA5 can function as part of the NuRD complex, which plays an important role in EWS/FLI-mediated repression of target genes (discussed previously) [104]. Whether any relationship exists between EWS/SMARCA5 and NuRD has not been tested.

CIC/DUX4 and *BCOR/CCNB3* fusions have also been described [136, 137]. However, it has not been fully determined whether these tumours represent Ewing sarcoma, "Ewing-like" sarcoma, or a distinct type of bone sarcoma. More in-depth study of the molecular mechanisms underlying these oncogenic chromosomal rearrangements must be undertaken to answer this question. Indeed, a clear molecular-based definition of Ewing sarcoma and its variations may hinge upon achieving a clearer picture of how these fusions generate an oncogenic phenotype.

15.9 Molecular Definitions of Ewing Sarcoma and Diagnostic Challenges

15.9.1 Defining the Disease

The classic diagnostic definition of Ewing sarcoma relies largely upon histopathological features of these tumours, assessed by light microscopy and/or immunohistochemistry [138, 139]. This cancer appears as a small, round cell cancer with hyperchromatic nuclei when viewed by light microscopy after H&E staining [140]. Immunohistochemical staining often reveals high levels of CD99 at the cell membrane, and is used as another diagnostic marker of Ewing sarcoma cells [115, 138].

Additionally, the presence of a balanced translocation involving *EWSR1* and one of the *ETS* family of transcription factors are considered pathognomonic for the disease [138]. However, as discussed in this chapter, a number of different translocations involving FET family members other than *EWSR1* (e.g., *FUS*) also exist.

Additionally, several "Ewing-like" cancers have been found with fusions of EWSR1 to non-ETS proteins. These alternate molecular lesions, rare as they may be, add complexity to the question of how to properly define this disease and its variations.

Generally, Ewing sarcoma can be broadly subdivided into three groups, based on the type of translocation present in the tumour cells: (1) *EWSR1/FLI1* and functionally similar translocations (i.e., FET/ETS fusions), (2) non-FET/ETS fusions (e.g., EWS/SMARCA5), and (3) totally distinct translocations (e.g., *CIC/DUX4*). Furthermore, tumours of EWS/FLI and other FET/ETS fusions (e.g., EWS/ERG) can be considered classic Ewing sarcoma, while rarer, non-FET/ETS fusions and distinct translocations can be generally termed "Ewing-like" sarcomas. These definitions provide a useful categorical structure for the various molecular lesions driving oncogenesis in these tumours, but definitions will be continuously refined as our understanding of the molecular mechanisms of this disease expands.

Accurate and useful definitions are important insomuch as they may assist in grouping patients in clinically useful ways, such as into groups receiving different treatments or with different prognoses. These goals are especially challenging considering the rarity of non-EWS/FLI fusion variants, and little variation currently exists in the clinical management of different types of fusions.

15.9.2 Challenges of Molecular Diagnosis

The existence of alternate chromosomal rearrangements has clear implications for the diagnosis of Ewing sarcoma. Current diagnostic methods utilized to identify the EWS/FLI fusion may not identify the less common translocations. For instance, breakapart FISH (fluorescence in situ hybridization) probes for *EWSR1* are commonly utilized to determine that a translocation involving EWSR1 exists and are, thus, useful for detecting the most common rearrangements in Ewing sarcoma (i.e., EWS/FLI and EWS/ERG) [138, 139]. This method, however, is unable to detect Ewing sarcoma driven by non-*EWSR1* rearrangements, such as the rarer FUS/ERG and FUS/FEV fusions (Fig. 15.6).

Reverse-transcriptase (RT)-PCR assays have also been utilized to detect the fusion transcript [139]. Such an approach suffers from the same weakness as the EWSR1 breakapart FISH assay in that it is unable to detect transcripts of all possible gene fusions. For instance, primers designed to amplify specific *EWSR1/FLI1* fusions will not anneal to *EWSR1/ERG* or other alternate transcripts. Despite this weakness, one potential benefit to using a PCR-based assay is the ability to detect specific breakpoints, although this may not be clinically useful, as discussed earlier [75, 76, 78].

Hence, the rare cases of Ewing sarcoma driven by alternate translocations may theoretically result in delayed or incorrect diagnosis in uncommon cases. Clearly, the correct diagnosis of Ewing sarcoma must not rely on one single test but rather on a collection of various criteria, including patient presentation, imaging studies (e.g., X-ray, CT, MRI), histopathology, and pathognomonic molecular lesions such

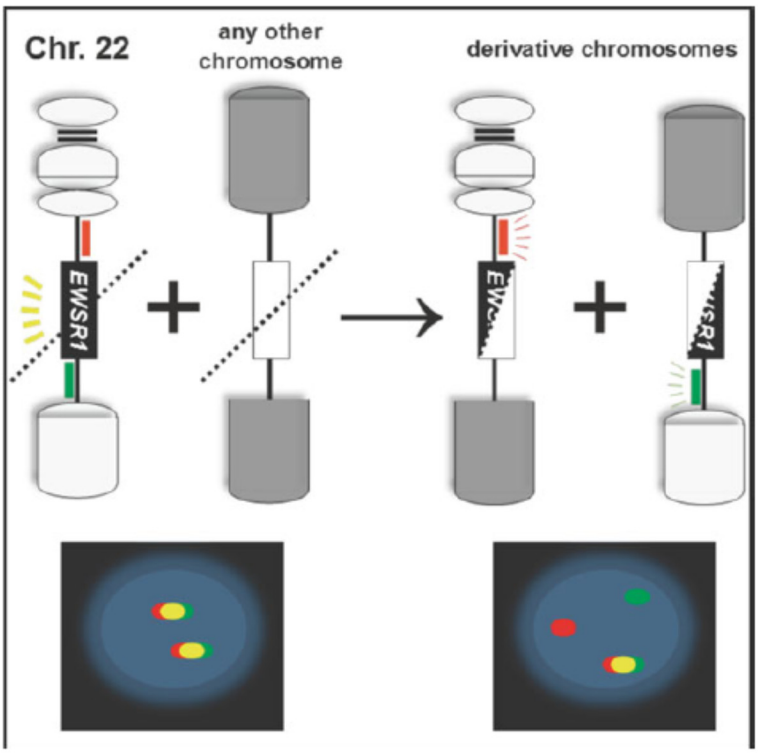

Fig. 15.6 Diagrammatic representation of a breakapart fluorescence in situ hybridization (FISH) assay for *EWSR1*. Fluorescent red and green probes flank the *EWSR1* gene. Intact *EWSR1* with both probes appears *yellow*. A translocation splits the gene, resulting in split *red* and *green* signals. In diploid cells, separate *red* and *green* signals result from the split chromosome, and the normal second allele appears *yellow*

as EWS/FLI. Such a practice of integrating distinct pieces of data to come to a definitive diagnosis is the current practice, allowing for prompt and accurate diagnosis in almost all cases.

15.10 Conclusions

Although it is rare compared to other malignancies, Ewing sarcoma is a devastating disease affecting many young people, resulting in many years of life lost to morbidity and mortality. Over the past 30 years, scientists have made great strides in understanding the molecular mechanisms underlying this cancer. Nevertheless, the increased knowledge gained through studying the cellular and molecular biology of this disease has not yet led to improvements in clinical management. Current standards of care rely on conventional therapies like surgery and chemotherapy, and

improved usage of these treatment modalities have achieved remarkable success in overall survival. No molecularly targeted therapy has been found to be efficacious against Ewing sarcoma, despite increased understanding of the molecular biology of the disease.

The EWS/FLI fusion protein, and the other fusions found in Ewing sarcoma, clearly offer a unique pathogenic feature of this disease that could be targeted. However, transcription factors have proven to be extraordinarily challenging targets for inhibition, often earning them the epithet "undruggable". Thus most efforts have focused on developing deeper understanding of the functions of critical effectors of EWS/FLI-driven oncogenesis. Although progress has been slow, a few promising targets have recently emerged [141]. Future work will continue to pursue a clearer understanding of the oncogenic consequences of the chromosomal rearrangements discussed in this chapter. Understanding why these translocations drive oncogenesis will assist in developing new therapies, likely increasing the odds of survival and bettering post-survival quality of life in these patients.

References

1. Ewing J (1921) Diffuse endothelioma of bone. Proc N Y Phytopathol Soc 21:17–24
2. Stiller CA, Bielack SS, Jundt G, Steliarova-Foucher E (2006) Bone tumours in European children and adolescents, 1978–1997. Report from the Automated Childhood Cancer Information System project. Eur J Cancer 42:2124–2135
3. Aurias A, Rimbaut C, Buffe D, Dubousset J, Mazabraud A (1983) Translocation of chromosome 22 in Ewing's sarcoma. C R Seances Acad Sci III Sci Vie 296:1105–1107
4. Turc-Carel C, Philip I, Berger MP, Philip T, Lenoir G (1983) Chromosomal translocation (11; 22) in cell lines of Ewing's sarcoma. C R Seances Acad Sci III Sci Vie 296:1101–1103
5. Janknecht R (2005) EWS-ETS oncoproteins: the linchpins of Ewing tumors. Gene 363:1–14
6. Horowitz ME, Malawer MM, Woo SY, Hicks MJ (1997) In: Pizzo PA, Poplack DG (eds) Principles and practice of pediatric oncology. Lippincott-Raven Publishers, Philadelphia, pp 831–863
7. Kimber C, Michalski A, Spitz L, Pierro A (1998) Primitive neuroectodermal tumours: anatomic location, extent of surgery, and outcome. J Pediatr Surg 33:39–41
8. Grier HE (1997) The Ewing family of tumors. Ewing's sarcoma and primitive neuroectodermal tumors. Pediatr Clin N Am 44:991–1004
9. Turc-Carel C, Philip I, Berger MP, Philip T, Lenoir GM (1984) Chromosome study of Ewing's sarcoma (ES) cell lines. Consistency of a reciprocal translocation t(11;22)(q24;q12). Cancer Genet Cytogenet 12:1–19
10. Kovar H (1998) Ewing's sarcoma and peripheral primitive neuroectodermal tumors after their genetic union. Curr Opin Oncol 10:334–342
11. Whang-Peng J et al (1984) Chromosome translocation in peripheral neuroepithelioma. N Engl J Med 311:584–585
12. Ries LAG et al (2001) SEER cancer statistics review, 1973–1998. National Cancer Institute, Bethesda
13. Surveillance, E., and End Results (SEER) Program (www.seer.cancer.gov) SEER*Stat Database: Incidence – SEER 9 Regs Research Data, Nov 2012 Sub (1973–2010) <Katrina/Rita Population Adjustment> – Linked to county attributes – total U.S., 1969–2011 Counties, National Cancer Institute, DCCPS, Surveillance Research Program, Surveillance Systems Branch, released April 2013, based on the November 2012 submission. Accessed February 2013

14. Stiller CA et al (2006) Cancer incidence and survival in European adolescents (1978–1997). Report from the Automated Childhood Cancer Information System project. Eur J Cancer 42:2006–2018
15. Denny CT (1998) Ewing's sarcoma – a clinical enigma coming into focus. J Pediatr Hematol Oncol 20:421–425
16. Paulussen M, Frohlich B, Jurgens H (2001) Ewing tumour: incidence, prognosis and treatment options. Pediatr Drugs 3:899–913
17. Parkin DM, Stiller CA, Nectoux J (1993) International variations in the incidence of childhood bone tumours. Int J Cancer 53:371–376
18. Polednak AP (1985) Primary bone cancer incidence in black and white residents of New York State. Cancer 55:2883–2888
19. Bahebeck J et al (2003) Bone tumours in Cameroon: incidence, demography and histopathology. Int Orthop 27:315–317
20. Settakorn J et al (2006) Spectrum of bone tumors in Chiang Mai University Hospital, Thailand according to WHO classification 2002: a study of 1,001 cases. J Med Assoc Thai 89:780–787
21. Guo W, Xu W, Huvos AG, Healey JH, Feng C (1999) Comparative frequency of bone sarcomas among different racial groups. Chin Med J (Engl) 112:1101–1104
22. Terrier P, Llombart-Bosch A, Contesso G (1996) Small round blue cell tumors in bone: prognostic factors correlated to Ewing's sarcoma and neuroectodermal tumors. Semin Diagn Pathol 13:250–257
23. Wang CC, Schulz MD (1953) Ewing's sarcoma; a study of fifty cases treated at the Massachusetts General Hospital, 1930–1952 inclusive. N Engl J Med 248:571–576
24. Dahlin DC, Coventry MB, Scanlon PW (1961) Ewing's sarcoma. A critical analysis of 165 cases. J Bone Joint Surg Am 43-A:185–192
25. Lahl M, Fisher VL, Laschinger K (2008) Ewing's sarcoma family of tumors: an overview from diagnosis to survivorship. Clin J Oncol Nurs 12:89–97. doi:10.1188/08.CJON.89-97
26. Lee ES (1971) Treatment of bone sarcoma. Proc R Soc Med 64:1179–1180
27. Rosen G et al (1978) Curability of Ewing's sarcoma and considerations for future therapeutic trials. Cancer 41:888–899
28. Sankar S, Lessnick SL (2011) Promiscuous partnerships in Ewing's sarcoma. Cancer Genet 204:351–365. doi:10.1016/j.cancergen.2011.07.008
29. Linabery AM, Ross JA (2008) Childhood and adolescent cancer survival in the US by race and ethnicity for the diagnostic period 1975–1999. Cancer 113:2575–2596
30. Randall RL et al (2010) Is there a predisposition gene for Ewing's sarcoma? J Oncol 2010:397632. doi:10.1155/2010/397632
31. May WA et al (2013) Characterization and drug resistance patterns of Ewing's sarcoma family tumor cell lines. PLoS One 8:e80060. doi:10.1371/journal.pone.0080060
32. Potratz J, Dirksen U, Jurgens H, Craft A (2012) Ewing sarcoma: clinical state-of-the-art. Pediatr Hematol Oncol 29:1–11. doi:10.3109/08880018.2011.622034
33. Turc-Carel C et al (1988) Chromosomes in Ewing's sarcoma. I. An evaluation of 85 cases of remarkable consistency of t(11;22)(q24;q12). Cancer Genet Cytogenet 32:229–238
34. Delattre O et al (1992) Gene fusion with an ETS DNA-binding domain caused by chromosome translocation in human tumours. Nature 359:162–165
35. Jeon IS et al (1995) A variant Ewing's sarcoma translocation (7;22) fuses the EWS gene to the ETS gene ETV1. Oncogene 10:1229–1234
36. Kaneko Y et al (1996) Fusion of an ETS-family gene, EIAF, to EWS by t(17;22)(q12;q12) chromosome translocation in an undifferentiated sarcoma of infancy. Gene Chromosome Cancer 15:115–121
37. Peter M et al (1997) A new member of the ETS family fused to EWS in Ewing tumors. Oncogene 14:1159–1164
38. Sorensen PH et al (1994) A second Ewing's sarcoma translocation, t(21;22), fuses the EWS gene to another ETS-family transcription factor, ERG. Nat Genet 6:146–151. doi:10.1038/ng0294-146

39. Urano F, Umezawa A, Hong W, Kikuchi H, Hata J (1996) A novel chimera gene between EWS and E1A-F, encoding the adenovirus E1A enhancer-binding protein, in extraosseous Ewing's sarcoma. Biochem Biophys Res Commun 219:608–612
40. Aman P et al (1996) Expression patterns of the human sarcoma-associated genes FUS and EWS and the genomic structure of FUS. Genomics 37:1–8
41. Ohno T et al (1994) The EWS gene, involved in Ewing family of tumors, malignant melanoma of soft parts and desmoplastic small round cell tumors, codes for an RNA binding protein with novel regulatory domains. Oncogene 9:3087–3097
42. May WA et al (1993) The Ewing's sarcoma EWS/FLI-1 fusion gene encodes a more potent transcriptional activator and is a more powerful transforming gene than FLI-1. Mol Cell Biol 13:7393–7398
43. Sutherland HG et al (2001) Large-scale identification of mammalian proteins localized to nuclear sub-compartments. Hum Mol Genet 10:1995–2011
44. Zakaryan RP, Gehring H (2006) Identification and characterization of the nuclear localization/retention signal in the EWS proto-oncoprotein. J Mol Biol 363:27–38
45. Araya N et al (2003) Cooperative interaction of EWS with CREB-binding protein selectively activates hepatocyte nuclear factor 4-mediated transcription. J Biol Chem 278:5427–5432
46. Bertolotti A et al (1998) EWS, but not EWS-FLI-1, is associated with both TFIID and RNA polymerase II: interactions between two members of the TET family, EWS and hTAFII68, and subunits of TFIID and RNA polymerase II complexes. Mol Cell Biol 18:1489–1497
47. Petermann R et al (1998) Oncogenic EWS-Fli1 interacts with hsRPB7, a subunit of human RNA polymerase II. Oncogene 17:603–610
48. Rossow KL, Janknecht R (2001) The Ewing's sarcoma gene product functions as a transcriptional activator. Cancer Res 61:2690–2695
49. Kwon I et al (2013) Phosphorylation-regulated binding of RNA polymerase II to fibrous polymers of low-complexity domains. Cell 155:1049–1060. doi:10.1016/j.cell.2013.10.033
50. Deloulme JC, Prichard L, Delattre O, Storm DR (1997) The prooncoprotein EWS binds calmodulin and is phosphorylated by protein kinase C through an IQ domain. J Biol Chem 272:27369–27377
51. Crozat A, Aman P, Mandahl N, Ron D (1993) Fusion of CHOP to a novel RNA-binding protein in human myxoid liposarcoma. Nature 363:640–644
52. Panagopoulos I et al (1999) Fusion of the RBP56 and CHN genes in extraskeletal myxoid chondrosarcomas with translocation t(9;17)(q22;q11). Oncogene 18:7594–7598
53. Zucman J et al (1993) EWS and ATF-1 gene fusion induced by t(12;22) translocation in malignant melanoma of soft parts. Nat Genet 4:341–345
54. Ladanyi M, Gerald W (1994) Fusion of the EWS and WT1 genes in the desmoplastic small round cell tumor. Cancer Res 54:2837–2840
55. Martini A et al (2002) Recurrent rearrangement of the Ewing's sarcoma gene, EWSR1, or its homologue, TAF15, with the transcription factor CIZ/NMP4 in acute leukemia. Cancer Res 62:5408–5412
56. Gill S et al (1995) Fusion of the EWS gene to a DNA segment from 9q22-31 in a human myxoid chondrosarcoma. Gene Chromosome Cancer 12:307–310
57. Sjogren H et al (2000) Fusion of the NH2-terminal domain of the basic helix-loop-helix protein TCF12 to TEC in extraskeletal myxoid chondrosarcoma with translocation t(9;15)(q22;q21). Cancer Res 60:6832–6835
58. Panagopoulos I et al (1996) Fusion of the EWS and CHOP genes in myxoid liposarcoma. Oncogene 12:489–494
59. Bertolotti A, Lutz Y, Heard DJ, Chambon P, Tora L (1996) hTAF(II)68, a novel RNA/ssDNA-binding protein with homology to the pro-oncoproteins TLS/FUS and EWS is associated with both TFIID and RNA polymerase II. EMBO J 15:5022–5031
60. Morohoshi F, Arai K, Takahashi EI, Tanigami A, Ohki M (1996) Cloning and mapping of a human RBP56 gene encoding a putative RNA binding protein similar to FUS/TLS and EWS proteins. Genomics 38:51–57

61. Stolow DT, Haynes SR (1995) Cabeza, a Drosophila gene encoding a novel RNA binding protein, shares homology with EWS and TLS, two genes involved in human sarcoma formation. Nucleic Acids Res 23:835–843
62. Kato M et al (2012) Cell-free formation of RNA granules: low complexity sequence domains form dynamic fibers within hydrogels. Cell 149:753–767. doi:10.1016/j.cell.2012.04.017
63. Seth A, Watson DK (2005) ETS transcription factors and their emerging roles in human cancer. Eur J Cancer 41:2462–2478
64. Sharrocks AD (2001) The ETS-domain transcription factor family. Nat Rev Mol Cell Biol 2:827–837
65. Ben-David Y, Giddens EB, Bernstein A (1990) Identification and mapping of a common proviral integration site Fli-1 in erythroleukemia cells induced by Friend murine leukemia virus. Proc Natl Acad Sci U S A 87:1332–1336
66. Ben-David Y, Giddens EB, Letwin K, Bernstein A (1991) Erythroleukemia induction by Friend murine leukemia virus: insertional activation of a new member of the ets gene family, Fli-1, closely linked to c-ets-1. Genes Dev 5:908–918
67. Bastian LS, Kwiatkowski BA, Breininger J, Danner S, Roth G (1999) Regulation of the megakaryocytic glycoprotein IX promoter by the oncogenic Ets transcription factor Fli-1. Blood 93:2637–2644
68. Athanasiou M et al (1996) Increased expression of the ETS-related transcription factor FLI-1/ERGB correlates with and can induce the megakaryocytic phenotype. Cell Growth Differ 7:1525–1534
69. Hart A et al (2000) Fli-1 is required for murine vascular and megakaryocytic development and is hemizygously deleted in patients with thrombocytopenia. Immunity 13:167–177
70. Smith R et al (2006) Expression profiling of EWS/FLI identifies NKX2.2 as a critical target gene in Ewing's sarcoma. Cancer Cell 9:405–416. doi:10.1016/j.ccr.2006.04.004
71. Zucman J et al (1992) Cloning and characterization of the Ewing's sarcoma and peripheral neuroepithelioma t(11;22) translocation breakpoints. Gene Chromosome Cancer 5:271–277
72. Zucman J et al (1993) Combinatorial generation of variable fusion proteins in the Ewing family of tumours. EMBO J 12:4481–4487
73. Zucman-Rossi J, Legoix P, Victor JM, Lopez B, Thomas G (1998) Chromosome translocation based on illegitimate recombination in human tumors. Proc Natl Acad Sci U S A 95:11786–11791
74. Lin PP et al (1999) Differential transactivation by alternative EWS-FLI1 fusion proteins correlates with clinical heterogeneity in Ewing's sarcoma. Cancer Res 59:1428–1432
75. de Alava E et al (1998) EWS-FLI1 fusion transcript structure is an independent determinant of prognosis in Ewing's sarcoma. J Clin Oncol 16:1248–1255
76. Zoubek A et al (1996) Does expression of different EWS chimeric transcripts define clinically distinct risk groups of Ewing tumor patients? J Clin Oncol 14:1245–1251
77. Le Deley MC et al (2010) Impact of EWS-ETS fusion type on disease progression in Ewing's sarcoma/peripheral primitive neuroectodermal tumor: prospective results from the cooperative Euro-E.W.I.N.G. 99 trial. J Clin Oncol Off J Am Soc Clin Oncol 28:1982–1988. doi:10.1200/JCO.2009.23.3585
78. van Doorninck JA et al (2010) Current treatment protocols have eliminated the prognostic advantage of type 1 fusions in Ewing sarcoma: a report from the Children's Oncology Group. J Clin Oncol Off J Am Soc Clin Oncol 28:1989–1994. doi:10.1200/JCO.2009.24.5845
79. Lessnick SL, Braun BS, Denny CT, May WA (1995) Multiple domains mediate transformation by the Ewing's sarcoma EWS/FLI- 1 fusion gene. Oncogene 10:423–431
80. May WA et al (1993) Ewing sarcoma 11;22 translocation produces a chimeric transcription factor that requires the DNA-binding domain encoded by FLI1 for transformation. Proc Natl Acad Sci U S A 90:5752–5756
81. Hancock JD, Lessnick SL (2008) A transcriptional profiling meta-analysis reveals a core EWS-FLI gene expression signature. Cell Cycle 7:250–256

82. Teitell MA et al (1999) EWS/ETS fusion genes induce epithelial and neuroectodermal differentiation in NIH 3T3 fibroblasts. Lab Invest 79:1535–1543
83. Thompson AD, Teitell MA, Arvand A, Denny CT (1999) Divergent Ewing's sarcoma EWS/ETS fusions confer a common tumorigenic phenotype on NIH3T3 cells. Oncogene 18:5506–5513. doi:10.1038/sj.onc.1202928
84. Chan D et al (2003) Transformation induced by Ewing's sarcoma associated EWS/FLI-1 is suppressed by KRAB/FLI-1. Br J Cancer 88:137–145
85. Chansky HA et al (2004) Targeting of EWS/FLI-1 by RNA interference attenuates the tumor phenotype of Ewing's sarcoma cells in vitro. J Orthop Res 22:910–917
86. Kovar H et al (1996) EWS/FLI-1 antagonists induce growth inhibition of Ewing tumor cells in vitro. Cell Growth Differ 7:429–437
87. Matsumoto Y et al (2001) Downregulation and forced expression of EWS-Fli1 fusion gene results in changes in the expression of G(1)regulatory genes. Br J Cancer 84:768–775
88. Ouchida M, Ohno T, Fujimura Y, Rao VN, Reddy ES (1995) Loss of tumorigenicity of Ewing's sarcoma cells expressing antisense RNA to EWS-fusion transcripts. Oncogene 11:1049–1054
89. Prieur A, Tirode F, Cohen P, Delattre O (2004) EWS/FLI-1 silencing and gene profiling of Ewing cells reveal downstream oncogenic pathways and a crucial role for repression of insulin-like growth factor binding protein 3. Mol Cell Biol 24:7275–7283
90. Tanaka K, Iwakuma T, Harimaya K, Sato H, Iwamoto Y (1997) EWS-Fli1 antisense oligodeoxynucleotide inhibits proliferation of human Ewing's sarcoma and primitive neuroectodermal tumor cells. J Clin Invest 99:239–247
91. Toretsky JA, Connell Y, Neckers L, Bhat NK (1997) Inhibition of EWS-FLI-1 fusion protein with antisense oligodeoxynucleotides. J Neuro Oncol 31:9–16
92. Kinsey M, Smith R, Lessnick SL (2006) NR0B1 is required for the oncogenic phenotype mediated by EWS/FLI in Ewing's sarcoma. Mol Cancer Res 4:851–859
93. Kauer M et al (2009) A molecular function map of Ewing's sarcoma. PLoS One 4:e5415
94. Kinsey M, Smith R, Iyer AK, McCabe ER, Lessnick SL (2009) EWS/FLI and its downstream target NR0B1 interact directly to modulate transcription and oncogenesis in Ewing's sarcoma. Cancer Res 69:9047–9055. doi:10.1158/0008-5472.CAN-09-1540
95. Baer C et al (2004) Profiling and functional annotation of mRNA gene expression in pediatric rhabdomyosarcoma and Ewing's sarcoma. Int J Cancer 110:687–694
96. Beauchamp E et al (2009) GLI1 is a direct transcriptional target of EWS-FLI1 oncoprotein. J Biol Chem 284:9074–9082
97. Zwerner JP et al (2008) The EWS/FLI1 oncogenic transcription factor deregulates GLI1. Oncogene 27:3282–3291. doi:10.1038/sj.onc.1210991, 1210991 [pii]
98. Jaishankar S, Zhang J, Roussel MF, Baker SJ (1999) Transforming activity of EWS/FLI is not strictly dependent upon DNA-binding activity. Oncogene 18:5592–5597
99. Welford SM, Hebert SP, Deneen B, Arvand A, Denny CT (2001) DNA binding domain-independent pathways are involved in EWS/FLI1-mediated oncogenesis. J Biol Chem 276:41977–41984
100. Gangwal K et al (2008) Microsatellites as EWS/FLI response elements in Ewing's sarcoma. Proc Natl Acad Sci U S A 105:10149–10154. doi:10.1073/pnas.0801073105
101. Mao X, Miesfeldt S, Yang H, Leiden JM, Thompson CB (1994) The FLI-1 and chimeric EWS-FLI-1 oncoproteins display similar DNA binding specificities. J Biol Chem 269:18216–18222
102. Gangwal K, Lessnick SL (2008) Microsatellites are EWS/FLI response elements: genomic "junk" is EWS/FLI's treasure. Cell Cycle 7:3127–3132
103. Guillon N et al (2009) The oncogenic EWS-FLI1 protein binds in vivo GGAA microsatellite sequences with potential transcriptional activation function. PLoS One 4:e4932
104. Sankar S et al (2013) Mechanism and relevance of EWS/FLI-mediated transcriptional repression in Ewing sarcoma. Oncogene 32(42):5089–5100

105. Sorna V et al (2013) High-throughput virtual screening identifies novel N′-(1-phenylethylidene)-benzohydrazides as potent, specific, and reversible LSD1 inhibitors. J Med Chem 56:9496–9508. doi:10.1021/jm400870h
106. Prasad DD, Rao VN, Lee L, Reddy ES (1994) Differentially spliced erg-3 product functions as a transcriptional activator. Oncogene 9:669–673
107. Ginsberg JP et al (1999) EWS-FLI1 and EWS-ERG gene fusions are associated with similar clinical phenotypes in Ewing's sarcoma. J Clin Oncol 17:1809–1814
108. Braunreiter CL, Hancock JD, Coffin CM, Boucher KM, Lessnick SL (2006) Expression of EWS-ETS fusions in NIH3T3 cells reveals significant differences to Ewing's sarcoma. Cell Cycle 5:2753–2759
109. Wang L et al (2007) Undifferentiated small round cell sarcomas with rare EWS gene fusions: identification of a novel EWS-SP3 fusion and of additional cases with the EWS-ETV1 and EWS-FEV fusions. J Mol Diagn 9:498–509
110. Ng TL et al (2007) Ewing sarcoma with novel translocation t(2;16) producing an in-frame fusion of FUS and FEV. J Mol Diagn 9:459–463
111. Shing DC et al (2003) FUS/ERG gene fusions in Ewing's tumors. Cancer Res 63:4568–4576
112. Chansky HA, Hu M, Hickstein DD, Yang L (2001) Oncogenic TLS/ERG and EWS/Fli-1 fusion proteins inhibit RNA splicing mediated by YB-1 protein. Cancer Res 61:3586–3590
113. Cironi L et al (2008) IGF1 is a common target gene of Ewing's sarcoma fusion proteins in mesenchymal progenitor cells. PLoS One 3:e2634
114. Rhodes M et al (1998) A high-resolution microsatellite map of the mouse genome. Genome Res 8:531–542
115. Kovar H et al (1990) Overexpression of the pseudoautosomal gene MIC2 in Ewing's sarcoma and peripheral primitive neuroectodermal tumor. Oncogene 5:1067–1070
116. Szuhai K et al (2009) The NFATc2 gene is involved in a novel cloned translocation in a Ewing sarcoma variant that couples its function in immunology to oncology. Clin Cancer Res 15:2259–2268
117. Chen L, Glover JN, Hogan PG, Rao A, Harrison SC (1998) Structure of the DNA-binding domains from NFAT. Fos and Jun bound specifically to DNA. Nature 392:42–48. doi:10.1038/32100
118. Macian F (2005) NFAT proteins: key regulators of T-cell development and function. Nat Rev Immunol 5:472–484. doi:10.1038/nri1632
119. Macian F, Lopez-Rodriguez C, Rao A (2001) Partners in transcription: NFAT and AP-1. Oncogene 20:2476–2489. doi:10.1038/sj.onc.1204386
120. Rao A, Luo C, Hogan PG (1997) Transcription factors of the NFAT family: regulation and function. Annu Rev Immunol 15:707–747. doi:10.1146/annurev.immunol.15.1.707
121. Kim S, Denny CT, Wisdom R (2006) Cooperative DNA binding with AP-1 proteins is required for transformation by EWS-ETS fusion proteins. Mol Cell Biol 26:2467–2478
122. Thomas RS et al (1997) ETS1, NFkappaB and AP1 synergistically transactivate the human GM-CSF promoter. Oncogene 14:2845–2855. doi:10.1038/sj.onc.1201125
123. Verger A et al (2001) Identification of amino acid residues in the ETS transcription factor Erg that mediate Erg-Jun/Fos-DNA ternary complex formation. J Biol Chem 276:17181–17189
124. Yamaguchi S et al (2005) EWSR1 is fused to POU5F1 in a bone tumor with translocation t(6;22)(p21;q12). Gene Chromosome Cancer 43:217–222
125. Nichols J et al (1998) Formation of pluripotent stem cells in the mammalian embryo depends on the POU transcription factor Oct4. Cell 95:379–391
126. Okamoto K et al (1990) A novel octamer binding transcription factor is differentially expressed in mouse embryonic cells. Cell 60:461–472
127. Rosner MH et al (1990) A POU-domain transcription factor in early stem cells and germ cells of the mammalian embryo. Nature 345:686–692. doi:10.1038/345686a0
128. Mastrangelo T et al (2000) A novel zinc finger gene is fused to EWS in small round cell tumor. Oncogene 19:3799–3804

129. Bossone SA, Asselin C, Patel AJ, Marcu KB (1992) MAZ, a zinc finger protein, binds to c-MYC and C2 gene sequences regulating transcriptional initiation and termination. Proc Natl Acad Sci U S A 89:7452–7456
130. Bochar DA et al (2000) A family of chromatin remodeling factors related to Williams syndrome transcription factor. Proc Natl Acad Sci U S A 97:1038–1043
131. Bozhenok L, Wade PA, Varga-Weisz P (2002) WSTF-ISWI chromatin remodeling complex targets heterochromatic replication foci. EMBO J 21:2231–2241. doi:10.1093/emboj/21.9.2231
132. LeRoy G, Loyola A, Lane WS, Reinberg D (2000) Purification and characterization of a human factor that assembles and remodels chromatin. J Biol Chem 275:14787–14790. doi:10.1074/jbc.C000093200
133. Percipalle P, Farrants AK (2006) Chromatin remodelling and transcription: be-WICHed by nuclear myosin 1. Curr Opin Cell Biol 18:267–274. doi:10.1016/j.ceb.2006.03.001
134. Strohner R et al (2001) NoRC – a novel member of mammalian ISWI-containing chromatin remodeling machines. EMBO J 20:4892–4900. doi:10.1093/emboj/20.17.4892
135. Sumegi J et al (2011) A novel t(4;22)(q31;q12) produces an EWSR1-SMARCA5 fusion in extraskeletal Ewing sarcoma/primitive neuroectodermal tumor. Mod Pathol Off J U S Can Acad Pathol 24:333–342. doi:10.1038/modpathol.2010.201
136. Machado I et al (2013) Superficial EWSR1-negative undifferentiated small round cell sarcoma with CIC/DUX4 gene fusion: a new variant of Ewing-like tumors with locoregional lymph node metastasis. Virchows Arch Int J Pathol 463:837–842. doi:10.1007/s00428-013-1499-9
137. Pierron G et al (2012) A new subtype of bone sarcoma defined by BCOR-CCNB3 gene fusion. Nat Genet 44:461–466. doi:10.1038/ng.1107
138. de Alava E, Lessnick SL, Sorensen PH (2013) In: Fletcher CDM, Bridge JA, Hogendoorn PCW, Mertens F (eds) WHO classification of tumours of soft tissue and bone. International Agency for Research on Cancer (IARC), Lyons, France, pp 305–309, Ch. 19
139. Carpentieri DF et al (2005) Protocol for the examination of specimens from pediatric and adult patients with osseous and extraosseous ewing sarcoma family of tumors, including peripheral primitive neuroectodermal tumor and ewing sarcoma. Arch Pathol Lab Med 129:866–873
140. Folpe AL et al (2005) Morphologic and immunophenotypic diversity in Ewing family tumors: a study of 66 genetically confirmed cases. Am J Surg Pathol 29:1025–1033
141. Bennani-Baiti IM, Machado I, Llombart-Bosch A, Kovar H (2012) Lysine-specific demethylase 1 (LSD1/KDM1A/AOF2/BHC110) is expressed and is an epigenetic drug target in chondrosarcoma, Ewing's sarcoma, osteosarcoma, and rhabdomyosarcoma. Hum Pathol 43:1300–1307. doi:10.1016/j.humpath.2011.10.010

CHAPTER 3

DETERMINING GENOME-WIDE LOCALIZATION OF EWS/FLI AND CTCF IN EWING SARCOMA CELLS

3.1 Abstract

The EWS/FLI fusion protein is the main oncogenic driver of Ewing sarcoma. Containing the transcriptional regulatory domain of *EWSR1* fused to the DNA-biding domain of *FLI1*, it functions as an aberrant transcription factor that alters the expression of several thousand genes. The result is an oncogenic phenotype that arises primarily in adolescents. Transcription profiling of Ewing sarcoma cells has been well characterized, and numerous targets have been identified as necessary, but not sufficient, for Ewing sarcoma tumorigenesis. Binding of EWS/FLI is associated with activation of some genes, and repression of others. However, the mechanisms utilized by EWS/FLI to induce such widespread transcriptional misregulation are not completely understood. It is hypothesized that EWS/FLI function is partly determined by its localization and ability to co-opt or disrupt regulatory factors normally involved in transcriptional regulation of distinct loci. This chapter presents preliminary data aimed at addressing such questions by assessing localization of EWS/FLI and its partners genome wide. We performed ChIP-seq analysis for EWS/FLI and CTCF in preparation for further investigation

of localization changes that result from deleting portions of the EWS/FLI fusion protein. These studies are being continued by the Lessnick Lab at Nationwide Children's Hospital in Columbus, Ohio.

3.2 Introduction

Ewing sarcoma is the second most common bone-associated tumor in children and adolescents, arising most frequently in the bones of the pelvis and femur (1). It is a relatively rare tumor, accounting for approximately 300 new diagnoses each year in the United States (2). Currently, therapeutic protocols rely mainly on surgical resection and adjuvant chemotherapy. And these approaches are remarkably efficacious, achieving 5-year survival rates approaching 90% (1,3–5). Nevertheless, patients who encounter metastasis or relapse of their disease have a poorer prognosis, with 5-year survival rates approaching 15% (1,6). Accordingly, there is a substantial need for novel therapeutic strategies targeting this cancer on the cellular and molecular level.

The primary molecular lesion responsible for tumorigenesis in Ewing sarcoma is a chromosomal translocation event between chromosomes 11 and 22, resulting in fusion of the *EWSR1* and *FLI1* genes (7–10). The in-frame fusion of these genes produces an aberrant protein known as EWS/FLI (EF). This protein contains the C-terminal transcriptional regulatory domain of EWSR1 joined to the DNA-binding domain of FLI1. Thus, EF is an aberrant transcription factor capable of altering gene expression across the genome. Indeed, the transcriptional misregulation driven by EF has been well characterized via both microarray and RNA-seq experiments (11–18).

Genome-wide localization of EF is an active area of study. Chromatin immunoprecipitation (ChIP) studies have been employed with microarrays (ChIP-on-ChIP) and high-throughput DNA sequencing (ChIP-Seq) to reveal that EF binds at canonical FLI1 binding sites, as well as sites for other ETS-family transcription factors (19–22). Interestingly, these studies have also shown that EF has a propensity to bind at regions of GGAA repeats, including near promoters of genes whose expression is altered by EF.

EF has also been shown to interact with regulatory complexes such as the nucleosome remodeling and deacetylase (NuRD) complex in order to repress expression of certain EF target genes (23). Additional epigenetic regulatory enzymes have also been shown to play important roles in Ewing sarcoma biology (24,25). Such evidence has led to the hypothesis that EF utilizes or hijacks a relatively small number of regulatory processes to alter chromatin state and subsequent gene transcription. Rather than employing a unique mechanism for each gene it alters, it is more likely that EF alters numerous genes via one or two mechanisms (or variations on one or two mechanistic themes). To this end, current work aims to better determine genome-wide localization of EF and its partners, with particular interest in assessing the mechanisms regulating EF localization. Specifically, we sought to determine whether deletion of certain functional portions of the EF protein would alter its ability to bind at promoters of target genes, and/or affect its interactions with regulatory partners.

The work presented in this chapter represents a portion of the initial efforts to ask these questions by means of ChIP-seq analysis. Here we show results of

our preliminary ChIP-seq analyses for EF, as well as for the chromatin binding factor CTCF. The remainder of this investigation is being continued by the Lessnick Lab at Nationwide Children's Hospital in Columbus, Ohio.

3.3 Results

3.3.1 ChIP-Seq of EF reveals numerous EF-bound loci across the genome

We performed ChIP experiments for EF in A673 cells, followed by high-throughput DNA sequencing. EF-bound loci were identified throughout the genome (Figure 3.1A). A total of 22,406 EF-bound sites were identified using a threshold Log2(ratio) of ≥ 0.585 and an AdjP value of ≥ 10. While many binding sites were located in intergenic regions, there was a prominent clustering of EF-bound loci within 1 kb of transcription start sites (Figure 3.1B). Indeed, the read count frequency was highest near the TSS (Figure 3.1C). This is consistent with the known role that EF has in transcriptional misregulation in Ewing sarcoma, and suggests that EF may alter transcription of numerous genes by binding near or within their promoter regions.

3.3.2 EF binds both high-affinity ETS sites and GGAA microsatellite repeats

The ETS (E26 transformation specific) family of transcription factors all contain a winged helix-turn-helix domain (known as the ETS domain) that binds with high affinity to DNA motifs containing a core sequence of GGAA or GGAT. The consensus sequence for ETS transcription factors, while somewhat variable,

is ACCGGAAGTG (26–28).

Consistent with previous work (19,20,29), we found that EF was present at binding sites for ETS-family transcription factors (Figure 3.2). Additionally, EF binding was detected at GGAA microsatellite repeats, including loci upstream of genes known to be altered by EF (Figure 3.3). Interestingly, EF-bound microsatellites could be found near both upregulated and downregulated targets of EF, suggesting distinct mechanisms of transcriptional activation versus transcriptional repression, beyond the mere presence of EF.

3.3.3 Increased gene expression is more common when EF binds nearby GGAA microsatellite repeats

ChIP-seq data were compared to transcriptional profiling data previously generated by RNA-seq. This RNA-seq dataset was also generated from experiments using A673 cells. EF-regulated genes were identified by knocking down EF via shRNA (shEF) and comparing expression of genes in shEF cells to a control shRNA targeting luciferase (shLuc). Differentially expressed genes in shEF versus shLuc cells were considered to be EF target genes.

In the RNA-seq data, 7,081 genes were found to be differentially expressed upon knockdown of EF. We found that only 1,457 of those differentially expressed genes contained EF-bound loci within 5 kb. These data suggest that only 20.6% (1,457 out of 7,081) of genes regulated by EF are likely direct targets of EF (Figure 3.4A). Thus, the majority of EF-driven transcriptional misregulation is likely due to downstream consequences of altering expression of direct targets of EF. For

instance, when EF increases expression of NR0B1 by binding directly to a GGAA microsatellite in the *NR0B1* promoter, increased levels of the NR0B1 transcription factor then transmit the effects of EF to an array of NR0B1 targets, which could themselves exert downstream effects on transcription of other genes (14).

These putative direct targets of EF are comprised of 696 (47.8%) EF-downregulated and 761 (52.2%) EF-upregulated genes (Figure 3.4B). These data further suggest that the mechanisms determining whether EF causes activation or repression of its targets likely depends upon other regulatory partners that interact with EF, such as the NuRD complex.

Interestingly, when we focused on the top 25 most upregulated and the 25 most downregulated EF target genes (based on the fold change values determined via RNA-seq analyses) we observed a correlation between the presence of nearby GGAA repeats and EF-upregulated genes (Figure 3.4C). Not one of the top 25 EF-downregulated targets had a nearby GGAA microsatellite (Figure 3.4D). These data further suggest that the mechanisms responsible for EF-mediated upregulation are distinct from the mechanisms responsible for EF-driven downregulation.

3.3.4 CTCF binding sites overlap with EF binding sites in a minority of instances

ChIP-seq was also performed for the chromatin binding protein CTCF. A total of 25,027 CTCF-bound loci were identified throughout the genome (Figure 3.5A). While CTCF sites could be found near the TSS of genes, the pattern was less tightly correlated to TSS (Figure 3.5B). Additionally, a sizeable proportion of

CTCF binding sites were identified in promoter regions (Figure 3.5C). However, consistent with the known insulator and other regulatory roles of CTCF, the correlation of peaks to TSS sites was less prominent compared to EF sites, and the majority of CTCF-bound loci were found in intergenic regions (Figure 3.5C).

When the genomic coordinates of EF-bound loci were compared against the genomic coordinates of CTCF-bound loci, we found that only a small proportion of binding sites overlapped between the two datasets (Figure 3.5D). This suggests that EF may, in a minority of cases, co-localize with CTCF and could potentially alter its insulator functions. Additional study is needed to determine the nature, abundance, and function of such interactions.

3.4 Discussion

The means by which EF transforms a healthy cell into a cancer cell has been – and continues to be – a subject of intense investigation. Early breakthroughs identified the presence of EF and its role as a neomorphic transcription factor with oncogenic consequences. Experiments revealed that EF could bind DNA and activate genes, and tumorigenesis was found to depend on the ability of EF to bind DNA and alter gene expression. Continuing research has led to more detailed understanding of these mechanisms, and it has become even more clear that these processes are complex and nuanced.

Here we began an exploration of the localization of EF across the genome. Consistent with earlier studies using microarray and other technologies, we demonstrated that EF binds to both high-affinity ETS consensus sequences (ACCGGAAGTG), as well as GGAA microsatellite repeats (Figures 3.2 & 3.3).

Importantly, we show that while EF-bound GGAA repeats appear to correlate more with activated targets of EF, some EF-repressed genes are also in close proximity to GGAA microsatellites. These data indicate that DNA binding alone is not sufficient to explain whether EF upregulates or downregulates target genes.

Indeed, these data suggest that local context at individual gene loci may play a role in determining the function of EF on that locus. Such an interplay between EF and individual loci would presumably depend upon what other regulatory factors and complexes potentially are involved in existing regulatory systems for a given gene. Work demonstrating the importance of complexes like NuRD, and epigenetic regulators such as LSD1, are consistent with this model (23,24). Continuation of these studies will foster development of a more detailed understanding of how EF transforms a healthy cell into a cancer cell, and promises to inform future therapeutic strategies directed at the cellular and molecular level.

3.5 Materials and Methods

3.5.1 Chromatin immunoprecipitation

Magnetic beads conjugated to anti-rabbit IgG (Dynabeads, ThermoFisher #11204D) were coated with either anti-FLI (Santa Cruz #sc-356), anti-CTCF (Santa Cruz, #sc-5916), or normal rabbit IgG (Santa Cruz, #sc-2027; negative control) antibodies. Specifically, 100 µL of beads were added to 2 mL of dilution buffer [20 mM Tris, pH 7.9, 2 mM EDTA, 150 mM NaCl, 1% Triton X-100, 20 mg/ml BSA plus protease inhibitor cocktail (Roche EDTA-free complete, Sigma #11836170001)] and 5 µg of antibody was added. All ChIP procedures were performed using DNA Lo Bind tubes (Eppendorf #022431021). Antibody-bead

mixtures were rotated overnight at 4° C.

A673 cells were grown in 15-cm tissue culture plates until approximately 90% confluency. Cross-linking was then performed by adding 1 mL of 16% (w/v) methanol-free formaldehyde solution (ThermoFisher #28906) directly to 15 mL of culture medium on cells (final concentration: 1%) and gently rocking for 15 minutes at room temperature. Cross-linking reactions were then quenched by adding 1 mL of 2 M glycine (final concentration: 125 mM) and rocking gently for 5 minutes at room temperature. Culture medium was then discarded and cells were washed with 20 mL ice-cold PBS. PBS was removed and 5 mL of ice-cold cell lysis buffer (50 mM HEPES-KOH, pH 8, 1 mM EDTA, 0.5 mM EGTA, 140 mM NaCl, 10% glycerol, 0.5% NP-40, 0.25% Triton X-100) was added, and cells were dissociated from the plate by a cell scraper. Cells and lysis buffer were collected and cells were rotated end over end for 10 minutes at 4° C, and then pelleted via centrifugation at 300 rcf and 4° C. The cell pellet was then resuspended in 10 mL ice-cold wash buffer (10 mM Tris, pH 7.9, 1 mM EDTA, 0.5 mM EGTA, 200 mM NaCl) and pelleted again via centrifugation at 300 rcf and 4° C. Cell pellets were then resuspended in 500 µL ice-cold nuclei lysis buffer (50 mM Tris, pH 7.9, 10 mM EDTA, 1% SDS, 1X protease inhibitor cocktail) and subjected to sonication using a probe sonicator. Cells were kept in ice during sonication, and sonication times and conditions were empirically determined by assessing DNA fragmentation using 10% agarose/TAE gel electrophoresis. Optimal fragment size was between 100 and 400 bp (Figure 3.6A). Following sonication, cell lysates were cleared by centrifugation at 20,000 rcf and 4° C for 15 minutes. The resulting

cell extract was added to magnetic beads (pre-coated with antibody or normal IgG; 250 µL of extract per ChIP reaction; one batch of extract is sufficient for approximately 4 ChIP reactions) and rotated overnight at 4° C. The following day, beads were pelleted with a magnet, and four washes were performed by 5 minute rotations at 4° C. IP washes were performed with increasing stringency; Wash #1: 20 mM Tris, pH 7.9, 2 mM EDTA, 250 mM NaCl, 0.05% SDS, 0.25% NP-40; Wash #2: 20 mM Tris, pH 7.9, 2 mM EDTA, 500 mM NaCl, 0.05% SDS, 0.25% NP-40; Washes #3 & 4: 20 mM Tris, pH 7.9, 2 mM EDTA, 500 mM LiCl, 0.05% SDS, 0.25% NP-40. Beads were finally rinsed in TE buffer (10 mM Tris, pH 8, 1 mM EDTA) and beads were resuspended in sodium bicarbonate solution (final concentration: 1 mM) and treated with 2 µL of 10 mg/ml RNAse A for 20 minutes at 37° C. Elution and cross-link reversal was performed by adding 10 µL of 20% SDS and incubating at 65° C overnight. Eluted DNA was then collected via ethanol precipitation by adding 20 µL of 3M sodium acetate, 15 µL glycogen (20 mg/ml) and 500 µL of ethanol (200 proof), and incubating overnight at -20° C. Precipitates were collected by centrifugation at 20,000 rcf for 20 minutes at 4° C, and rinsed twice with ice-cold 70% ethanol/water followed by centrifugation. Pellets were air dried, and dissolved in 20 µL nuclease-free water. Successful ChIP assays were verified by qPCR of known EF-bound loci near *GSTM4* and *NR0B1* (Figure 3.6B). Fold enrichment was determined by comparing to the normal IgG negative control ChIP at target genes and gene desert negative control loci.

3.5.2 Library construction and sequencing

Libraries were constructed using the NEBNext library prep kit for Illumina sequencing (New England BioLabs #E7645) and AMPure XP magnetic beads (Beckman Coulter #A63881) according to manufacturer instructions. Unique index primers were selected for each ChIP and input sample to permit multiplexing on sequencing flowcells. DNA concentrations were determined using Qubit dsDNA HS assay kit (ThermoFisher #Q32851) and enrichment of signal at target genes was confirmed by qPCR of library DNA.

High-throughput sequencing was performed at the High Throughput Genomics core facility at the Huntsman Cancer Institute. Briefly, ChIP DNA libraries were sequenced by Illumina HiSeq 50 cycle single read sequencing, version 4. Between 21 x 10^6 and 37 x 10^6 sequence reads were obtained for each sample, multiplexed on a single flowcell.

3.5.3 Alignment to reference genome and sequence analysis

Sequence data were aligned to the February 2009 (GRCh37/hg19) build of the human genome using Novoalign (Novocraft Technologies) (30). Aligned sequence tracks were visualized using Integrated Genome Browser (IGB; BioViz) (31).

Identification of ChIP peak loci was performed using the ChIPSeq wrapper of applications in the USeq software package (32). ChIP peaks were normalized to their corresponding input samples.

Two methods were used to identify genes near peaks: the FNG (Find

Neighboring Genes) application in the USeq package, and the R application ChIPpeakAnno (33,34). Overlaps between EF and CTCF ChIP-seq peaks was determined using the findOverlappingPeaks function in the ChIPpeakAnno package. Venn diagrams were also produced using R.

Other analyses (e.g., proximity of peaks to transcription start sites, genomic region annotations, and comparisons to transcriptional profiling/RNA-seq data) were performed and figures were generated using the ChIPSeeker package in R (35). RNA-seq data were previously published, and are publicly available in the NCBI BioProject database, accession #PRJNA176544, and the Sequence Read Archive, accession #SRA059329 (24,36). ChIP-seq data for EF and CTCF presented herein remain unpublished and are currently not available to the public.

3.6 References

1. Pradhan A, Grimer RJ, Spooner D, Peake D, Carter SR, Tillman RM, et al. Oncological outcomes of patients with Ewing's sarcoma: is there a difference between skeletal and extra-skeletal Ewing's sarcoma? J Bone Joint Surg Br. 2011 Apr;93(4):531–6.

2. Esiashvili N, Goodman M, Marcus RB. Changes in incidence and survival of Ewing sarcoma patients over the past 3 decades: surveillance epidemiology and end results data. J Pediatr Hematol Oncol. 2008 Jun;30(6):425–30.

3. Wang CC, Schulz MD. Ewing's sarcoma; a study of fifty cases treated at the Massachusetts General Hospital, 1930-1952 inclusive. N Engl J Med. 1953 Apr 2;248(14):571–6.

4. Lahl M, Fisher VL, Laschinger K. Ewing's sarcoma family of tumors: an overview from diagnosis to survivorship. Clin J Oncol Nurs. 2008 Feb;12(1):89–97.

5. Dahlin DC, Coventry MB, Scanlon PW. Ewing's sarcoma. A critical analysis of 165 cases. J Bone Joint Surg Am. 1961 Mar;43–A:185–92.

6. Linabery AM, Ross JA. Childhood and adolescent cancer survival in the US

by race and ethnicity for the diagnostic period 1975-1999. Cancer. 2008 Nov 1;113(9):2575–96.

7. Delattre O, Zucman J, Plougastel B, Desmaze C, Melot T, Peter M, et al. Gene fusion with an ETS DNA-binding domain caused by chromosome translocation in human tumours. Nature. 1992 Sep 10;359(6391):162–5.

8. Turc-Carel C, Aurias A, Mugneret F, Lizard S, Sidaner I, Volk C, et al. Chromosomes in Ewing's sarcoma. I. An evaluation of 85 cases of remarkable consistency of t(11;22)(q24;q12). Cancer Genet Cytogenet. 1988 Jun;32(2):229–38.

9. Turc-Carel C, Philip I, Berger MP, Philip T, Lenoir G. [Chromosomal translocation (11; 22) in cell lines of Ewing's sarcoma]. Comptes Rendus Seances Acad Sci Ser III Sci Vie. 1983;296(23):1101–3.

10. Aurias A, Rimbaut C, Buffe D, Dubousset J, Mazabraud A. [Translocation of chromosome 22 in Ewing's sarcoma]. Comptes Rendus Seances Acad Sci Ser III Sci Vie. 1983;296(23):1105–7.

11. Smith R, Owen LA, Trem DJ, Wong JS, Whangbo JS, Golub TR, et al. Expression profiling of EWS/FLI identifies NKX2.2 as a critical target gene in Ewing's sarcoma. Cancer Cell. 2006 May;9(5):405–16.

12. Hancock JD, Lessnick SL. A transcriptional profiling meta-analysis reveals a core EWS-FLI gene expression signature. Cell Cycle Georget Tex. 2008 Jan 15;7(2):250–6.

13. Prieur A, Tirode F, Cohen P, Delattre O. EWS/FLI-1 silencing and gene profiling of Ewing cells reveal downstream oncogenic pathways and a crucial role for repression of insulin-like growth factor binding protein 3. Mol Cell Biol. 2004 Aug;24(16):7275–83.

14. Kinsey M, Smith R, Iyer AK, McCabe ERB, Lessnick SL. EWS/FLI and its downstream target NR0B1 interact directly to modulate transcription and oncogenesis in Ewing's sarcoma. Cancer Res. 2009 Dec 1;69(23):9047–55.

15. Hu-Lieskovan S, Zhang J, Wu L, Shimada H, Schofield DE, Triche TJ. EWS-FLI1 fusion protein up-regulates critical genes in neural crest development and is responsible for the observed phenotype of Ewing's family of tumors. Cancer Res. 2005 Jun 1;65(11):4633–44.

16. Tirode F, Laud-Duval K, Prieur A, Delorme B, Charbord P, Delattre O. Mesenchymal stem cell features of Ewing tumors. Cancer Cell. 2007 May;11(5):421–9.

17. Deneen B, Welford SM, Ho T, Hernandez F, Kurland I, Denny CT. PIM3 proto-oncogene kinase is a common transcriptional target of divergent EWS/ETS oncoproteins. Mol Cell Biol. 2003 Jun;23(11):3897–908.

18. Lessnick SL, Dacwag CS, Golub TR. The Ewing's sarcoma oncoprotein EWS/FLI induces a p53-dependent growth arrest in primary human fibroblasts. Cancer Cell. 2002 May;1(4):393–401.

19. Gangwal K, Sankar S, Hollenhorst PC, Kinsey M, Haroldsen SC, Shah AA, et al. Microsatellites as EWS/FLI response elements in Ewing's sarcoma. Proc Natl Acad Sci. 2008 Jul 22;105(29):10149–54.

20. Gangwal K, Close D, Enriquez CA, Hill CP, Lessnick SL. Emergent properties of EWS/FLI regulation via GGAA microsatellites in Ewing's sarcoma. Genes Cancer. 2010 Feb;1(2):177–87.

21. Riggi N, Knoechel B, Gillespie SM, Rheinbay E, Boulay G, Suvà ML, et al. EWS-FLI1 utilizes divergent chromatin remodeling mechanisms to directly activate or repress enhancer elements in Ewing sarcoma. Cancer Cell. 2014 Nov 10;26(5):668–81.

22. Guillon N, Tirode F, Boeva V, Zynovyev A, Barillot E, Delattre O. The oncogenic EWS-FLI1 protein binds in vivo GGAA microsatellite sequences with potential transcriptional activation function. PLOS ONE. 2009 Mar 23;4(3):e4932.

23. Sankar S, Bell R, Stephens B, Zhuo R, Sharma S, Bearss DJ, et al. Mechanism and relevance of EWS/FLI-mediated transcriptional repression in Ewing sarcoma. Oncogene. 2013 Oct 17;32(42):5089–100.

24. Sankar S, Theisen ER, Bearss J, Mulvihill T, Hoffman LM, Sorna V, et al. Reversible LSD1 inhibition interferes with global EWS/ETS transcriptional activity and impedes Ewing sarcoma tumor growth. Clin Cancer Res. 2014 Sep 1;20(17):4584–97.

25. Theisen ER, Pishas KI, Saund RS, Lessnick SL. Therapeutic opportunities in Ewing sarcoma: EWS-FLI inhibition via LSD1 targeting. Oncotarget. 2016 Feb 2;

26. Sharrocks AD. The ETS-domain transcription factor family. Nat Rev Mol Cell Biol. 2001 Nov;2(11):827–37.

27. Seth A, Watson DK. ETS transcription factors and their emerging roles in human cancer. Eur J Cancer Oxf Engl 1990. 2005 Nov;41(16):2462–78.

28. Cooper CDO, Newman JA, Aitkenhead H, Allerston CK, Gileadi O. Structures

of the Ets protein DNA-binding domains of transcription factors Etv1, Etv4, Etv5, and Fev. J Biol Chem. 2015 May 29;290(22):13692–709.

29. Luo W, Gangwal K, Sankar S, Boucher KM, Thomas D, Lessnick SL. GSTM4 is a microsatellite-containing EWS/FLI target involved in Ewing's sarcoma oncogenesis and therapeutic resistance. Oncogene. 2009 Aug 31;28(46):4126–32.

30. Thankaswamy-Kosalai S, Sen P, Nookaew I. Evaluation and assessment of read-mapping by multiple next-generation sequencing aligners based on genome-wide characteristics. Genomics. 2017 Mar 9;

31. Freese NH, Norris DC, Loraine AE. Integrated genome browser: visual analytics platform for genomics. Bioinforma Oxf Engl. 2016 Jul 15;32(14):2089–95.

32. Nix DA, Courdy SJ, Boucher KM. Empirical methods for controlling false positives and estimating confidence in ChIP-Seq peaks. BMC Bioinformatics. 2008 Dec 5;9:523.

33. Zhu L. Integrative Analysis of ChIP-Chip and ChIP-Seq Dataset. In: Lee T-L, Shui Luk AC, Luk ACS, editors. Tiling Arrays [Internet]. Humana Press; 2013 [cited 2017 May 13]. p. 105–24. (Methods in Molecular Biology).

34. Zhu LJ, Gazin C, Lawson ND, Pagès H, Lin SM, Lapointe DS, et al. ChIPpeakAnno: a Bioconductor package to annotate ChIP-seq and ChIP-chip data. BMC Bioinformatics. 2010;11:237.

35. Yu G, Wang L-G, He Q-Y. ChIPseeker: an R/Bioconductor package for ChIP peak annotation, comparison and visualization. Bioinformatics. 2015 Jul 15;31(14):2382–3.

36. Sankar S, Gomez NC, Bell R, Patel M, Davis IJ, Lessnick SL, et al. EWS and RE1-silencing transcription factor inhibit neuronal phenotype development and oncogenic transformation in Ewing sarcoma. Genes Cancer. 2013 May;4(5–6):213–23.

Figure 3.1 EF ChIP-Seq identifies numerous binding site across the genome. A) EF ChIP-Seq peaks visualized across all chromosomes. A total of 22,406 EF bound loci were identified by peak-calling algorithms (see Materials and Methods). These experiments were performed using A673 cells, which were derived from a female patient, and hence no peaks were mapped to the Y chromosome. **B & C)** EF-bound loci are found predominantly within 1kb of the transcription start sites (TSS) of genes. While EF binding sites can be found great distances from genes (not shown), a great number of EF-bound loci are found in promoter regions, consistent with the ability of EF to alter gene expression.

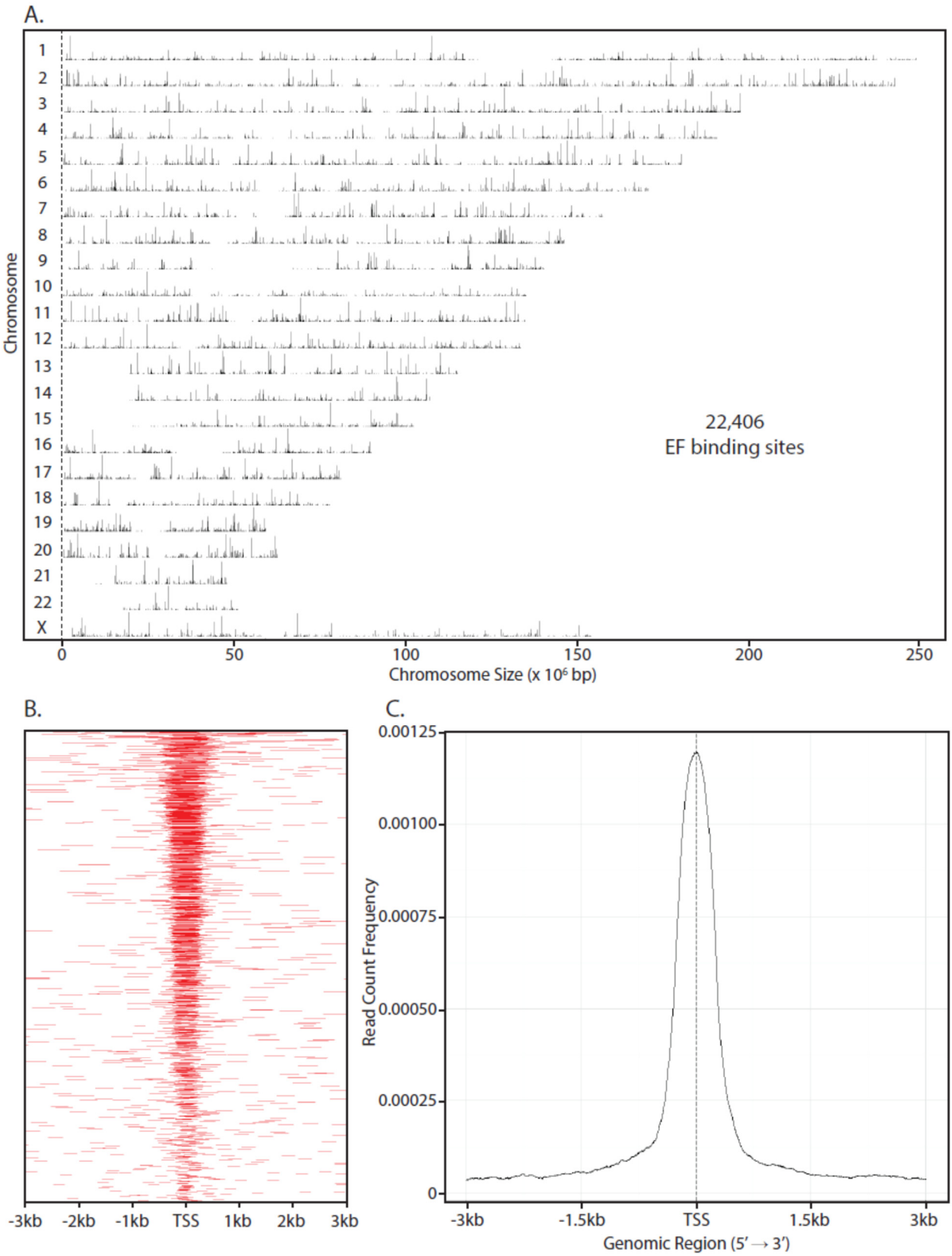
A.
Chromosome
1
2
3
4
5
6
7
8
9
10
11
12
13
14
15
16
17
18
19
20
21
22
X
22,406
EF binding sites
0
50
100
150
200
250
Chromosome Size (x 10⁶ bp)
B.
-3kb
-2kb
-1kb
TSS
1kb
2kb
3kb
C.
0.00125
0.00100
0.00075
0.00050
0.00025
0
Read Count Frequency
-3kb
-1.5kb
TSS
1.5kb
3kb
Genomic Region (5′ → 3′)

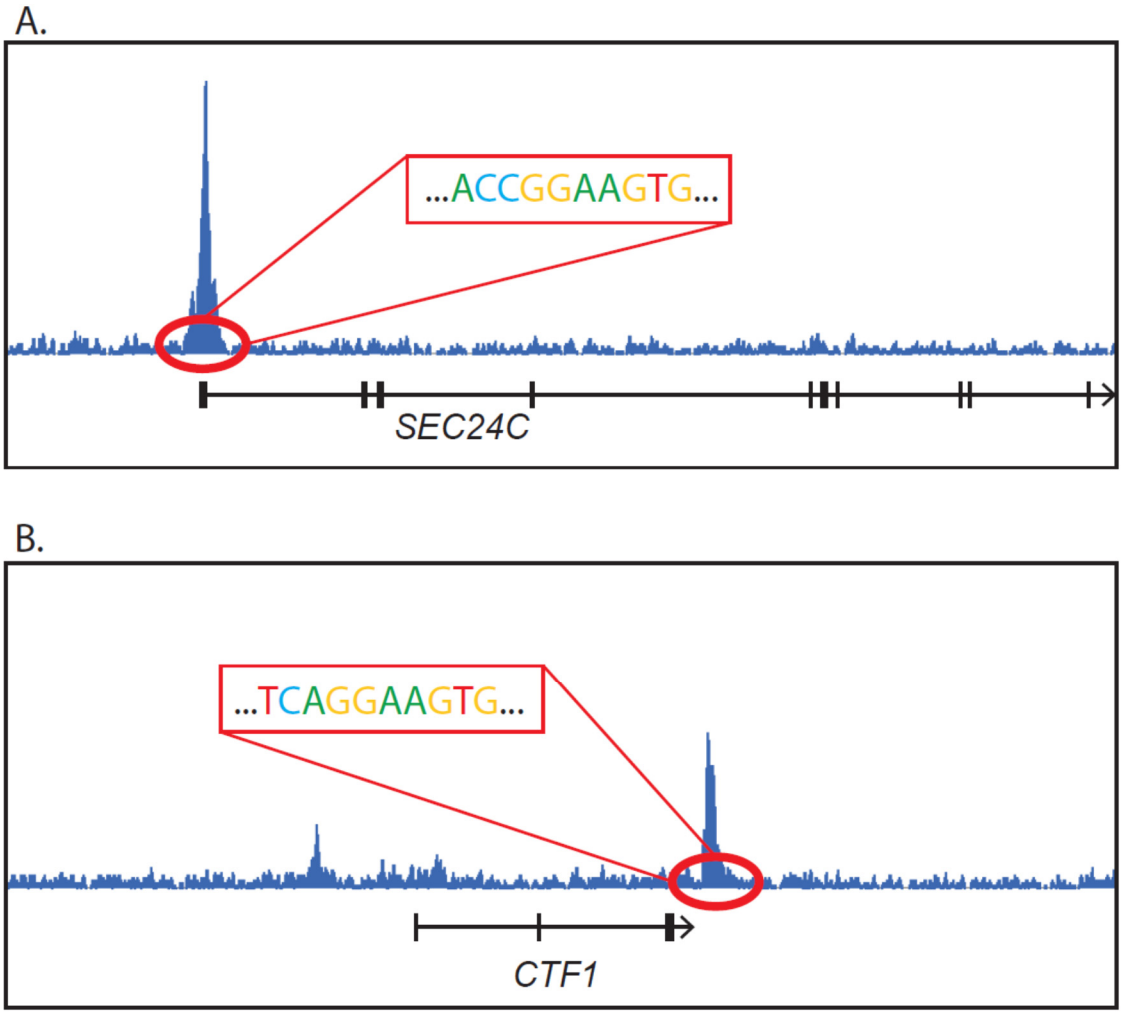

Figure 3.2 EF binds high-affinity ETS-sites. EF ChIP-Seq reveals peaks at high-affinity consensus sequences for ETS-family transcription factors [ACCGGAAGT(G/A)]. Representative tracks are shown: **A)** EF binds at the 5' end of *SEC24C*, and **B)** EF binds at the 3' end of *CTF1*.

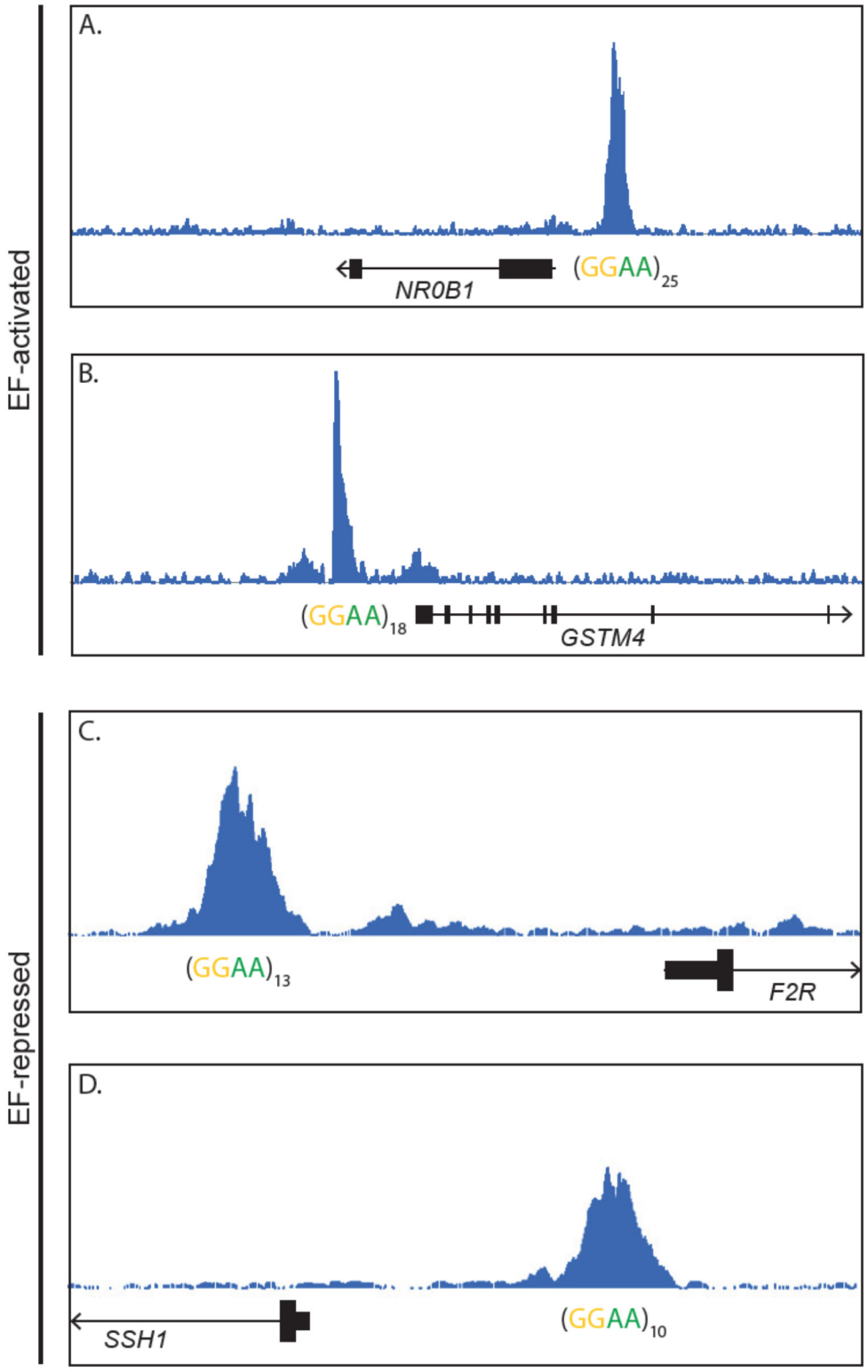

Figure 3.3 EF binds GGAA repeats. A & B) EF-bound GGAA repeats were observed near genes known to be upregulated by EF. **C & D)** EF-bound GGAA repeats were also observed near genes known to be downregulated targets of EF, though further away.

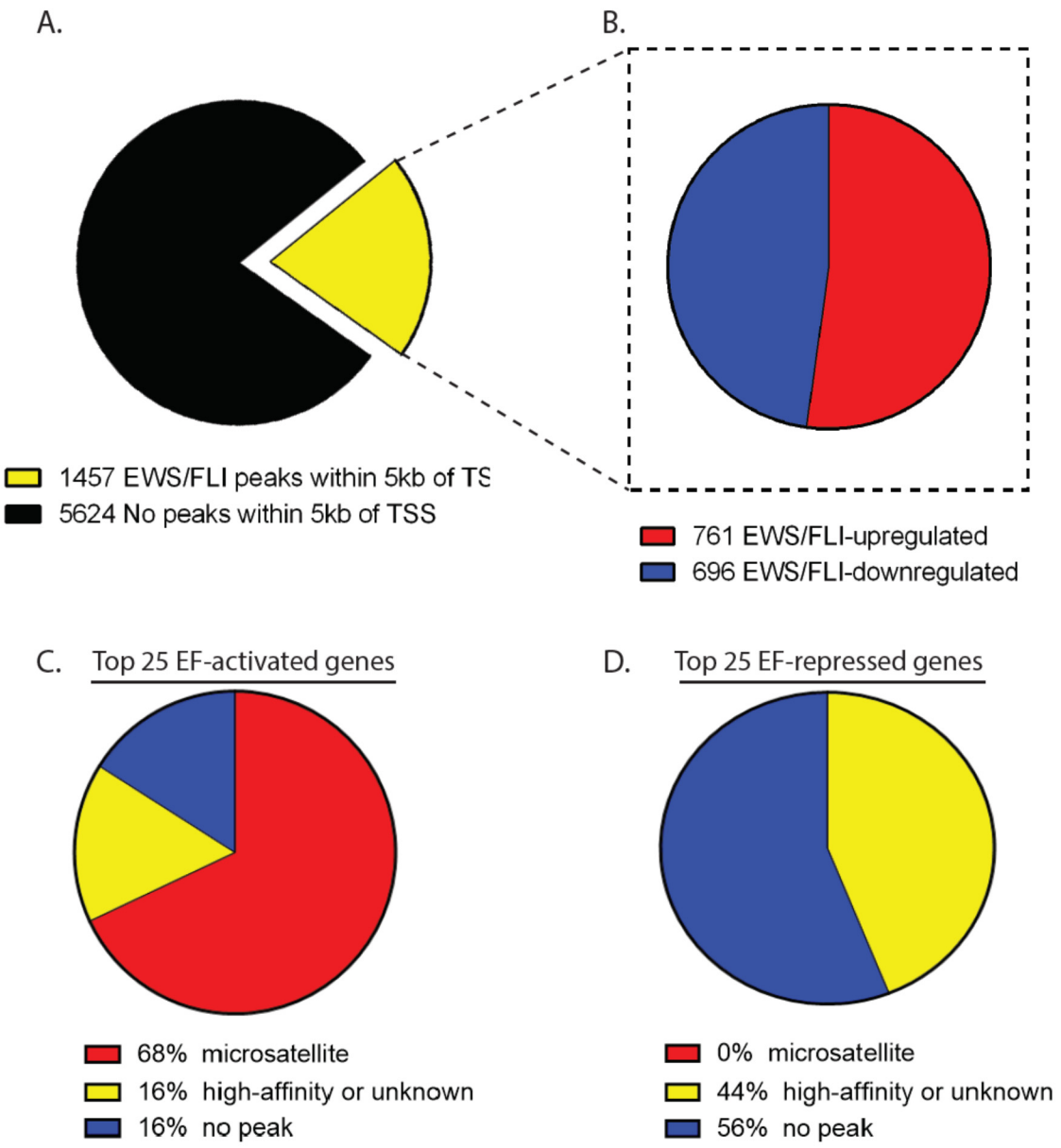

Figure 3.4 EF-binding at GGAA repeats is correlated with upregulation of neighboring genes. A) 1,457 genes were found to be differentially expressed after EF knockdown *and* have EF-bound loci within 5kb. This amounts to 20.6% of all genes identified by RNA-seq as differentially expressed after EF knockdown. **B)** Of these 1,457 genes, 761 (52.2%) are activated by EF, and 696 (47.8%) are repressed by EF. **C & D)** The 25 genes with the greatest magnitude of change after EF knockdown (EF-activated or EF-downregulated) were investigated to determine presence of nearby EF ChIP-seq peaks. Among EF-upregulated genes, 68% had a GGAA microsatellite within 5kb of the TSS, compared to none of the top 25 EF-downregulated genes.

Figure 3.5 CTCF ChIP-Seq reveals few loci where both EF and CTCF can bind. **A)** CTCF ChIP-Seq peaks visualized across all chromosomes. A total of 25,027 CTCF- bound loci were identified by peak-calling algorithms (see Materials and Methods). These experiments were performed using A673 cells, which were derived from a female patient, and hence no peaks were mapped to the Y chromosome. **B)** CTCF-bound loci can be found within 3 kb of the transcription start sites (TSS) of genes. **C)** The majority of CTCF-bound loci were found in distal intergenic regions, although numerous sites are found in other regions, including promoters and introns. **D)** Peaks in the CTCF ChIP-seq data did not overlap significantly with peaks from the EF ChIP-seq data. 2,059 peaks were omitted from the overlap analysis as some enriched regions originally counted as multiple peaks were merged and considered as a single peak to facilitate overlap analysis.

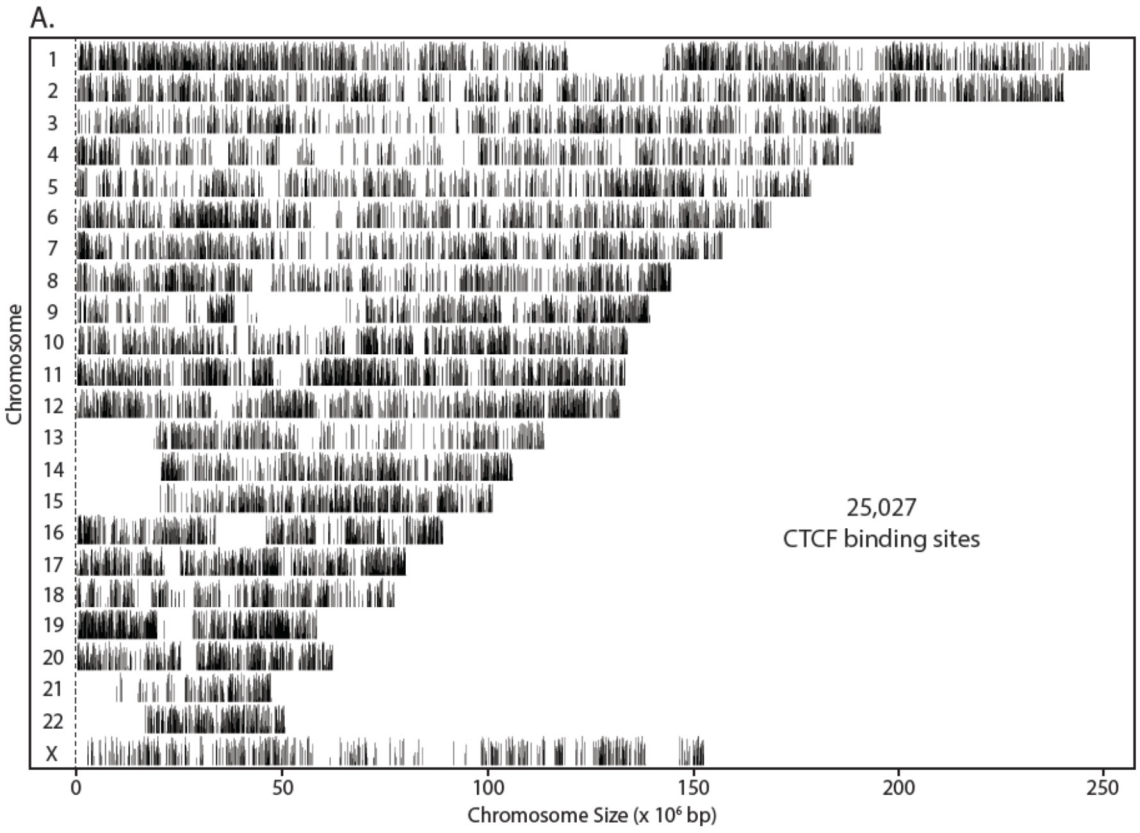
A.
Chromosome
1
2
3
4
5
6
7
8
9
10
11
12
13
14
15
16
17
18
19
20
21
22
X
25,027
CTCF binding sites
0
50
100
150
200
250
Chromosome Size (x 10⁶ bp)

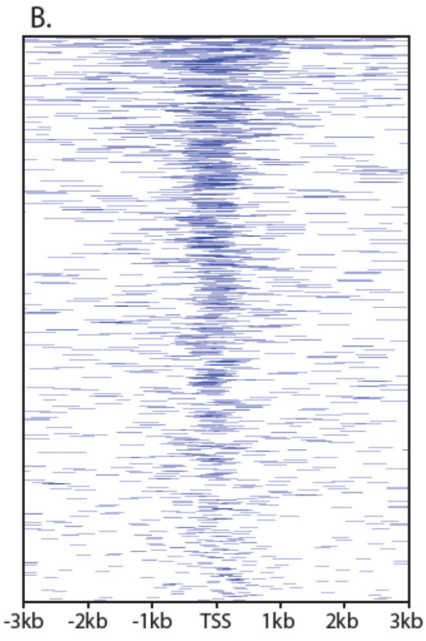
B.
-3kb
-2kb
-1kb
TSS
1kb
2kb
3kb

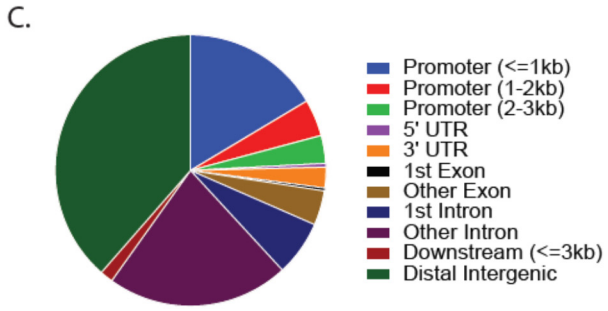
C.
Promoter (<=1kb)
Promoter (1-2kb)
Promoter (2-3kb)
5' UTR
3' UTR
1st Exon
Other Exon
1st Intron
Other Intron
Downstream (<=3kb)
Distal Intergenic

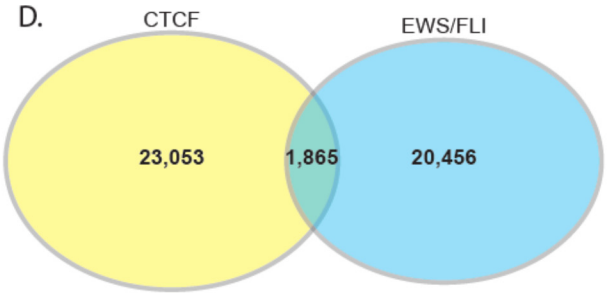
D.
CTCF
EWS/FLI
23,053
1,865
20,456

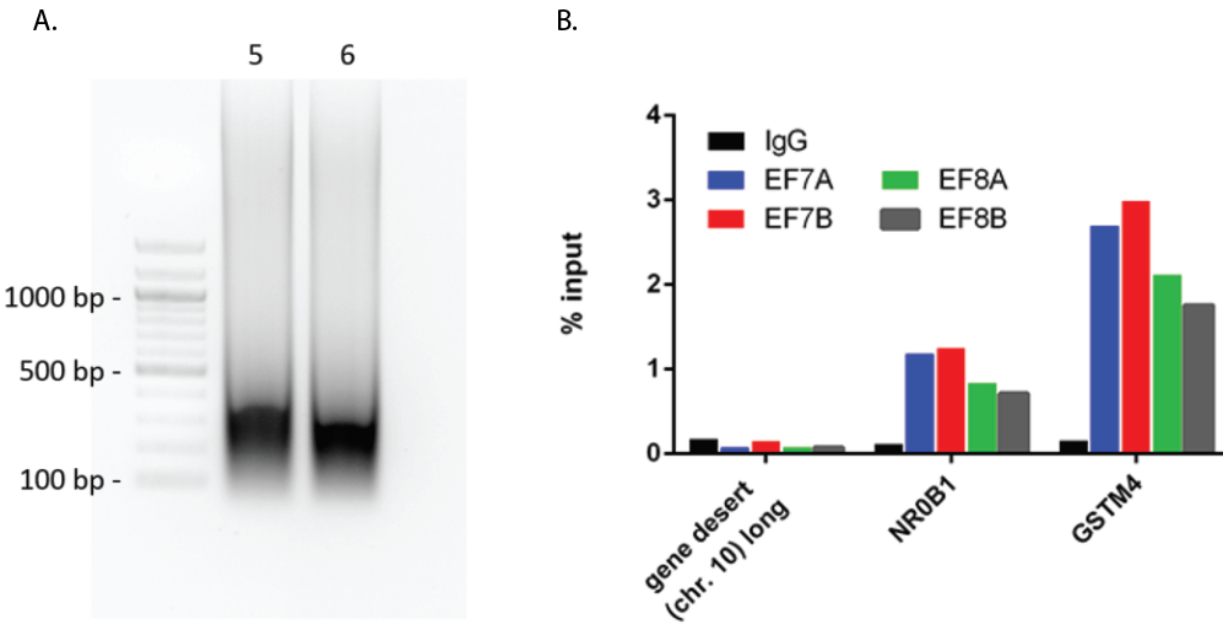

Figure 3.6 Verification of ChIP procedure. A) DNA fragmentation was verified after sonication by 10% agarose/TAE electrophoresis of fragmented DNA. We aimed for a fragment size of 100-400 bp. **B)** qPCR results showing enrichment at known EWS/FLI-bound targets. *NR0B1* and *GSTM4* both have GGAA microsatellites just upstream of their TSS. Primers were designed within the GGAA region and qPCR was performed to determine whether ChIPs were successful. Enrichment was determined by comparing ChIP samples to IgG negative controls and gene desert regions where EF does not bind.

CHAPTER 4

YOU ARE WHAT YOU EAT… OR ARE YOU?

A preview article that accompanied publication of work demonstrating the biosynthetic program of cellular metabolism utilized by cells undergoing rapid growth and proliferation.

Developmental Cell, Vol. 36 (5), p. 483-485

Developmental Cell
Previews

You Are What You Eat… or Are You?

Jason M. Tanner[1] and Jared Rutter[1,2,*]
[1]Department of Biochemistry, University of Utah School of Medicine, Salt Lake City, UT 84112-5650, USA
[2]Howard Hughes Medical Institute, University of Utah School of Medicine, Salt Lake City, UT 84112-5650, USA
*Correspondence: rutter@biochem.utah.edu
http://dx.doi.org/10.1016/j.devcel.2016.02.021

In this issue of *Developmental Cell*, Hosios et al. (2016) take a rigorous and quantitative approach to analyze metabolite acquisition and allocation in proliferating cultured mammalian cells. This work clarifies what we know while providing a new analytical framework to undergird future work on the metabolism of proliferating cells.

In order to meet the metabolic demands associated with duplicating their mass, it appears that proliferating cells employ a metabolic program optimized for the synthesis of macromolecular components rather than ATP (Deberardinis et al., 2008; Vander Heiden et al., 2009). Cells voraciously consume glucose, which is metabolized to lactate through glycolysis to generate two molecules of ATP, rather than being oxidized in the mitochondria via the tricarboxylic acid (TCA) cycle (which can generate as many as ~34 molecules of ATP) (Figure 1). This aerobic glycolysis metabolic program, known as the Warburg effect, belies the apparent fact that proliferation demands macromolecule synthesis more than it does energy. Hence aerobic glycolysis, rather than conversion to usable energy in the form of ATP, serves as a mechanism for diverting metabolic intermediates toward synthetic pathways.

With most of the glucose-derived carbon being converted to lactate and exported from the cell, TCA cycle intermediates—which are needed for some essential biosynthetic reactions—are at risk of being depleted. As a result, proliferating cells have been shown to rely on input from other molecules to replenish the TCA cycle—a phenomenon termed anaplerosis (Owen et al., 2002). Glutamine is robustly consumed in most proliferating mammalian cells in vitro, apparently to fill this role (DeBerardinis et al., 2007; Yuneva et al., 2007) (Figure 1). Since cell mass must be duplicated in each round of proliferation, and duplication of cell mass is accomplished through the acquisition and generation of new molecular components, the logical assumption has been that the majority of new cell mass is derived from the most highly consumed molecules, glucose and glutamine. However, despite an extensive qualitative understanding of the fates of glucose and glutamine, the degree to which these molecules contribute to the biomass of proliferating cells, and to which fractions of that biomass, has not been comprehensively determined. In this issue of *Developmental Cell*, Hosios et al. (2016) impressively fill this void through a rigorous and quantitative assessment of the contributions of glucose, glutamine, and other molecules to the mass of proliferating mammalian cells in culture.

Utilizing a combination of isotopic labeling and mass spectrometry, the authors were able to quantitatively determine the consumption rates of specific molecules, as well as their contribution to total cell mass. Additionally, they traced the fates of nutrient-derived carbon and nitrogen to different macromolecular fractions (protein, nucleic acid, lipid, etc.), thus determining the biosynthetic contributions of the most highly consumed nutrients in proliferative mammalian cells.

The authors first confirm the long-standing observation that glucose is by far the most highly consumed nutrient in proliferating mammalian cells in culture. Although the analysis is not presented in a way to easily assess this, it is likely that more carbon is consumed in the form of glucose than from all other sources combined. In spite of that, the authors make the very surprising observation that glucose-derived carbon accounts for only 10%–15% of total cell mass, distributed more or less equally among the macromolecular fractions (i.e., protein, nucleic acids, lipids, and soluble metabolites) (Figure 1). Where does all of the glucose-derived carbon go? Consistent with the Warburg effect dogma, they find that the vast majority of glucose is converted to lactate and exported from the cell.

With glucose carbon being mostly lost as lactate, the need of a source for TCA cycle intermediates seems to be mostly filled by glutamine, which also contributes around 10% of total cell mass. Interestingly, proliferative cells also exported large amounts of glutamate, derived by removal of an amine from a relatively small fraction of the consumed glutamine. While these data are not such that a definitive conclusion can be reached, they do suggest that most of the glutamine-derived carbon is retained by the cell and is presumably incorporated into the cell's biomass, while a fraction is deaminated and exported as glutamate. Consistent with this, glutamine-derived nitrogen contributed to almost 50% of total cellular nitrogen.

Hosios et al. (2016) further demonstrate that the vast majority of the glutamine-derived carbon assimilated by the cell is fated to end up in cellular protein, with smaller amounts being found in polar metabolites, nucleic acids, and lipids (Figure 1). Although they do not explicitly trace glutamine through the pathways required to convert glutamine into α-ketoglutarate and TCA cycle-derived amino acids, the fact that glutamine itself is not over-represented in total cellular protein permits the authors to infer that glutamine carbon must be utilized to produce other amino acids. Thus, they provide a quantitative example of how glutamine anaplerosis provides a means to synthesize TCA cycle-derived amino acids in rapidly proliferative cells (DeBerardinis et al., 2007), opening the door for further in-depth examination of this phenomenon.

CellPress

Developmental Cell
Previews

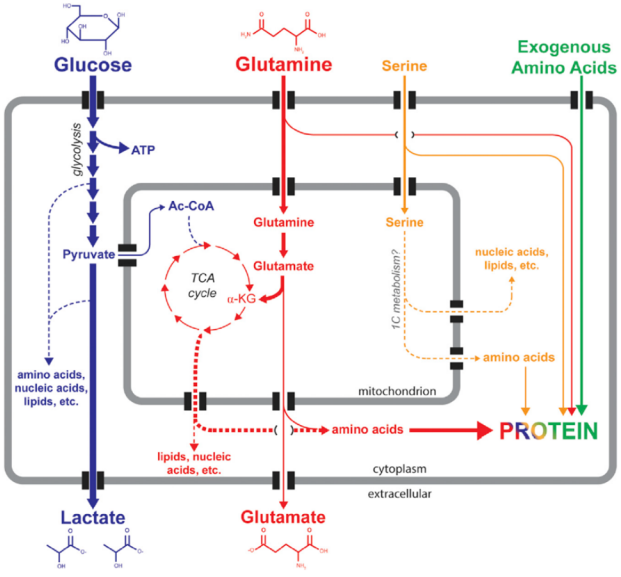

Figure 1. Acquisition and Disposition of Macromolecules in Proliferating Cells
Solid lines signify direct contributions. Dashed lines signify multiple steps and/or conversion to other molecules. Thicker lines correspond with greater relative contribution. Colors signify that the metabolites were at least partially derived from the original nutrient (blue denotes glucose-derived, red denotes glutamine-derived, etc.).

The authors also show that, in addition to protein, serine contributes significantly to nucleic acid lipid synthesis, presumably through the one-carbon metabolism pathway, which produces precursors for several biosynthetic pathways, most prominently nucleic acids (Fan et al., 2014; Locasale, 2013). Valine, on the other hand, contributed almost exclusively in the protein fraction.

So if the majority of cell mass is not derived from glucose or glutamine—the two most highly consumed nutrients in vitro—then what are the principal sources of total cell mass? The authors demonstrate that the majority of cell mass is derived from exogenous amino acids, which is not necessarily surprising, given that the majority of cell mass is made up of protein (Bonarius et al., 1996). When cells were grown in medium containing a pool of 15 isotopically labeled amino acids (not including glutamine), these labeled amino acids comprised the majority of cellular carbon in proliferating cells and made up approximately 20%–40% of total cell mass. Importantly, these amino acids were consumed at much lower rates than glucose and glutamine, revealing a clearer view of a seemingly counterintuitive phenomenon: the most highly consumed nutrient in proliferating cells (glucose) contributes less to cellular biomass, while nutrients consumed at lower rates (amino acids) comprise the majority of total cell mass.

These findings provide a clear and quantitative understanding of carbon acquisition and disposition in proliferating cells, but they also raise many provocative questions. First, to what extent do these phenomena—observed in this manuscript exclusively in vitro—exist in vivo? Interestingly, the same group led by Matt Vander Heiden recently studied the metabolism of glucose and glutamine in vivo using a mouse model of non-small-cell lung cancer (NSCLC) (Davidson et al., 2016). They demonstrated that in vivo NSCLC cells consumed high amounts of glucose, which was predominantly converted to lactate. However, tumor cells were minimally reliant on glutamine, and in vivo tumor formation required contribution of glucose- rather than glutamine-derived carbon to the TCA cycle. Second, although the majority of cell protein is comprised of amino acids imported from the environment, why do cultured cells—awash in amino-acid-rich culture medium—utilize glutamine to synthesize other amino acids de novo even when those amino acids are available for import? Might this have to do with limited import capacity, or is there a separate unforeseen advantage to biosynthesis? Finally, the finding that glucose-derived carbon contributes to a small fraction of cell mass raises still more questions. Why don't proliferating cells utilize the large amounts of carbon consumed as glucose to meet their biosynthetic needs? What is the purpose of such a carbon-wasting metabolic program? Is it simply that this program enables the rapid production of adequate ATP while maintaining the NAD/NADH redox balance, or is there more to it?

Apart from raising important new questions, these experiments reveal important details that reinforce our fundamental understanding of the metabolic underpinnings of molecular biosynthesis and cellular proliferation. Aerobic glycolysis and robust consumption of glucose and glutamine are well-known phenomena in proliferating cells in culture. Accordingly, one might expect that the majority of the duplicated cell biomass results from intake of carbon from these two nutrients. But Hosios et al. (2016) show that it is not quite so simple. In addition to shedding new light on some surprising aspects of the metabolic physiology of cells proliferating in culture, they also provide an important reference for future in vivo and in vitro studies of metabolic programming in proliferative cells of many types.

REFERENCES

Bonarius, H.P., Hatzimanikatis, V., Meesters, K.P., de Gooijer, C.D., Schmid, G., and Tramper, J. (1996). Biotechnol. Bioeng. *50*, 299–318.

Davidson, S.M., Papagiannakopoulos, T., Olenchock, B.A., Heyman, J.E., Keibler, M.A., Luengo, A., Bauer, M.R., Jha, A.K., O'Brien, J.P., Pierce,

Developmental Cell
Previews

K.A., et al. (2016). Cell Metab. http://dx.doi.org/10.1016/j.cmet.2016.01.007.

DeBerardinis, R.J., Mancuso, A., Daikhin, E., Nissim, I., Yudkoff, M., Wehrli, S., and Thompson, C.B. (2007). Proc. Natl. Acad. Sci. USA *104*, 19345–19350.

Deberardinis, R.J., Sayed, N., Ditsworth, D., and Thompson, C.B. (2008). Curr. Opin. Genet. Dev. *18*, 54–61.

Fan, J., Ye, J., Kamphorst, J.J., Shlomi, T., Thompson, C.B., and Rabinowitz, J.D. (2014). Nature *510*, 298–302.

Hosios, A.M., Hecht, V.C., Danai, L.V., Johnson, M.O., Rathmell, J.C., Steinhauser, M.L., Manalis, S.R., and Vander Heiden, M.G. (2016). Dev. Cell *36*, this issue, 540–549.

Locasale, J.W. (2013). Nat. Rev. Cancer *13*, 572–583.

Owen, O.E., Kalhan, S.C., and Hanson, R.W. (2002). J. Biol. Chem. *277*, 30409–30412.

Vander Heiden, M.G., Cantley, L.C., and Thompson, C.B. (2009). Science *324*, 1029–1033.

Yuneva, M., Zamboni, N., Oefner, P., Sachidanandam, R., and Lazebnik, Y. (2007). J. Cell Biol. *178*, 93–105.

CHAPTER 5

THE EWS/FLI FUSION PROTEIN IS REQUIRED FOR METABOLIC MISREGULATION IN EWING SARCOMA

5.1 Abstract

Ewing sarcoma is a bone malignancy driven by the fusion protein EWS/FLI (EF). EF functions as an aberrant transcription factor that misregulates the expression of thousands of genes. Previous work has focused principally on determining important transcriptional targets of EF, as well as characterizing important regulatory partnerships in EF-dependent transcriptional misregulation. Less is known, however, about EF-dependent metabolic changes or their role in Ewing sarcoma biology. We determined the metabolic effects of silencing EF in Ewing sarcoma cells. Metabolomic analyses revealed distinct separation of metabolic profiles in EF-knockdown vs. control-knockdown cells. Mitochondrial stress tests demonstrated that knockdown of EF increased respiratory as well as glycolytic functions. Enzymes and metabolites in several metabolic pathways were altered, including *de novo* serine synthesis and elements of one-carbon metabolism. We found that phosphoglycerate dehydrogenase (PHGDH) is highly expressed in Ewing sarcoma, correlating with worse patient survival. PHGDH knockdown or inhibition *in vitro* caused impaired proliferation and cell death.

Interestingly, PHGDH modulation also led to elevated histone expression and methylation. These studies demonstrate that the translocation-derived fusion protein EF is a master regulator of metabolic reprogramming in Ewing sarcoma, diverting metabolites toward biosynthesis. These data further suggest that the metabolic aberrations induced by EF are important contributors to the oncogenic biology of these tumors. This previously unexplored role of EF as a driver of metabolic reprogramming expands the understanding of Ewing sarcoma biology, and has potential to significantly inform development of therapeutic strategies.

5.2 Introduction

Ewing sarcoma is an aggressive malignancy that most often emerges from bone and bone-associated tissues of children and adolescents. It is the second most common pediatric bone tumor; second only to osteosarcoma. Surgical strategies have achieved very good outcomes for many of these patients. But truly effective molecular therapies continue to evade discovery, translating to especially poor prognosis for patients who fall victim to metastasis or relapse (1). Indeed, the rate of relapse after surgery is ~35%, and the probability of 5-year survival after relapse is ~20% (2,3). Continued investigation of the molecular underpinnings of this disease is thus crucial, and has the promise of providing additional candidate therapies to these patients.

Ewing sarcoma tumors are uniquely devoid of recurrent mutations in classical oncogenes or tumor suppressors (4). Instead, oncogenesis of Ewing sarcoma is almost entirely due to the far-reaching consequences of a single genetic lesion: a translocation event between chromosomes 11 and 22. This

chromosomal rearrangement generates an in-frame fusion product merging the *EWSR1* and *FLI1* genes, giving rise to the oncogenic fusion protein known as EWS/FLI (EF). EF contains the N-terminal transcriptional regulatory domain of EWS and the DNA-binding domain of FLI1. Interestingly, while EF can affect known targets of FLI1 by binding to canonical FLI1 binding sites, it also influences expression of genes that are not targets of FLI1 or EWSR1 (5,6). Thus, EF is an aberrant transcription factor with neomorphic functions and tumorigenic consequences.

The transcriptional reprogramming driven by EF has been well profiled (7–15). In-depth study of EF targets has revealed that this master regulator exerts its oncogenic effects on numerous processes, contributing to many of the hallmark capabilities of cancer cells. These include: proliferation and growth (16,17), resistance to cell death (18), immortality (19), angiogenesis (20), invasion and metastasis (18,21), and evading immune destruction (22). However, very little is known about how EF affects another characteristic feature of cancer cells – the pro-oncogenic reprogramming of cellular metabolism.

Cancer cells characteristically adopt programs that modify substrate utilization and alter metabolite abundance in ways that support the biosynthetic requirements of these highly proliferative and resilient cells (23). Evidence increasingly indicates that metabolic alterations observed in cancer are not mere spectator phenomena, but are active contributors to oncogenesis (23). Significant interrelationships exist linking cellular metabolic processes to nuclear control, and vice versa (23,24). As a result, defining the metabolic processes undergirding

cancer cells provides promising new opportunities for discovery of potentially actionable therapeutic targets.

Currently, there is a paucity of data concerning the role of EF in altering metabolic processes in Ewing sarcoma. Given its relatively low mutation burden compared to other cancers (4), Ewing sarcoma provides a unique model to study metabolic alterations that are important to oncogenesis. Changes in cellular metabolism that result from EF transcriptional misregulation likely contribute directly to oncogenesis. Thus, studying cellular metabolism in Ewing sarcoma promises to increase our understanding of metabolic reprogramming in general, and inform development of novel therapeutic strategies for Ewing sarcoma specifically. With these goals in mind, we set out to investigate EF-driven metabolic reprogramming in Ewing sarcoma.

5.3 Results

5.3.1 EWS/FLI misregulates numerous genes involved in metabolism

Transcription profiling of Ewing sarcoma cells has been previously performed by microarray and RNA-seq experiments after silencing EWS/FLI (EF) in A673 cells (7,25,26). We analyzed data from a publicly available RNA-seq dataset wherein EF was silenced by shRNA (shEF) and compared to control knockdown (shLUC). Our analysis identified 7,094 genes that are differentially expressed in shEF vs. control shLUC cells (gene lists found as Excel files in Supplemental Data). We defined significant changes in expression as a fold change of ≥ 1.5-fold and a p-value of < 0.05. After EF knockdown, 4,140 genes

exhibited increased expression, while 2,954 genes were less expressed. Gene ontology (GO) analysis was performed on the list of all EF-misregulated genes, revealing metabolic processes (GO: 0008152) as the second most enriched GO term (2,058 genes; 33.7%) (Fig. 5.1A). These genes were further subdivided into primary metabolic processes (GO: 0044238), revealing that the majority of these genes were involved in nucleobase-containing compound metabolism (GO: 0006139) and protein metabolism (GO: 0019538) (Fig. 5.1B).

To further assess whether EF significantly alters genes of metabolic importance, gene set enrichment analysis (GSEA) was performed comparing our dataset of differentially expressed genes in shEF cells to gene sets from the Molecular Signatures Database (MSigDB) (27). Significant correlations were observed between differentially expressed genes and genes in the Hallmark-Glycolysis gene set and the KEGG-Pathways in Cancer gene set (Fig. 5.1C & 1D). Significant correlations were also observed with gene sets of Hallmark-Reactive Oxygen Species, Hallmark-Epithelial-Mesenchymal Transition, but not in the Hallmark-Oxidative Phosphorylation gene set (Fig. 5.2A).

5.3.2 Knockdown of EWS/FLI causes changes in cellular metabolism

To more directly study whether EF alters cellular metabolism, we performed stress tests on glycolysis and mitochondrial function using the Seahorse XF96 analysis system. During the glycolysis stress test, addition of glucose and oligomycin caused greater increases of extracellular acidification rate (ECAR) in shEF vs. shLUC cells (Fig. 5.3A). Oxygen consumption rate was not different

between shEF and shLUC cells throughout the glycolysis stress test (Fig. 5.3B). These data suggest that silencing of EF results in increased utilization of glucose by glycolysis (Fig. 5.2B). Basal ECAR was not different between shEF and shLUC cells at the beginning of the glycolysis stress test, reflecting the lower glucose (10 mM) conditions required for a glycolysis stress test (Fig. 5.3B). However, in the mitochondrial stress test, glucose is present at typical cell culture levels (25 mM), allowing us to observe that basal ECAR is higher in shEF vs. shLUC cells (Fig. 5.3C). The apparent increase of glycolytic rate caused by EF knockdown is surprising, and is possibly explained by de-repression of hexokinase 1 (HK1) by shEF (Fig. 5.3E). Indeed, uptake of 2-deoxy-2-[(7-nitro-2,1,3-benzoxadiazol-4-yl)amino]-D-glucose (2-NBDG; a fluorescently-labeled analog of deoxyglucose) is elevated in shEF vs. shLUC A673 cells (Fig. 5.3F).

Tests of mitochondrial respiration showed enhanced response to mitochondrial uncoupling by carbonyl cyanide-4 (trifluoromethoxy) phenylhydrazone (FCCP) in shEF vs. shLUC cells (Fig. 5.3D). These data indicate that silencing EF results in increased maximal respiration and spare respiratory capacity, with no change in basal respiration, ATP production, proton leak, non-mitochondrial respiration, and coupling efficiency (Fig. 5.2B). To additionally assess mitochondrial respiratory function, cells were treated with the membrane potential-sensitive Mitotracker Red FM dye. Comparisons were made relative to a membrane potential-independent mitochondrial dye (Mitotracker Green). Consistent with increased maximal respiration and respiratory capacity, shEF cells also had elevated mitochondrial membrane potential compared to shLUC cells

(Fig. 5.3G). Together, these data suggest that EF increases the proportion of glucose-derived carbon that is shunted away from oxidative metabolism consistent with a biosynthetic, pro-oncogenic metabolic program.

5.3.3 EWS/FLI is required for global changes in metabolite abundance

Global changes in metabolite abundance were assessed by performing steady-state metabolomics analyses comparing shEF with shLUC A673 cells. Examining metabolomic data by principal components analysis revealed that EF knockdown results in a distinct metabolic profile compared to control cells (Fig. 5.4A & 5.3B). Topological analysis of metabolites within metabolic pathways highlighted several metabolic pathways that were more significantly impacted by silencing of EF (Fig. 5.4C) (28,29). Pathways significantly affected by EF silencing included alanine, aspartate, and glutamine metabolism, and glycine, serine, and threonine metabolism.

Additionally, metabolomic profiling data were combined with transcription profiling data to perform analyses of pathways in which both metabolite abundance and gene expression were significantly altered in shEF vs. shLUC cells. This allowed us to determine which pathways were impacted the most by shEF, potentially by altering expression of enzymes and metabolites in that pathway. Intriguingly, the enzymes of serine and glycine synthesis were found to be significantly downregulated by EF silencing in the RNA-seq dataset, and corresponding decreases in serine and glycine were observed in our metabolomic dataset (Fig. 5.4C & Fig. 5.5A).

5.3.4 EWS/FLI upregulates expression of serine and glycine synthesis enzymes

The *de novo* serine synthesis pathway is one way by which glycolytic intermediates can be shunted toward biosynthetic processes, and this has been implicated in many cancers (30,31). Specifically, phosphoglycerate dehydrogenase (PHGDH) commits the glycolytic intermediate 3-phosphoglycerate to serine and glycine synthesis, providing important precursors for protein, lipid, and nucleic acid synthesis. Increased PHGDH has been linked to the oncogenic biology of other tumors (30,32). In fact, PHGDH expression is higher in Ewing sarcoma than all other cancer cell lines in the Cancer Cell Line Encyclopedia (Fig. 5.6A).

In concordance with RNA-seq data, protein levels of PHGDH were decreased in shEF vs. shLUC cells (Fig. 5.7A). Protein levels of phosphoserine aminotransferase (PSAT) and phosphoserine phosphatase (PSPH) – the two enzymes downstream of PHGDH in the serine synthesis pathway – were also lower upon silencing of EF (Fig. 5.7A). Similar patterns of expression were observed for serine hyrdroxymethyltransferase (SHMT1 and SHMT2), which converts serine to glycine and feeds into one-carbon folate metabolism cycles, as well as dihydrofolate reductase (DHFR) and thymidylate synthetase (TYMS) – important enzymes in one-carbon folate metabolism cycles (Fig. 5.7B and Fig. 5.5D & E).

5.3.5 PHGDH is elevated in high-risk Ewing sarcoma patients

To explore correlations between PHGDH expression and clinical outcome, we used the SurvExpress tool to perform Cox survival analysis of a Ewing sarcoma dataset (33,34). Patients who were categorized as high-risk had significantly higher expression of PHGDH and SHMT1/2 (Fig. 5.7C & D). Similarly, higher expression of PSPH, DHFR, TYMS, MTHFD2, and SHMT2 was correlated with poorer survival in Ewing sarcoma patients (Fig. 5.6B & C). Similar correlations were also observed between expression levels and event-free survival (data not shown).

Furthermore, PHGDH expression was assessed in histological samples from Ewing sarcoma patients. PHGDH staining was much higher in tumor (defined by IHC for CD99) than in adjacent normal tissue (Fig. 5.8A). CD99 exhibited staining along cell surface boundaries, while PHGDH staining appeared diffusely cytoplasmic.

5.3.6 PHGDH is required for proliferation and normal chromatin modification

Inhibition of PHGDH function by NCT502 and NCT503 caused growth defects and cell death in Ewing sarcoma cell lines, including the EWS/ERG-harboring TTC466 line (Fig. 5.8B-E). This effect was less prominent in 293T or U2OS cells (Fig. 5.8F & G). This and previous data indicate that upregulated expression of serine synthesis and 1-carbon metabolism contributes importantly to the oncogenic phenotype in Ewing sarcoma (Fig. 5.8H).

While the major product of PHGDH is 3 phosphohydroxypyruvate (3-PP) from 3-phosphoglycerate (3-PG), the enzyme also produces relatively small amounts of 2-hydroxyglutarate (2-HG) from α-ketoglutarate (Fig. 5.9A) (35). 2-HG has been shown to be oncogenic in high amounts, typically resulting from neomorphic mutations of isocitrate dehydrogenase enzymes (35,36). Interestingly, we observed that 2-HG was lower in shEF vs. shLUC cells (Fig. 5.9B), suggesting that EF might be driving elevated production of 2-HG via increased expression of PHGDH.

To test whether elevated levels of 2-HG in Ewing sarcoma cells were due to PHGDH, we assessed 2-HG levels after inhibition of PHGDH function with NCT502. 2-HG was lower in cells treated by NCT502 vs. its inactive analog (Fig. 5.9C). Importantly, the levels of 2-HG in Ewing sarcoma cells were lower than previously observed in cells harboring mutations in isocitrate dehydrogenase (IDH) enzymes (37,38). To test whether 2-HG generated from PHGDH had effects on DNA methylation, we silenced PHGDH expression and determined 5-methylcytosine (5-mC) content of LINE-1 elements (a surrogate for bulk DNA methylation). However, knockdown of EF or PHGDH had no effect on 5-mC levels (Fig. 5.9D). PSPH was also silenced to distinguish between serine synthesis and 2-HG producing functions of PHGDH, and disruption of serine synthesis downstream of PHGDH also had no effect on 5-mC levels.

To further assess whether modulation of PHGDH affects chromatin, we immunoblotted histone proteins. This was performed with A673 cells, as well as another more recently established patient-derived EF-harboring Ewing sarcoma

cell line (UTES-14-01872) (Fig. 5.5C). Interestingly, methylation of histone H3 at lysine (K) 9 and K27 was increased by PHGDH knockdown in UTES-14-01872 and TTC466 cells, but not in A673 cells (Fig. 5.9E & F). Additionally, total histone protein was increased by PHGDH knockdown in two of the three cell lines. These data raise the possibility of a role for PHGDH in chromatin regulation, possibly by affecting abundance of metabolites used as cofactors for histone modifying enzymes.

5.4 Discussion

EF has long been recognized as the primary oncogenic driver of Ewing sarcoma. Overexpression of EF in NIH3T3 murine fibroblasts results in oncogenic transformation, and silencing EF expression in patient-derived cell lines results in a loss of tumorigenesis (8,39–48). However, effective therapeutic strategies directly targeting transcription factors have been notoriously elusive. For this reason, studies of the biology of Ewing sarcoma have primarily focused on identifying important EF target genes, as well as the interacting partners EF requires to elicit its effects. Indeed, numerous EF targets have been shown to be necessary, but not sufficient, for oncogenesis in these tumors (7,10,21,25,49–53). Unfortunately, many of these critical EF targets and partners lack enzymatic function and are themselves not susceptible to pharmacological modulation. With this in mind, we sought to determine whether EF generates an oncogenic program of cellular metabolism by misregulating the transcription of genes encoding key metabolic enzymes.

By analyzing existing EF transcriptional datasets, we were able to identify

significant patterns of altered metabolic gene expression (Fig. 5.1). Specifically, gene ontology analysis revealed significant alterations in the expression of genes involved in glycolysis, nucleobase-containing metabolic processes, and protein metabolism. Consistent with a cancerous phenotype, Ewing sarcoma cells are hyperproliferative and require increased macromolecule synthesis to sustain accelerated growth and proliferation. It has been shown that Ewing sarcoma cells are therefore vulnerable to replicative stress, and inhibition of DNA repair pathways has been explored as a therapeutic option for Ewing sarcoma (54,55). Additionally, EF-driven alterations in nucleobase-containing metabolic processes such as (NAD salvage) could be sensitive to inhibition and therapeutic exploitation (56). The increased metabolic demands of rapid proliferation and growth could be exploited in similar ways.

We also observed that EF knockdown resulted in increased maximal respiration and mitochondrial membrane potential (Fig. 5.3D & 5.2G). This is in line with studies of other malignancies, wherein various oncogenic processes lead to a metabolic program of aerobic glycolysis – diverting metabolites toward pathways that are important for various kinds of macromolecule synthesis (23). As more carbon is diverted to biosynthetic pathways from glycolysis, flux through the TCA cycle may decrease, resulting in oncogene-induced reduction in respiratory capacity, as suggested by our data. These findings reinforce the concept that such a shift away from oxidative metabolism is a characteristic feature of oncogenesis, important in all cancers, and not a spectator phenomenon merely correlating with oncogenic processes. Furthermore, they demonstrate that EF is a driver of

oncogenic metabolic reprogramming, in addition to and as a consequence of transcriptional reprogramming.

Surprisingly, we also observed an increase of glycolysis in shEF vs. shLUC cells (Fig. 5.3A & C). Such observations appear to run contrary to the known glycolytic metabolism that predominates in the vast majority of cancer cells. This unique phenomenon could be explained by transcriptional downregulation of genes important for glucose import or utilization. Indeed, we observed that hexokinase 1 (HK1) is increased in shEF vs. shLUC cells (Fig. 5.3E). In such a scenario, EF may restrict glucose entry into glycolysis, effectively reducing the cell's ability to metabolize additional glucose (as seen in our Seahorse analysis data). However, if this restriction is not so severe to cause cell death by starvation, glucose uptake may remain sufficient to fulfill cellular energy requirements. Simultaneously, EF upregulates genes of biosynthetic pathways such as *de novo* serine synthesis (Fig. 5.7A), resulting in an increased proportion of glycolytic intermediates being shunted into biosynthetic pathways. Thus it may be possible to generate the net effect of oncogenic and biosynthetic reprogramming of metabolism by increasing the proportion of glucose-derived carbon shunted towards biosynthetic pathways, even in the face of EF-induced downregulation of HK1. Additionally, considering that the putative cell of origin for Ewing sarcoma is a mesenchymal stem cell, and that EF is known to repress mesenchymal features, the baseline glycolytic metabolism of these stem cells may provide ample flexibility to be permissive to decreased HK1 within the context of oncogenic metabolic reprogramming induced by EF (12,57). These and other hypotheses are a subject

of current and future study.

Our findings also suggest that EF drives global shifts in metabolite abundance in Ewing sarcoma cells (Fig. 5.4). Integrating metabolomic and transcriptomic data enabled us to identify EF-driven upregulation of *de novo* serine synthesis via PHGDH as an important candidate for further study. PHGDH is amplified in various tumors, and has been implicated previously in tumor biology (30,35,58). PHGDH commits the glycolytic intermediate 3-PG to *de novo* serine synthesis, and EF-driven upregulation of PHGDH expression appears to be an important factor in diverting metabolites toward macromolecule synthesis (Fig. 5.7A). Increased *de novo* serine synthesis also may create a positive feedback loop whereby elevated levels of serine inhibit PKM2, enhancing entry of metabolites into the serine synthesis pathway via PHGDH (59,60). While perhaps not a major oncogenic outcome of elevated serine synthesis, such a feedback loop could amplify the effects of such increases. Whether such a phenomenon exists in Ewing sarcoma has not been tested. Importantly, elevated expression of PHGDH also correlates with a poor prognosis in Ewing sarcoma patients, suggesting that these phenomena have important clinical implications (Fig. 5.7C). Our findings are similar to previous findings demonstrating upregulation of serine synthesis by other oncogenes. PHGDH, PSPH, and PSAT are upregulated in some Myc-driven lymphomas (61). Additionally, oncogene-driven transcriptional misregulation in other malignancies (e.g., HER2, SP1, NFY, NRF2, ATF4) has been shown to increase expression of enzymes of *de novo* serine synthesis (62–64). EF thus appears to generate a metabolic program of upregulated serine

synthesis similar to other malignancies, and further study is required to determine whether EF exerts its effects by co-opting any of the aforementioned regulatory factors.

Downstream of *de novo* serine synthesis, conversion of serine to glycine is carried out by serine hydroxymethyltransferase (SHMT). This reaction is coupled to the conversion of tetrahydrofolate to 5,10-methylenetetrahydrofolate, and is a major provider of 1-carbon units needed for multiple cellular functions (65–67). Our data suggest that EF is also driving upregulation of these processes, further establishing a pro-oncogenic, biosynthetic metabolic program in these cells (Fig. 5.5H). It is likely that this is also clinically relevant, as patients with high levels of SHMT also have worse overall survival (Fig. 5.7D). Together, these data also raise the interesting possibility of utilizing expression levels of metabolic enzymes such as PHGDH and SHMT to inform predictions of patient prognosis, or even using metabolic indices to define different patient populations.

The nature of the relationship between patient survival and expression levels of these genes deserves further consideration. Several hypotheses exist for why increased expression of these enzymes correlate with poorer prognosis. For instance, upregulation of *de novo* serine synthesis may contribute importantly to increased synthesis of glycine and cysteine. Such a process would contribute more amino acids to meet the biosynthetic requirements of proliferative cancer cells. Additionally, since glycine and cysteine both contribute to production of glutathione, increased serine synthesis also potentially contributes to greater redox buffering. Indeed, serine metabolism has been shown to be activated under

conditions of increased ROS production, perhaps contributing to increased capacity to confront redox stress (68). Furthermore, the conversion of serine to glycine contributes importantly to one-carbon metabolism and the folate cycle. The *de novo* synthesis of adenosine, guanosine, and thymidylate requires one-carbon units derived from serine. Thus, increased serine synthesis could contribute to greater nucleotide synthesis in general. Upregulation of SHMT1/2 and TYMS is consistent with these hypotheses. Upregulation of such processes could permit cancer cells to become more proliferative or aggressive, thus contributing to poorer prognosis in patients. However, as these hypotheses have yet to be tested, more in-depth investigation is clearly needed.

Upregulation of *de novo* serine synthesis and one-carbon metabolism has far-reaching consequences for cancer cells, as flux through these pathways is important for regulation of methyl donor (methionine) recycling and epigenetic states. In addition, previous work has suggested that amplified PHGDH may play a role in cancer through production of 2-HG (69). 2-HG is a known oncometabolite when overproduced by neomorphic mutations in IDH enzymes (70–72). Intriguingly, our data also suggest that important links exist between *de novo* serine synthesis (specifically PHGDH) and nuclear processes. We observed decreased amounts of 2-HG in shEF vs. shLUC cells (Fig. 5.9B & C). However, the amounts of 2-HG generated by EF-induced upregulation of PHGDH are lower than levels seen in other malignancies with IDH mutations, and 2-HG likely has less of a role in Ewing sarcoma biology. Additionally, IDH mutations are rare in Ewing sarcoma (73). Some work has shown that the small amounts of 2-HG

produced by PHGDH may be sufficient to promote histone methylation, contributing to an oncogenic hypermethylation of histones and, possibly, DNA (69). However, our results suggest that this is not the case in Ewing sarcoma. Rather, knockdown of PHGDH did not affect DNA methylation (Fig. 5.9D), but did cause significant increases in histone methylation (Fig. 5.9E & F). Interestingly, these histone alterations were observed in EF-expressing cells (UTES-14-01872) as well as in TTC466 cells, which harbor the alternate translocation EWS/ERG (found in ~10% of Ewing sarcomas) (74,75). While the mechanisms responsible for these chromatin changes are unclear, we hypothesize that abundance of metabolites important for the function of other enzymes (either as substrates or cofactors) might play a role. Future efforts are aimed at testing these hypotheses and further elucidating the mechanisms linking metabolism and nuclear control.

Taken together, our findings demonstrate that EF drives metabolic misregulation, resulting in diversion of metabolites toward biosynthetic pathways in order to meet the increased demands of oncogenesis. EF induces increased expression of PHGDH, PSAT, and PSPH, shunting glycolytic intermediates into serine and glycine synthesis, and contributing to 1-carbon metabolism through upregulated SHMT. This and further study of the role of EF as a driver of oncogenic metabolism promises to reveal new actionable targets for therapeutic intervention. Such efforts aspire to inform the development of hitherto elusive molecular targeted therapies for Ewing sarcoma.

5.5 Materials and Methods

5.5.1 Cell culture

Cell lines expressing EWS/FLI (A673, UTES-14-01872; see Fig. 5.5B & C) or EWS/ERG (TTC466) were grown in 10%FBS/DMEM or 10% FBS/RPMI (RPMI 1640 Glutamax; ThermoFisher), respectively. DMEM (Corning) contained 25 mM glucose, 4 mM L-glutamine, and 1 mM sodium pyruvate. Media were supplemented with 3 μg/ml puromycin for selection of shRNA-expressing cells. 293T cells were grown in 10% FBS/DMEM. Population doublings were assessed using a 3T5 growth assay as previously described (14). A673 and TTC466 lines were validated prior to experimentation by STR analysis (Genetica DNA Labs). The patient-derived cell lines A673 and TTC466 were acquired from stocks maintained S. Lessnick. UTES-14-01872 is a recently-derived cell line of Ewing sarcoma established in 2014 by S. Schiffman.

5.5.2 Virus production, shRNA constructs, and infections

EWS/FLI- and Luciferase-siRNA sequences were used previously for transcriptional profiling of Ewing sarcoma (7,25,49,76). siRNA sequences for PHGDH and PSPH were designed using the Whitehead Institute siRNA Selection Program (77). shRNA-encoding inserts containing these sequences were ligated into the pMKO.1p retroviral vector. siRNA sequences are found in Supplemental Materials and Methods. Retrovirus was produced by transfecting 293T cells with Optimem and Lipofectamine 2000, and viral supernatant was collected at 48h and 72h post-infection. Viral supernatant was filtered at 0.45 μm, aliquoted, and stored

at -80° C. Infections were performed by adding viral supernatant (plus 8 μg/ml polybrene) to sub-confluent cultures. Selection in puromycin-containing media was continued for 3 days, and puromycin efficacy was confirmed by observing cell death in uninfected cells.

As EF is the primary oncogenic driver of Ewing sarcoma, most Ewing sarcoma cell lines do not tolerate its silencing well. A673 cells are known to best tolerate EF knockdown. Accordingly, we have had the most success using A673 cells, and limited success performing such experiments in other lines.

5.5.3 Mitotracker staining

A673 cells expressing shLUC or shEF were seeded onto 1.5 borosilicate chambered coverglass slides (Thermo Fisher) and incubated overnight. Media was replaced with phenol red-free DMEM containing 25 mM glucose, 1% Glutamax, 1% sodium pyruvate, 100 nM Mitotracker Red FM, 200 nM Mitotracker Green FM, and 5 μg/ml Hoechst stain (Thermo Fisher). Cells were incubated in staining medium for 10 minutes, after which staining medium was removed and cells were washed twice with phenol red-free medium. Cells were immediately imaged using a Zeiss Axio Observer Z1 microscope.

Images were quantified using ImageJ software. Three cells were selected in each of 5 high-power field images for a total of 15 quantified cells. Integrated density measurements were taken for Mitotracker Red and Mitotracker Green channels for each cell with identical areas, and corrected total cell fluorescence (CTCF) was calculated for each channel as described previously (78). CTCF calculations were done as: CTCF = integrated density – (area of selected cell x

mean fluorescence of background readings).

5.5.4 Western blotting

Whole cell extract (WCE) was prepared using RIPA buffer containing protease inhibitor cocktail (Sigma). Total protein content was determined via BCA assay, and WCE was prepared for SDS-PAGE by adding Laemmli buffer. Immunoblotting was done using the following antibodies: Fli1 (Abcam, 1:1,000), PHGDH (Cell Signaling, 1:1,000), PSAT (Abcam, 1:1,000), PSPH (Abcam, 1:1,000), SHMT1 (Cell Signaling, 1:1,000), SHMT2 (Cell Signaling, 1:1000), TYMS (Cell Signaling, 1:1,000), DHFR (Abcam, 1:1,000), HK1 (Abcam, 1:1000), H3K9me3 (Abcam, 1:1,000), H3K27me3 (Cell Signaling, 1:1,000), Histone H3 (Abcam, 1:5,000), α-tubulin (Cell Signaling, 1:5,000), β-actin (Sigma, 1:5,000).

5.5.5 Immunohistochemistry

Procedures for immunohistochemistry (IHC) are previously described (79–81). Briefly, paraffin was removed and tissue was subjected to high pressure antigen retrieval (Vector Unmasking Solution; Vector Laboratories, Burlingame, CA). Samples were incubated in primary antibody (PHGDH, Cell Signaling) overnight at 4°C. Secondary antibodies, raised in donkey (Jackson Immunoresearch, West Grove, PA), were used at a dilution of 1:250 at room temperature for 1-hour. Vectastain reagents and diaminobenzidine (DAB) (Vector Laboratories) were used to develop IHC. Images were subsequently taken on a Zeiss Axio Observer Z1 microscope. Tissue samples from human patients were obtained with patient consent and approval from the University of Utah Institutional

Review Board.

5.5.6 PHGDH inhibition, 2-HG and %5-mC

The PHGDH inhibitors NCT502 and NCT503 (Cayman) and the inactive control molecule called PHGDH-inactive (Cayman) were reconstituted in DMSO. Final concentrations of inhibitors were 3.7 μM, 18.5 μM, and 37 μM for PHGDH-inactive and NCT502; and 2.5 μM, 12.5 μM, and 25 μM for NCT503. These concentrations were chosen to achieve maximal levels of inhibition at the highest doses based on previously published IC_{50} data (82).

Global 5-methylcytosine levels were assessed using the Global DNA Methylation Assay – LINE1 (Active Motif). D-2-hydroxyglutarate was quantified using a colorimetric D2HG assay kit (BioVision). All procedures were carried out as indicated by the manufacturer.

5.5.7 Analysis of functional metabolism via seahorse XFe96 analyzer

Cells were seeded into 96-well format Seahorse analyzer plates 24 hours prior to performing Seahorse experiments. We performed side-by-side Mito Stress Tests and a Glycolysis Stress Tests in 96-well format using the XF96e analyzer. The Mito Stress Test was performed in standard assay media (DMEM, 25 mM Glucose, 1 mM pyruvate, 2 mM Glutamine, pH 7.4) with the final concentrations of drugs as follows [Oligomycin: 2 μM; carbonyl cyanide-4 (trifluoromethoxy) phenylhydrazone (FCCP): 2 μM; Rotenone: 0.5 μM; Antimycin A: 0.5 μM]. Assay protocol was standard (3 measurements per phase, acute injection followed by 3

min mixing, 0 min waiting, and 3 min measuring). Data were normalized to cell number because morphological changes that result from EF silencing potentially confound normalization to total cellular protein (Fig. 5.2D) (57). The Glycolysis Stress test was performed in standard assay media (DMEM, 2 mM Glutamine, pH 7.4) and the following final concentrations (glucose: 10 mM; Oligomycin: 2 μM; 2-deoxy-glucose: 50 mM). Results were normalized as above and analyzed in WAVE software and processed through the XF Mito Stress Test Report and Glycolysis Stress Test Generators. All statistics were generated through GraphPad Prism 7 using unpaired two-tailed student t-tests.

5.5.8 Gene ontology, geneset enrichment analysis, and survival-expression analyses

Gene ontology analysis was performed on lists of differentially expressed genes from RNA-seq data (Lg2Rto: 0.585; AdjP≥10). Gene lists and data are available in Supplemental Data. Methodology of the PANTHER gene ontology platform and gene set enrichment analysis (GSEA) are described elsewhere (27,83,84). Ewing sarcoma patient survival data were compared with gene expression by analyzing a publicly available dataset (GSE17679) with the SurvExpress online tool (33,34). Risk groups were defined by prognostic index, with low-risk being defined as less than the median prognostic index, and high-risk being defined as greater than the median prognostic index.

5.5.9 RNA-Seq dataset

RNA-Seq of A673 cells treated with shLUC or shEF was previously performed (25,26). The datasets we acquired are publicly available in the NCBI BioProject database, accession # PRJNA176544, and the Sequence Read Archive (SRA059329). We re-analyzed these data to determine differential expression analysis using USeq (useq.sourceforge.net) version 8.8.3. Lists of differentially expressed genes are provided in Supplementary Data.

5.5.10 Steady-state metabolomics

All GC-MS analysis was performed with a Waters GCT Premier mass spectrometer fitted with an Agilent 6890 gas chromatograph and a Gerstel MPS2 autosampler. Dried samples were suspended in 40 µL of a 40 mg/mL O-methoxylamine hydrochloride (MOX) in pyridine and incubated for 1 hour at 30°C. To autosampler vials was added 25 µL of this solution. 40 µL of N-methyl-N-trimethylsilyltrifluoracetamide (MSTFA) was added automatically via the autosampler and incubated for 60 minutes at 37°C with shaking. After incubation, 3 µL of a fatty acid methyl ester standard (FAMES) solution was added via the autosampler then 1 µL of the prepared sample was injected to the gas chromatograph inlet in the split mode with the inlet temperature held at 250°C. A 10:1 split ratio was used for analysis. The gas chromatograph had an initial temperature of 95°C for 1 minute followed by a 40°C/min ramp to 110°C and a hold time of 2 minutes. This was followed by a second 5°C/min ramp to 250°C, a third ramp to 350°C, then a final hold time of 3 minutes. A 30 m Phenomex ZB5-5 MSi column with a 5 m long guard column was employed for chromatographic

separation. Helium was used as the carrier gas at 1 mL/min. Due to the high amounts of several metabolites, the samples were analyzed once more at a 10-fold dilution. Data were collected using MassLynx 4.1 software (Waters). Metabolites were identified and their peak area was recorded using QuanLynx. These data were transferred to an Excel spread sheet (Microsoft, Redmond WA). Metabolite identity was established using a combination of an in-house metabolite library developed using pure purchased standards and the commercially available NIST library. Metabolomic data were further analyzed using MetaboAnalyst 3.0 (28,29,85–89).

5.6 Grant Support

J. Rutter was supported by HHMI and NIH grant GM 110755. J. Schiffman was supported by St. Baldrick's Foundation, Sarcoma Alliance for Research through Collaboration (SARC) Career Development Award, Damon Runyon Clinical Investigator Award, and the Eunice Kennedy Shriver Children's Health Research Career Development Award NICHD 5K12HD001410. Metabolomics analysis was performed at the Metabolomics Core Facility at the University of Utah, which is supported by 1 S10 OD016232-01, 1 S10 OD021505-01 and 1 U54 DK110858-01. The authors also acknowledge the support of the Huntsman Cancer Institute (P30CA042014) and the Huntsman Cancer Foundation.

5.7 Acknowledgments

The authors would like to thank Dr. Kevin Jones, Dr. Emily Theisen, Dr. Ranajeet Saund, and Dr. Kathleen Pishas, and all members of the Lessnick and

Rutter labs for many useful and thought-provoking discussions throughout the course of these studies.

5.8 References

1. Linabery AM, Ross JA. Childhood and adolescent cancer survival in the US by race and ethnicity for the diagnostic period 1975-1999. Cancer. 2008;113:2575–96.

2. Rodriguez-Galindo C, Billups CA, Kun LE, Rao BN, Pratt CB, Merchant TE, et al. Survival after recurrence of Ewing tumors: the St Jude Children's Research Hospital experience, 1979-1999. Cancer. 2002;94:561–9.

3. Lahl M, Fisher VL, Laschinger K. Ewing's sarcoma family of tumors: an overview from diagnosis to survivorship. Clin J Oncol Nurs. 2008;12:89–97.

4. Brohl AS, Solomon DA, Chang W, Wang J, Song Y, Sindiri S, et al. The genomic landscape of the Ewing sarcoma family of tumors reveals recurrent STAG2 mutation. PLOS Genet. 2014;10:e1004475.

5. Gangwal K, Sankar S, Hollenhorst PC, Kinsey M, Haroldsen SC, Shah AA, et al. Microsatellites as EWS/FLI response elements in Ewing's sarcoma. Proc Natl Acad Sci. 2008;105:10149–54.

6. Mao X, Miesfeldt S, Yang H, Leiden JM, Thompson CB. The FLI-1 and chimeric EWS-FLI-1 oncoproteins display similar DNA binding specificities. J Biol Chem. 1994;269:18216–22.

7. Smith R, Owen LA, Trem DJ, Wong JS, Whangbo JS, Golub TR, et al. Expression profiling of EWS/FLI identifies NKX2.2 as a critical target gene in Ewing's sarcoma. Cancer Cell. 2006;9:405–16.

8. Hancock JD, Lessnick SL. A transcriptional profiling meta-analysis reveals a core EWS-FLI gene expression signature. Cell Cycle Georget Tex. 2008;7:250–6.

9. Prieur A, Tirode F, Cohen P, Delattre O. EWS/FLI-1 silencing and gene profiling of Ewing cells reveal downstream oncogenic pathways and a crucial role for repression of insulin-like growth factor binding protein 3. Mol Cell Biol. 2004;24:7275–83.

10. Kinsey M, Smith R, Lessnick SL. NR0B1 is required for the oncogenic phenotype mediated by EWS/FLI in Ewing's sarcoma. Mol Cancer Res MCR. 2006;4:851–9.

11. Hu-Lieskovan S, Zhang J, Wu L, Shimada H, Schofield DE, Triche TJ. EWS-FLI1 fusion protein up-regulates critical genes in neural crest development and is responsible for the observed phenotype of Ewing's family of tumors. Cancer Res. 2005;65:4633–44.

12. Tirode F, Laud-Duval K, Prieur A, Delorme B, Charbord P, Delattre O. Mesenchymal stem cell features of Ewing tumors. Cancer Cell. 2007;11:421–9.

13. Deneen B, Welford SM, Ho T, Hernandez F, Kurland I, Denny CT. PIM3 proto-oncogene kinase is a common transcriptional target of divergent EWS/ETS oncoproteins. Mol Cell Biol. 2003;23:3897–908.

14. Lessnick SL, Dacwag CS, Golub TR. The Ewing's sarcoma oncoprotein EWS/FLI induces a p53-dependent growth arrest in primary human fibroblasts. Cancer Cell. 2002;1:393–401.

15. Riggi N, Cironi L, Provero P, Suvà M-L, Kaloulis K, Garcia-Echeverria C, et al. Development of Ewing's sarcoma from primary bone marrow-derived mesenchymal progenitor cells. Cancer Res. 2005;65:11459–68.

16. Cironi L, Riggi N, Provero P, Wolf N, Suvà M-L, Suvà D, et al. IGF1 is a common target gene of Ewing's sarcoma fusion proteins in mesenchymal progenitor cells. PloS One. 2008;3:e2634.

17. Benini S, Manara MC, Cerisano V, Perdichizzi S, Strammiello R, Serra M, et al. Contribution of MEK/MAPK and PI3-K signaling pathway to the malignant behavior of Ewing's sarcoma cells: therapeutic prospects. Int J Cancer. 2004;108:358–66.

18. Lissat A, Joerschke M, Shinde DA, Braunschweig T, Meier A, Makowska A, et al. IL6 secreted by Ewing sarcoma tumor microenvironment confers anti-apoptotic and cell-disseminating paracrine responses in Ewing sarcoma cells. BMC Cancer [Internet]. 2015 [cited 2017 Mar 29];15. Available from: http://www.ncbi.nlm.nih.gov/pmc/articles/PMC4517368/

19. Douglas D, Hsu JH-R, Hung L, Cooper A, Abdueva D, van Doorninck J, et al. BMI-1 promotes Ewing sarcoma tumorigenicity independent of CDKN2A-repression. Cancer Res. 2008;68:6507–15.

20. Katuri V, Gerber S, Qiu X, McCarty G, Goldstein SD, Hammers H, et al. WT1 regulates angiogenesis in Ewing Sarcoma. Oncotarget. 2014;5:2436–49.

21. Sankar S, Tanner JM, Bell R, Chaturvedi A, Randall RL, Beckerle MC, et al. A novel role for keratin 17 in coordinating oncogenic transformation and

cellular adhesion in Ewing sarcoma. Mol Cell Biol. 2013;33:4448–60.

22. Peters HL, Yan Y, Nordgren TM, Cutucache CE, Joshi SS, Solheim JC. Amyloid precursor-like protein 2 suppresses irradiation-induced apoptosis in Ewing sarcoma cells and is elevated in immune-evasive Ewing sarcoma cells. Cancer Biol Ther. 2013;14:752–60.

23. Pavlova NN, Thompson CB. The emerging hallmarks of cancer metabolism. Cell Metab. 2016;23:27–47.

24. Kinnaird A, Zhao S, Wellen KE, Michelakis ED. Metabolic control of epigenetics in cancer. Nat Rev Cancer. 2016;16:694–707.

25. Sankar S, Theisen ER, Bearss J, Mulvihill T, Hoffman LM, Sorna V, et al. Reversible LSD1 inhibition interferes with global EWS/ETS transcriptional activity and impedes Ewing sarcoma tumor growth. Clin Cancer Res. 2014;20:4584–97.

26. Sankar S, Gomez NC, Bell R, Patel M, Davis IJ, Lessnick SL, et al. EWS and RE1-silencing transcription factor inhibit neuronal phenotype development and oncogenic transformation in Ewing sarcoma. Genes Cancer. 2013;4:213–23.

27. Subramanian A, Tamayo P, Mootha VK, Mukherjee S, Ebert BL, Gillette MA, et al. Gene set enrichment analysis: A knowledge-based approach for interpreting genome-wide expression profiles. Proc Natl Acad Sci. 2005;102:15545–50.

28. Xia J, Wishart DS. MetPA: a web-based metabolomics tool for pathway analysis and visualization. Bioinforma Oxf Engl. 2010;26:2342–4.

29. Xia J, Wishart DS. Web-based inference of biological patterns, functions and pathways from metabolomic data using MetaboAnalyst. Nat Protoc. 2011;6:743–60.

30. Locasale JW, Grassian AR, Melman T, Lyssiotis CA, Mattaini KR, Bass AJ, et al. Phosphoglycerate dehydrogenase diverts glycolytic flux and contributes to oncogenesis. Nat Genet. 2011;43:869–74.

31. Locasale JW. Serine, glycine and the one-carbon cycle: cancer metabolism in full circle. Nat Rev Cancer. 2013;13:572–83.

32. Possemato R, Marks KM, Shaul YD, Pacold ME, Kim D, Birsoy K, et al. Functional genomics reveal that the serine synthesis pathway is essential in breast cancer. Nature. 2011;476:346–50.

33. Aguirre-Gamboa R, Gomez-Rueda H, Martínez-Ledesma E, Martínez-Torteya A, Chacolla-Huaringa R, Rodriguez-Barrientos A, et al. SurvExpress: an online biomarker validation tool and database for cancer gene expression data using survival analysis. PLOS ONE. 2013;8:e74250.

34. Savola S, Klami A, Myllykangas S, Manara C, Scotlandi K, Picci P, et al. High expression of complement component 5 (C5) at tumor site associates with superior survival in Ewing's sarcoma family of tumour patients. ISRN Oncol. 2011;2011:168712.

35. Fan J, Teng X, Liu L, Mattaini KR, Looper RE, Vander Heiden MG, et al. Human phosphoglycerate dehydrogenase produces the oncometabolite d-2-hydroxyglutarate. ACS Chem Biol. 2015;10:510–6.

36. Xu W, Yang H, Liu Y, Yang Y, Wang P, Kim S-H, et al. Oncometabolite 2-hydroxyglutarate is a competitive inhibitor of α-ketoglutarate-dependent dioxygenases. Cancer Cell. 2011;19:17–30.

37. Dang L, White DW, Gross S, Bennett BD, Bittinger MA, Driggers EM, et al. Cancer-associated IDH1 mutations produce 2-hydroxyglutarate. Nature. 2009;462:739–44.

38. Ward PS, Patel J, Wise DR, Abdel-Wahab O, Bennett BD, Coller HA, et al. The common feature of leukemia-associated IDH1 and IDH2 mutations is a neomorphic enzyme activity converting alpha-ketoglutarate to 2-hydroxyglutarate. Cancer Cell. 2010;17:225–34.

39. May WA, Lessnick SL, Braun BS, Klemsz M, Lewis BC, Lunsford LB, et al. The Ewing's sarcoma EWS/FLI-1 fusion gene encodes a more potent transcriptional activator and is a more powerful transforming gene than FLI-1. Mol Cell Biol. 1993;13:7393–8.

40. Delattre O, Zucman J, Plougastel B, Desmaze C, Melot T, Peter M, et al. Gene fusion with an ETS DNA-binding domain caused by chromosome translocation in human tumours. Nature. 1992;359:162–5.

41. Lessnick SL, Braun BS, Denny CT, May WA. Multiple domains mediate transformation by the Ewing's sarcoma EWS/FLI-1 fusion gene. Oncogene. 1995;10:423–31.

42. May WA, Gishizky ML, Lessnick SL, Lunsford LB, Lewis BC, Delattre O, et al. Ewing sarcoma 11;22 translocation produces a chimeric transcription factor that requires the DNA-binding domain encoded by FLI1 for transformation. Proc Natl Acad Sci. 1993;90:5752–6.

43. Chansky HA, Barahmand-pour F, Mei Q, Kahn-Farooqi W, Zielinska-

Kwiatkowska A, Blackburn M, et al. Targeting of EWS/FLI-1 by RNA interference attenuates the tumor phenotype of Ewing's sarcoma cells in vitro. J Orthop Res. 2004;22:910–7.

44. Kovar H, Aryee DN, Jug G, Henöckl C, Schemper M, Delattre O, et al. EWS/FLI-1 antagonists induce growth inhibition of Ewing tumor cells in vitro. Cell Growth Differ Mol Biol J Am Assoc Cancer Res. 1996;7:429–37.

45. Ouchida M, Ohno T, Fujimura Y, Rao VN, Reddy ES. Loss of tumorigenicity of Ewing's sarcoma cells expressing antisense RNA to EWS-fusion transcripts. Oncogene. 1995;11:1049–54.

46. Tanaka K, Iwakuma T, Harimaya K, Sato H, Iwamoto Y. EWS-Fli1 antisense oligodeoxynucleotide inhibits proliferation of human Ewing's sarcoma and primitive neuroectodermal tumor cells. J Clin Invest. 1997;99:239–47.

47. Toretsky JA, Connell Y, Neckers L, Bhat NK. Inhibition of EWS-FLI-1 fusion protein with antisense oligodeoxynucleotides. J Neurooncol. 1997;31:9–16.

48. Thompson AD, Teitell MA, Arvand A, Denny CT. Divergent Ewing's sarcoma EWS/ETS fusions confer a common tumorigenic phenotype on NIH3T3 cells. Oncogene. 1999;18:5506–13.

49. Owen LA, Kowalewski AA, Lessnick SL. EWS/FLI mediates transcriptional repression via NKX2.2 during oncogenic transformation in Ewing's sarcoma. PLOS ONE. 2008;3:e1965.

50. Kinsey M, Smith R, Iyer AK, McCabe ERB, Lessnick SL. EWS/FLI and its downstream target NR0B1 interact directly to modulate transcription and oncogenesis in Ewing's sarcoma. Cancer Res. 2009;69:9047–55.

51. Beauchamp E, Bulut G, Abaan O, Chen K, Merchant A, Matsui W, et al. GLI1 is a direct transcriptional target of EWS-FLI1 oncoprotein. J Biol Chem. 2009;284:9074–82.

52. Zwerner JP, Joo J, Warner KL, Christensen L, Hu-Lieskovan S, Triche TJ, et al. The EWS/FLI1 oncogenic transcription factor deregulates GLI1. Oncogene. 2008;27:3282–91.

53. Sankar S, Bell R, Stephens B, Zhuo R, Sharma S, Bearss DJ, et al. Mechanism and relevance of EWS/FLI-mediated transcriptional repression in Ewing sarcoma. Oncogene. 2013;32:5089–100.

54. Nieto-Soler M, Morgado-Palacin I, Lafarga V, Lecona E, Murga M, Callen E, et al. Efficacy of ATR inhibitors as single agents in Ewing sarcoma. Oncotarget. 2016;7:58759–67.

55. Brenner JC, Feng FY, Han S, Patel S, Goyal SV, Bou-Maroun LM, et al. PARP-1 inhibition as a targeted strategy to treat Ewing's sarcoma. Cancer Res. 2012;72:1608–13.

56. Mutz CN, Schwentner R, Aryee DNT, Bouchard EDJ, Mejia EM, Hatch GM, et al. EWS-FLI1 confers exquisite sensitivity to NAMPT inhibition in Ewing sarcoma cells. Oncotarget. 2017;

57. Chaturvedi A, Hoffman LM, Welm AL, Lessnick SL, Beckerle MC. The EWS/FLI oncogene drives changes in cellular morphology, adhesion, and migration in Ewing sarcoma. Genes Cancer. 2012;3:102–16.

58. Unterlass JE, Baslé A, Blackburn TJ, Tucker J, Cano C, Noble MEM, et al. Validating and enabling phosphoglycerate dehydrogenase (PHGDH) as a target for fragment-based drug discovery in PHGDH-amplified breast cancer. Oncotarget [Internet]. 2016 [cited 2016 Oct 21];5. Available from: http://www.impactjournals.com/oncotarget/index.php?journal=oncotarget&page=article&op=view&path[]=11487&pubmed-linkout=1

59. Ye J, Mancuso A, Tong X, Ward PS, Fan J, Rabinowitz JD, et al. Pyruvate kinase M2 promotes *de novo* serine synthesis to sustain mTORC1 activity and cell proliferation. Proc Natl Acad Sci U S A. 2012;109:6904–9.

60. Chaneton B, Hillmann P, Zheng L, Martin ACL, Maddocks ODK, Chokkathukalam A, et al. Serine is a natural ligand and allosteric activator of pyruvate kinase M2. Nature. 2012;491:458–62.

61. Sun L, Song L, Wan Q, Wu G, Li X, Wang Y, et al. cMyc-mediated activation of serine biosynthesis pathway is critical for cancer progression under nutrient deprivation conditions. Cell Res. 2015;25:429–44.

62. Jun DY, Park HS, Lee JY, Baek JY, Park H-K, Fukui K, et al. Positive regulation of promoter activity of human 3-phosphoglycerate dehydrogenase (PHGDH) gene is mediated by transcription factors Sp1 and NF-Y. Gene. 2008;414:106–14.

63. Bollig-Fischer A, Dewey TG, Ethier SP. Oncogene activation induces metabolic transformation resulting in insulin-independence in human breast cancer cells. PloS One. 2011;6:e17959.

64. DeNicola GM, Chen P-H, Mullarky E, Sudderth JA, Hu Z, Wu D, et al. NRF2 regulates serine biosynthesis in non-small cell lung cancer. Nat Genet. 2015;47:1475–81.

65. Ducker GS, Rabinowitz JD. One-carbon metabolism in health and disease. Cell Metab [Internet]. 2016 [cited 2017 Jan 10];0. Available from:

http://www.cell.com/cell-metabolism/abstract/S1550-4131(16)30425-9

66. Yang M, Vousden KH. Serine and one-carbon metabolism in cancer. Nat Rev Cancer. 2016;16:650–62.

67. Ben-Sahra I, Hoxhaj G, Ricoult SJH, Asara JM, Manning BD. mTORC1 induces purine synthesis through control of the mitochondrial tetrahydrofolate cycle. Science. 2016;351:728–33.

68. Ye J, Fan J, Venneti S, Wan Y-W, Pawel BR, Zhang J, et al. Serine catabolism regulates mitochondrial redox control during hypoxia. Cancer Discov. 2014;4:1406–17.

69. Fan J, Teng X, Liu L, Looper R, Rabinowitz J. Human phosphoglycerate dehydrogenase produces the oncometabolite D-2-hydroxyglutarate and promotes histone methylation. Cancer Metab. 2014;2:P75.

70. Figueroa ME, Abdel-Wahab O, Lu C, Ward PS, Patel J, Shih A, et al. Leukemic IDH1 and IDH2 mutations result in a hypermethylation phenotype, disrupt TET2 function, and impair hematopoietic differentiation. Cancer Cell. 2010;18:553–67.

71. Lu C, Ward PS, Kapoor GS, Rohle D, Turcan S, Abdel-Wahab O, et al. IDH mutation impairs histone demethylation and results in a block to cell differentiation. Nature. 2012;483:474–8.

72. Turcan S, Rohle D, Goenka A, Walsh LA, Fang F, Yilmaz E, et al. IDH1 mutation is sufficient to establish the glioma hypermethylator phenotype. Nature. 2012;483:479–83.

73. Na KY, Noh B-J, Sung J-Y, Kim YW, Santini Araujo E, Park Y-K. IDH mutation analysis in Ewing sarcoma family tumors. J Pathol Transl Med. 2015;49:257–61.

74. Sorensen PH, Lessnick SL, Lopez-Terrada D, Liu XF, Triche TJ, Denny CT. A second Ewing's sarcoma translocation, t(21;22), fuses the EWS gene to another ETS-family transcription factor, ERG. Nat Genet. 1994;6:146–51.

75. Ginsberg JP, de Alava E, Ladanyi M, Wexler LH, Kovar H, Paulussen M, et al. EWS-FLI1 and EWS-ERG gene fusions are associated with similar clinical phenotypes in Ewing's sarcoma. J Clin Oncol Off J Am Soc Clin Oncol. 1999;17:1809–14.

76. Braunreiter CL, Hancock JD, Coffin CM, Boucher KM, Lessnick SL. Expression of EWS-ETS fusions in NIH3T3 cells reveals significant differences to Ewing's sarcoma. Cell Cycle Georget Tex. 2006;5:2753–9.

77. Yuan B, Latek R, Hossbach M, Tuschl T, Lewitter F. siRNA Selection Server: an automated siRNA oligonucleotide prediction server. Nucleic Acids Res. 2004;32:W130–4.

78. McCloy RA, Rogers S, Caldon CE, Lorca T, Castro A, Burgess A. Partial inhibition of Cdk1 in G2 phase overrides the SAC and decouples mitotic events. Cell Cycle. 2014;13:1400–12.

79. O J-PDL, Emerson LL, Goodman JL, Froebe SC, Illum BE, Curtis AB, et al. Notch and Kras reprogram pancreatic acinar cells to ductal intraepithelial neoplasia. Proc Natl Acad Sci. 2008;105:18907–12.

80. Keefe MD, Wang H, O J-PDL, Khan A, Firpo MA, Murtaugh LC. β-catenin is selectively required for the expansion and regeneration of mature pancreatic acinar cells in mice. Dis Model Mech. 2012;5:503–14.

81. Kopinke D, Brailsford M, Pan FC, Magnuson MA, Wright CVE, Murtaugh LC. Ongoing Notch signaling maintains phenotypic fidelity in the adult exocrine pancreas. Dev Biol. 2012;362:57–64.

82. Pacold ME, Brimacombe KR, Chan SH, Rohde JM, Lewis CA, Swier LJYM, et al. A PHGDH inhibitor reveals coordination of serine synthesis and one-carbon unit fate. Nat Chem Biol. 2016;12:452–8.

83. Mi H, Muruganujan A, Casagrande JT, Thomas PD. Large-scale gene function analysis with the PANTHER classification system. Nat Protoc. 2013;8:1551–66.

84. Mi H, Huang X, Muruganujan A, Tang H, Mills C, Kang D, et al. PANTHER version 11: expanded annotation data from gene ontology and reactome pathways, and data analysis tool enhancements. Nucleic Acids Res. 2017;45:D183–9.

85. Xia J, Wishart DS. Using metaboanalyst 3.0 for comprehensive metabolomics data analysis. Curr Protoc Bioinforma. 2016;55:14.10.1-14.10.91.

86. Xia J, Wishart DS. Metabolomic data processing, analysis, and interpretation using MetaboAnalyst. Curr Protoc Bioinforma. 2011;Chapter 14:Unit 14.10.

87. Xia J, Sinelnikov IV, Han B, Wishart DS. MetaboAnalyst 3.0—making metabolomics more meaningful. Nucleic Acids Res. 2015;43:W251–7.

88. Xia J, Psychogios N, Young N, Wishart DS. MetaboAnalyst: a web server for metabolomic data analysis and interpretation. Nucleic Acids Res.

2009;37:W652–60.

89. Xia J, Wishart DS. MSEA: a web-based tool to identify biologically meaningful patterns in quantitative metabolomic data. Nucleic Acids Res. 2010;38:W71-77.

Figure 5.1 EWS/FLI exerts significant effects on expression of genes important for metabolism. A. Gene ontology analysis of 5,698 EWS/FLI-regulated genes from publicly available RNA-seq data using the PANTHER GO-Slim Biological Process annotation dataset. Threshold of significance for differential expression was log2(ratio) ≥ 0.585 and AdjP ≥ 10. Of these, 1,920 (33.7%) were annotated as metabolic processes (GO: 0008152). **B.** Among these metabolic processes (GO: 0008152), genes annotated as primary metabolic processes (GO: 0044238) were mostly involved in nucleobase-containing compound metabolism (GO: 0006139) and protein metabolism (GO: 0019538). **C & D.** Gene set enrichment analysis comparing a rank-ordered dataset (ranked by AdjP) of EWS/FLI knockdown RNA-seq data to the gene sets Hallmark-Glycolysis and KEGG-Pathways In Cancer, available from the Molecular Signatures Database (MSigDB) version 5.2. Differentially expressed genes (blue shaded region) in shEF vs. shLUC correlate significantly with genes important for glycolysis and pathways commonly altered in cancer. NES = normalized enrichment score.

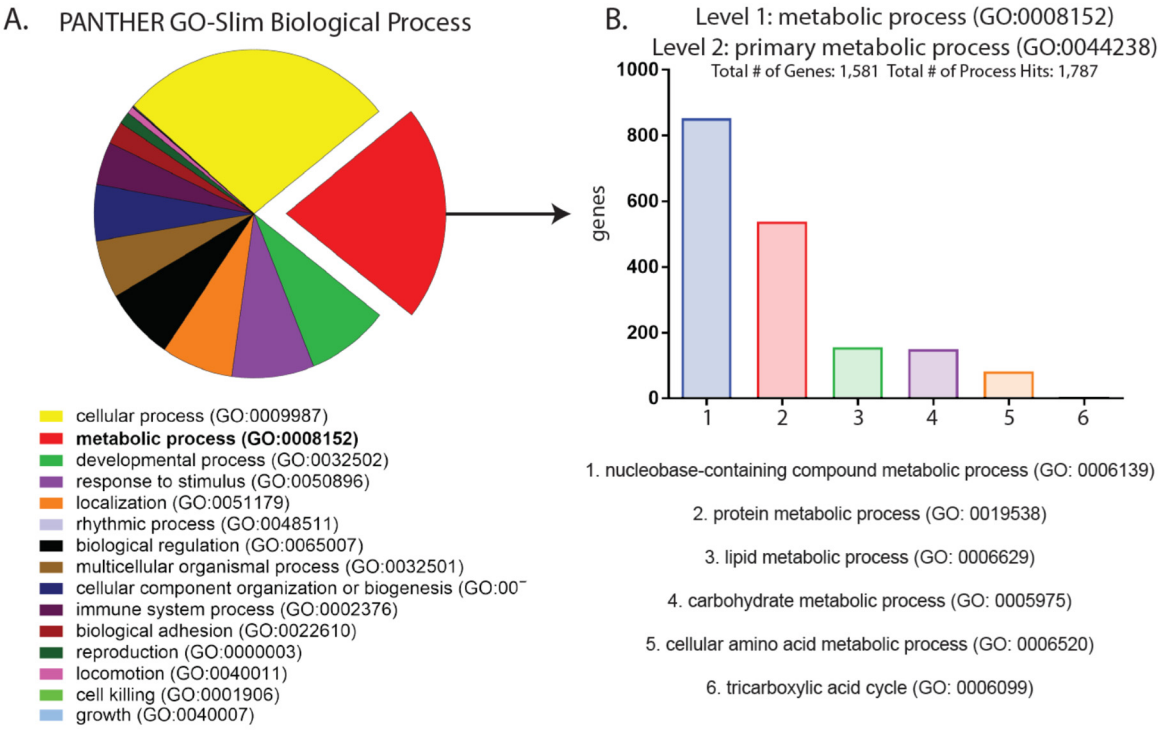

dataset: shEF RNA-seq (PRJNA176544)

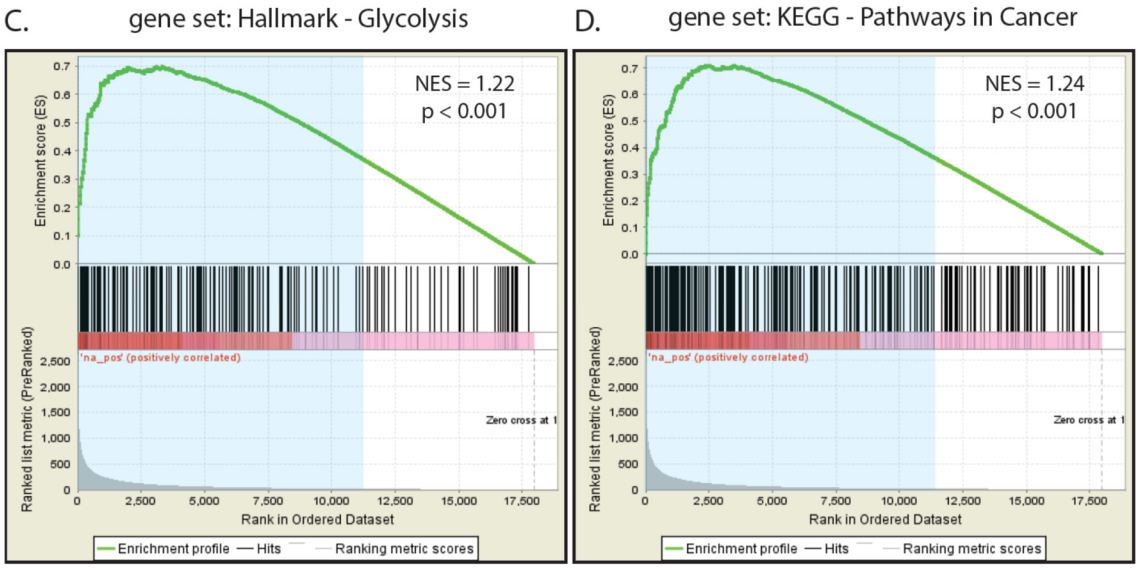

Figure 5.2 EWS/FLI affects glycolytic and oxidative metabolism. A. Gene set enrichment analysis comparing a rank-ordered dataset (ranked by AdjP) of EWS/FLI knockdown RNA-seq data to the gene sets Hallmark-Epthelial-Mesenchymal Transition, Hallmark-Oxidative Phosphorylation, Hallmark-Reactive Oxygen Species, available from the Molecular Signatures Database (MSigDB) version 5.2. Differentially expressed genes in shEF vs. shLUC are indicated by the blue shaded region. NES = normalized enrichment score. **B.** Results of glycolysis stress test. **C.** Results of mito stress test. **D.** Photomicrograph of A673 cells with shLUC and shEF, showing larger cells in shEF vs. shLUC. Scale bars are 100 μm. **E.** FPKM values from RNA-seq data, indicating an increase in transcript abundance of hexokinase 1 (HK1) in shEF vs. shLUC cells.

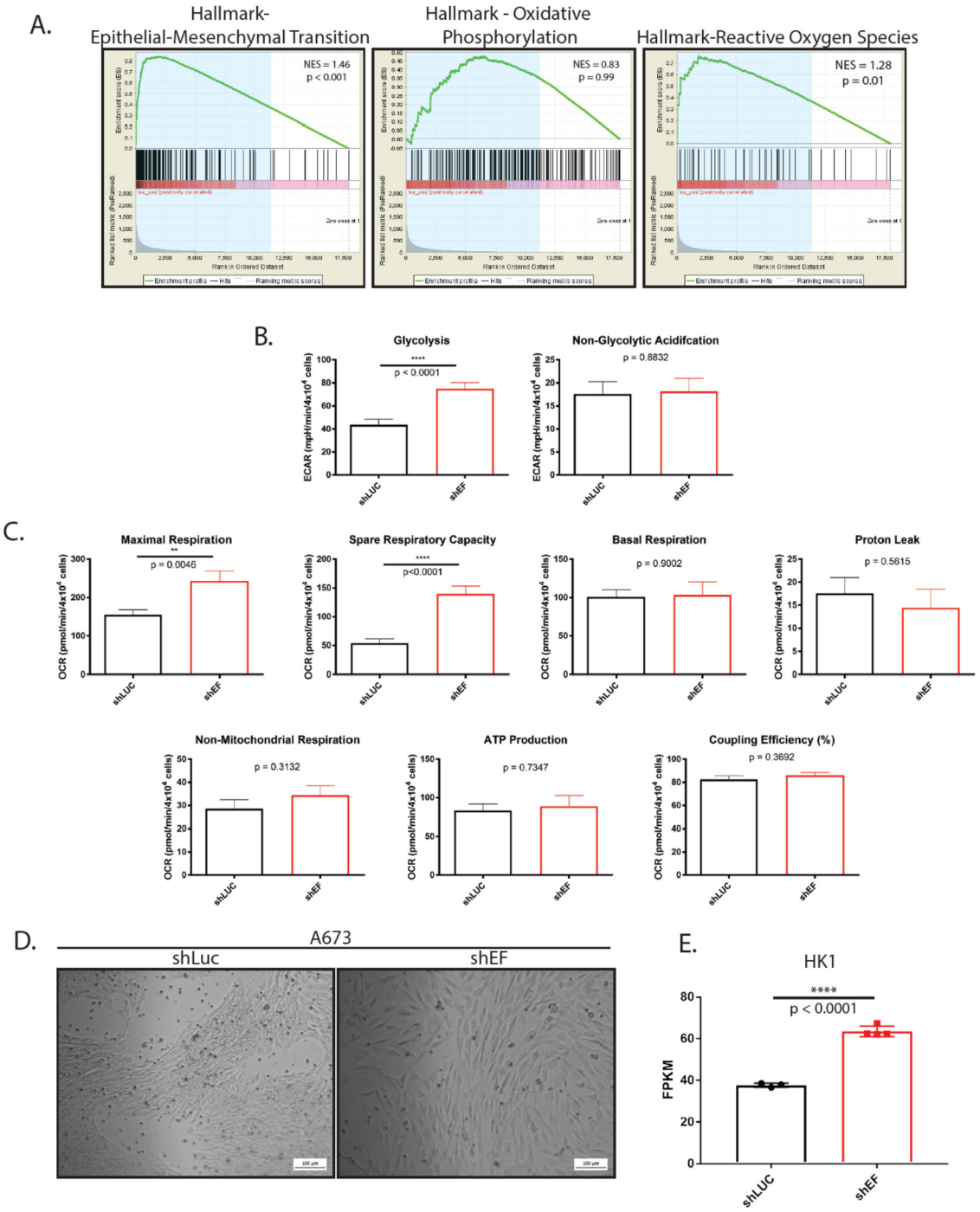
A.
Hallmark-
Epithelial-Mesenchymal Transition
NES = 1.46
p < 0.001
Hallmark - Oxidative
Phosphorylation
NES = 0.83
p = 0.99
Hallmark-Reactive Oxygen Species
NES = 1.28
p = 0.01
B.
Glycolysis
****
p < 0.0001
ECAR (mpH/min/4x10^4 cells)
shLUC
shEF
Non-Glycolytic Acidifcation
p = 0.8832
C.
Maximal Respiration
**
p = 0.0046
Spare Respiratory Capacity
****
p<0.0001
Basal Respiration
p = 0.9002
Proton Leak
p = 0.5615
OCR (pmol/min/4x10^4 cells)
Non-Mitochondrial Respiration
p = 0.3132
ATP Production
p = 0.7347
Coupling Efficiency (%)
p = 0.3692
D.
A673
shLuc
shEF
E.
HK1
****
p < 0.0001
FPKM

Figure 5.3 Silencing EWS/FLI results in functional metabolic changes. A & B. Glycolysis stress tests demonstrate an increased extracellular acidification rate (ECAR) in response to a glucose bolus in shEF vs. shLUC A673 cells. No difference was seen in oxygen consumption rate in the glycolysis stress test. **C & D.** Basal ECAR is higher in shEF vs. shLUC cells, a reflection of different basal glucose concentrations in different test media. Mito stress tests reveal increased oxygen consumption rate (OCR) after treatment with the FCCP mitochondrial uncoupler, indicating increased maximal respiration in shEF vs. shLUC A673 cells. Basal respiration was similar between groups. **E.** Hexokinase 1 (HK1) was increased in A673 and UTES-14-01872 cells after EF knockdown. **F.** Uptake of the fluorescent glucose molecule 2-NBDG was increased in shEF vs. shLUC cells, as measured by flow cytometry. **G.** Mitotracker red signal was elevated in shEF vs. shLUC cells, suggesting increased mitochondrial membrane potential. A representative image from A673 cells is shown, and quantification was done on 3 cells from each of 5 high-power field images, shown as the corrected total cell fluorescence (CTCF) ratio of mitotracker red / mitotracker green (mean ± standard deviation).

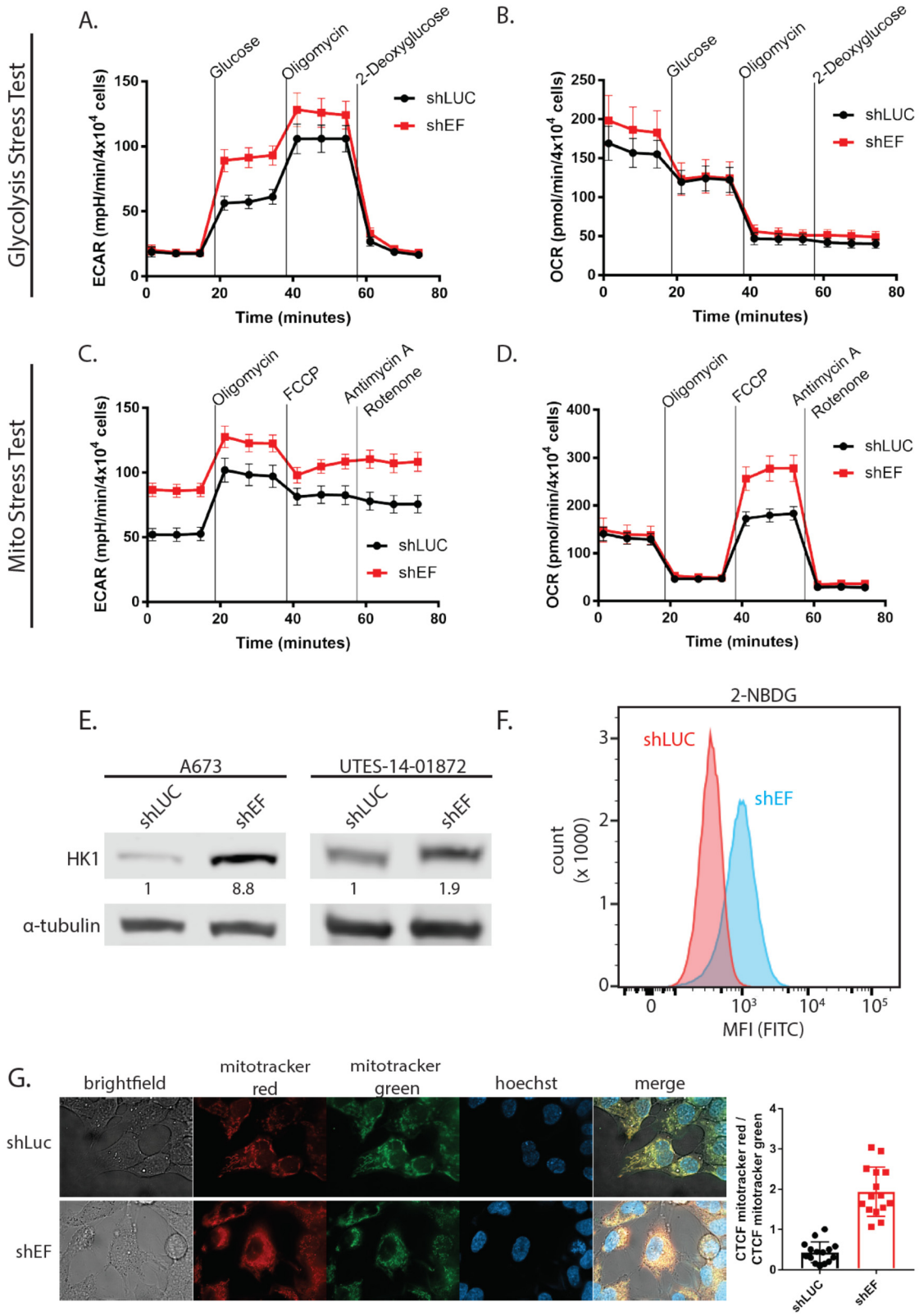
Glycolysis Stress Test
A.
ECAR (mpH/min/4x10^4 cells)
Glucose
Oligomycin
2-Deoxyglucose
shLUC
shEF
Time (minutes)
B.
OCR (pmol/min/4x10^4 cells)
Glucose
Oligomycin
2-Deoxyglucose
shLUC
shEF
Time (minutes)
Mito Stress Test
C.
ECAR (mpH/min/4x10^4 cells)
Oligomycin
FCCP
Antimycin A
Rotenone
shLUC
shEF
Time (minutes)
D.
OCR (pmol/min/4x10^4 cells)
Oligomycin
FCCP
Antimycin A
Rotenone
shLUC
shEF
Time (minutes)
E.
A673
UTES-14-01872
shLUC
shEF
shLUC
shEF
HK1
1
8.8
1
1.9
α-tubulin
F.
2-NBDG
shLUC
shEF
count (x 1000)
MFI (FITC)
G.
brightfield
mitotracker red
mitotracker green
hoechst
merge
shLuc
shEF
CTCF mitotracker red / CTCF mitotracker green
shLUC
shEF

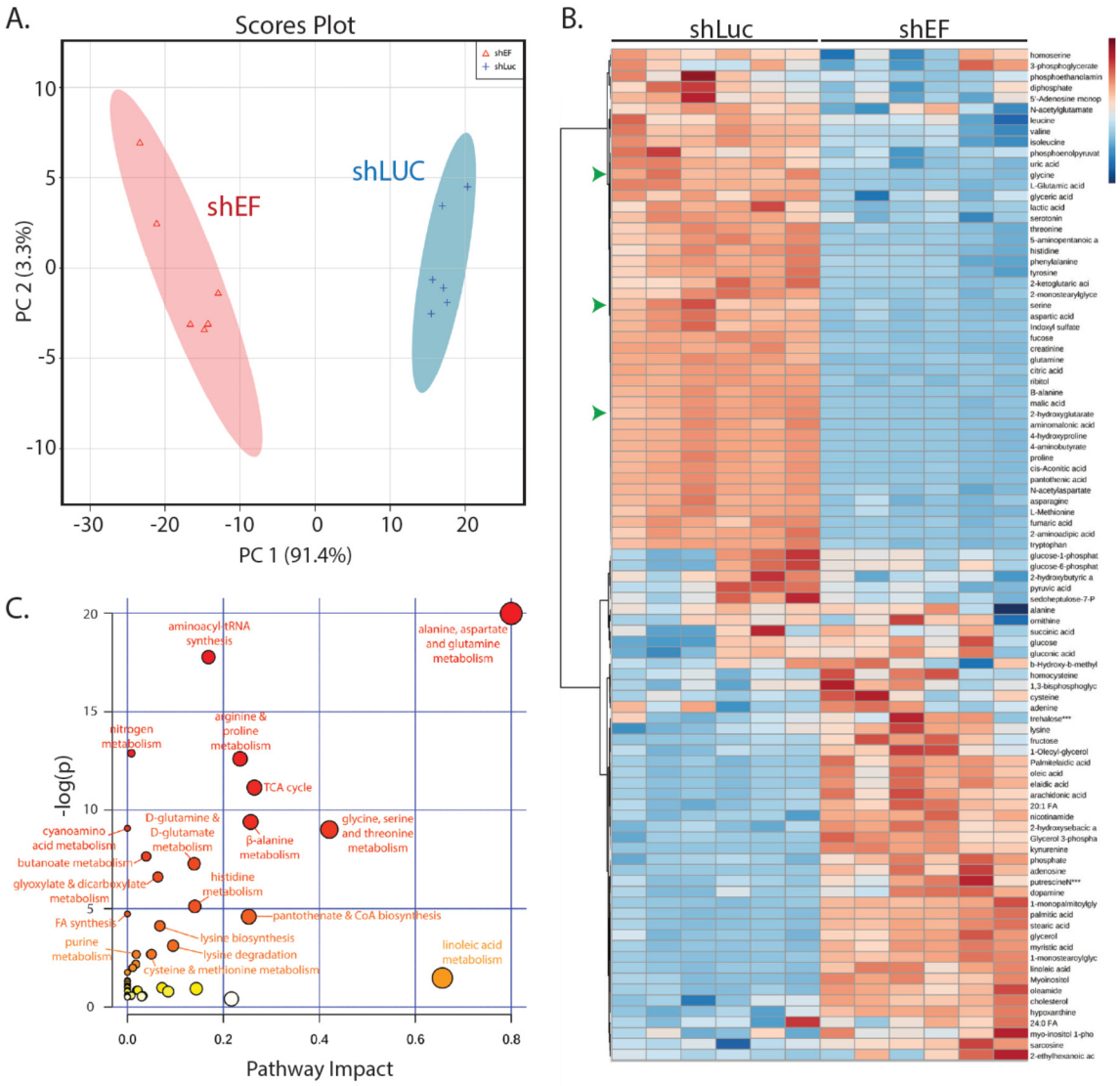

Figure 5.4 The global profile of cellular metabolite abundance is altered by EWS/FLI. **A.** Principal components analysis of metabolite abundance data (assessed by GC-MS) demonstrates distinct metabolic profiles in shEF vs. shLUC A673 cells. **B.** Hierarchichal clustering of differential metabolite abundance after EF knockdown was done by Euclidean distances and a Ward statistic. Metabolite abundances cluster into two distinct groups corresponding to shEF and shLUC conditions. Serine, glycine, and 2-hydroxyglutarate are indicated by green arrowheads. **C.** Topological analysis of metabolite data was performed by MetaboAnalyst 3.0. Circle color represents p value and node size represents pathway impact value. Pathway impact is calculated as the cumulative percentage of centrality measures of metabolites notes within pathways.

Figure 5.5 EWS/FLI affects metabolic pathways and enzyme levels. A. KEGG pathway results from Metaboanalyst comparisons of metabolite changes and gene expression changes in the pathways of glycine, serine, and threonine metabolism. Elements that change are indicated in yellow. **B & C.** Western blots of EF in A673 and UTES-14-01872 cells, indicating expression of EF is decreased in shEF vs. shLUC. **D & E.** Western blots of SHMT2, showing decreased expression after EF knockdown. **F & G.** PHGDH is decreased after EF knockdown in other Ewing sarcoma cell lines, although knockdown is more difficult to achieve in these cells.

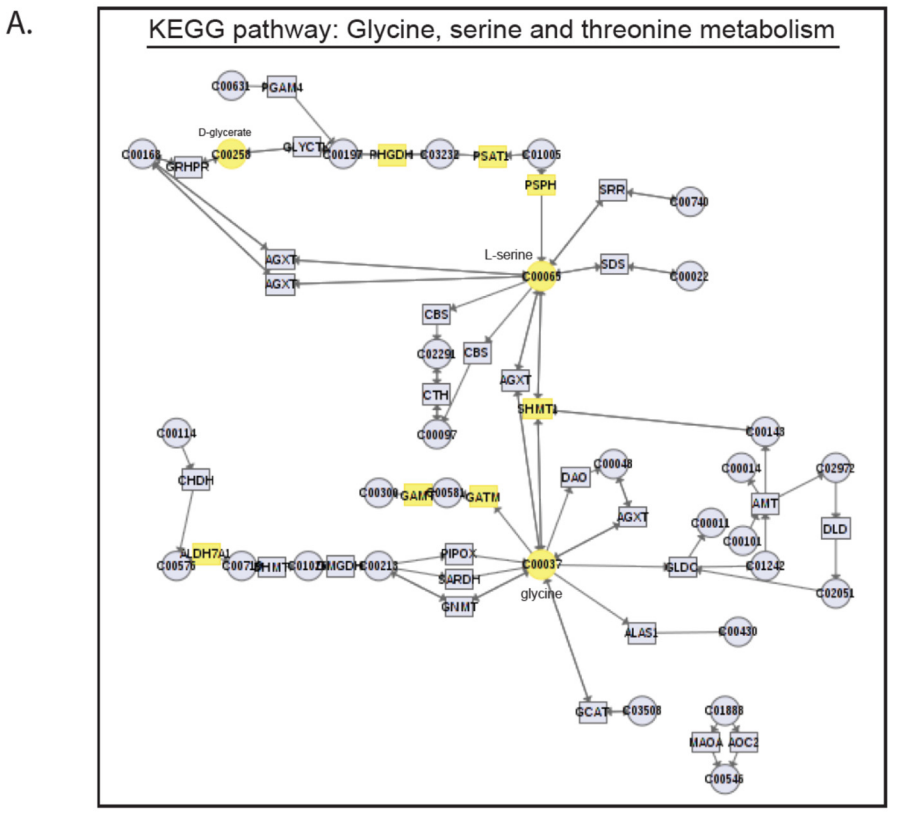
A.
KEGG pathway: Glycine, serine and threonine metabolism
D-glycerate
L-serine
glycine
PSPH
SRR
SDS
AGXT
CBS
CTH
SHMT1
CHDH
DAO
AMT
DLD
GLDC
PIPOX
SARDH
GNMT
ALAS1
GCAT
MAOA
AOC2

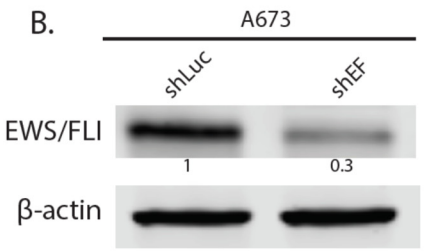
B.
A673
shLuc
shEF
EWS/FLI
1
0.3
β-actin

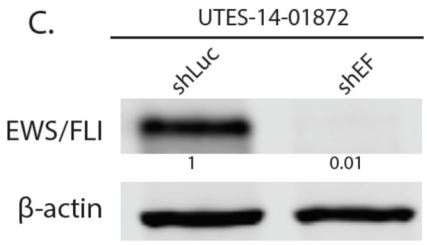
C.
UTES-14-01872
shLuc
shEF
EWS/FLI
1
0.01
β-actin

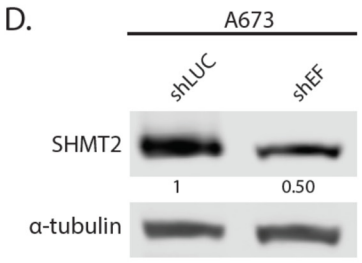
D.
A673
shLUC
shEF
SHMT2
1
0.50
α-tubulin

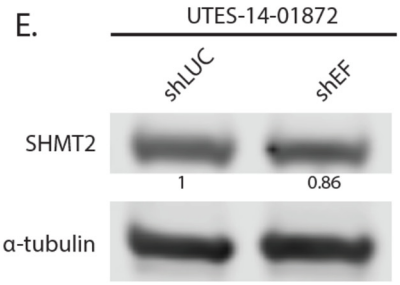
E.
UTES-14-01872
shLUC
shEF
SHMT2
1
0.86
α-tubulin

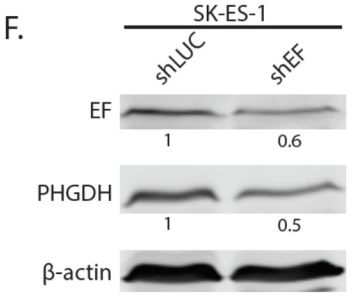
F.
SK-ES-1
shLUC
shEF
EF
1
0.6
PHGDH
1
0.5
β-actin

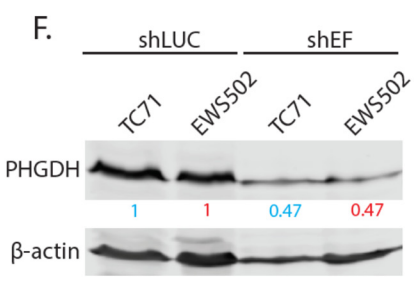
F.
shLUC
shEF
TC71
EWS502
TC71
EWS502
PHGDH
1
1
0.47
0.47
β-actin

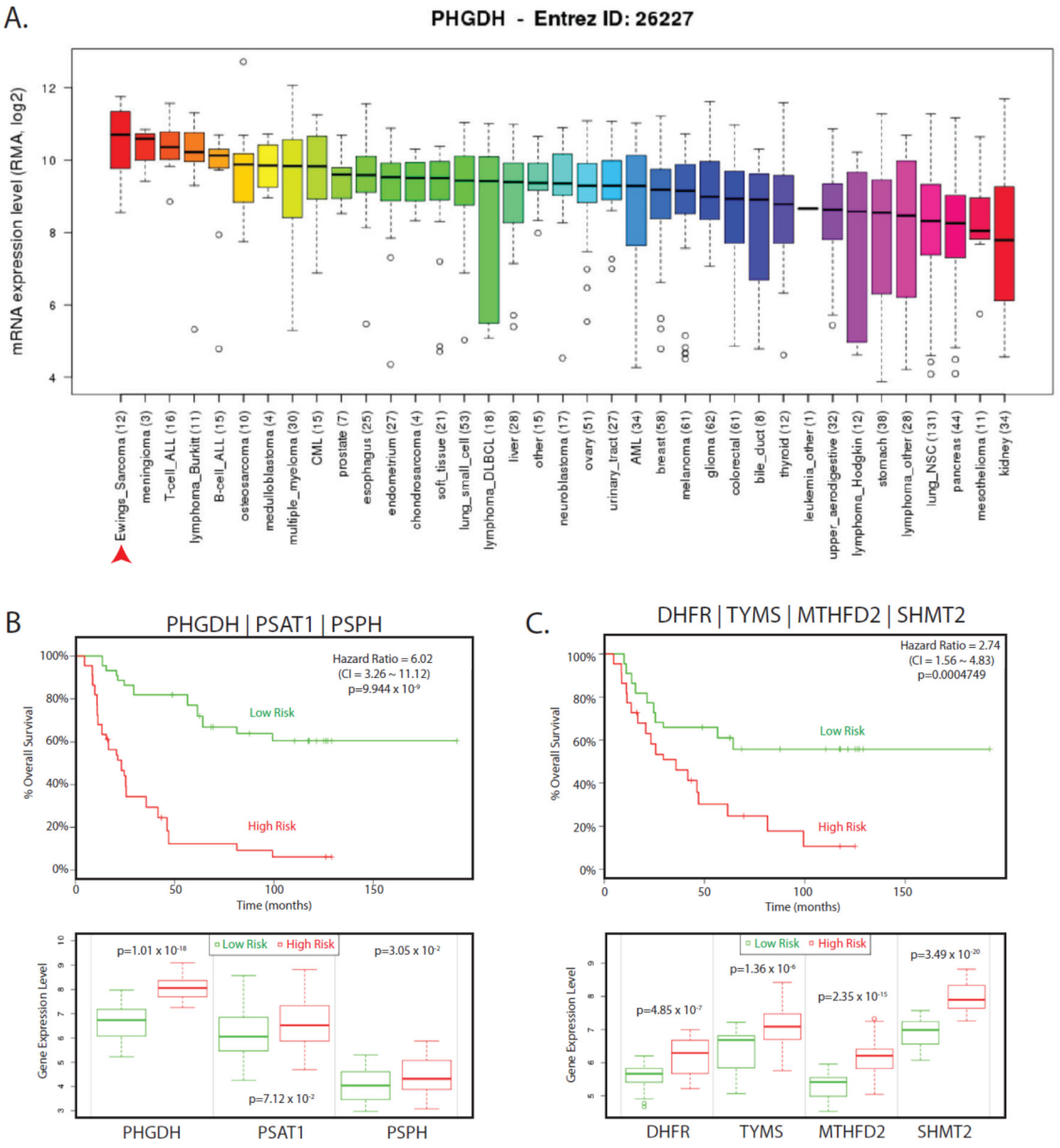

Figure 5.6 Serine synthesis and 1-carbon enzymes are highly expressed in high-risk Ewing sarcoma patients. **A.** Plot from the Cancer Cell Line Encyclopedia (CCLE) indicating that Ewing sarcoma highly expresses PHGDH, more than other cancer cell lines. **B & C.** SurvExpress plots of enzymes of *de novo* serine synthesis and key enzymes of 1-carbon metabolism. Percent overall survival is plotted, correlating expression of these genes with patient outcome. CI = confidence interval.

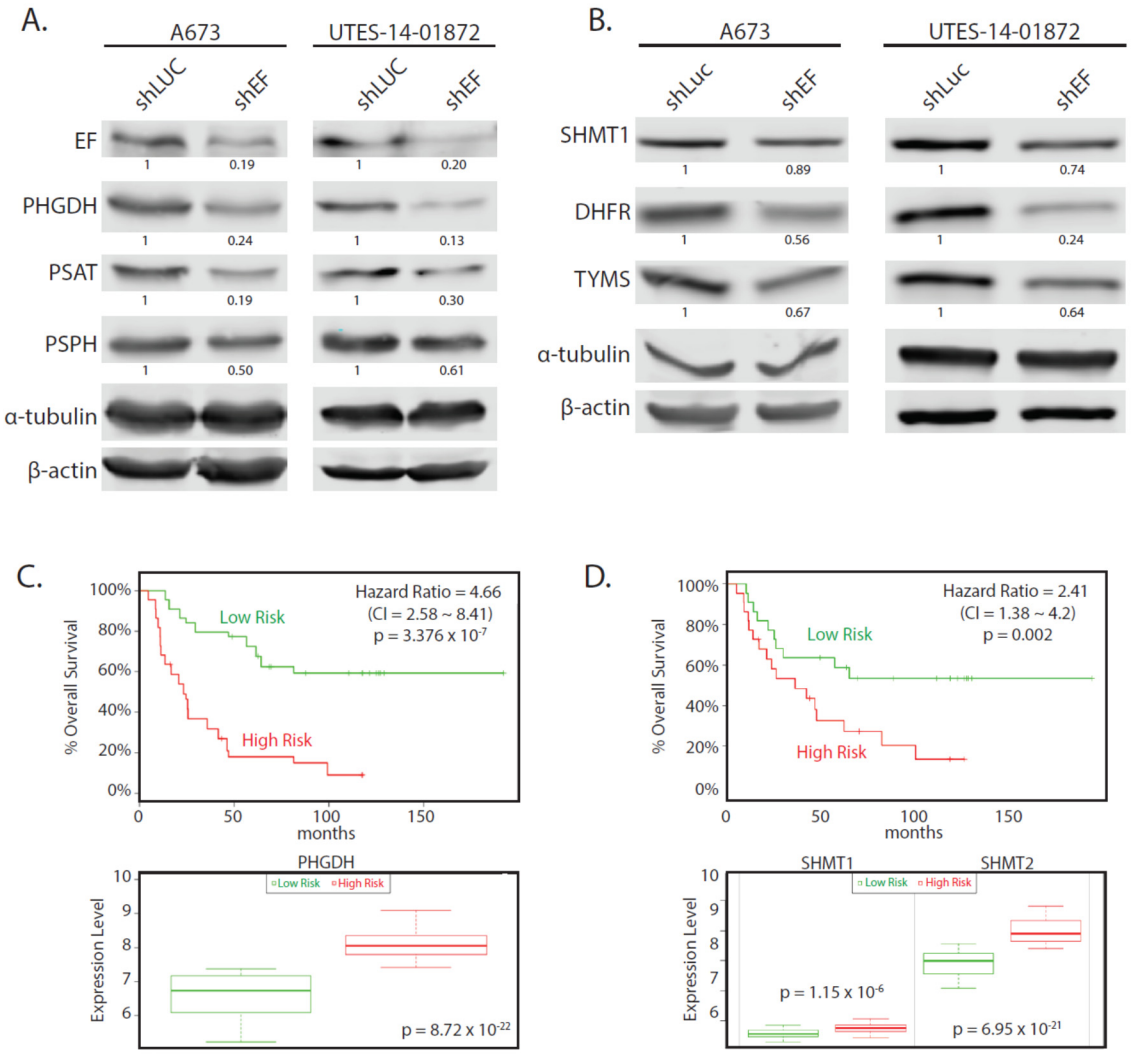

Figure 5.7 Key enzymes of serine and glycine synthesis, and 1-carbon metabolism, are altered by silencing EWS/FLI. A. Western blots of enzymes of serine synthesis in A673 and UTES-14-01872 cells treated by shEF and shLUC. PHGDH, PSAT, and PSPH are lower in shEF vs. shLUC. **B.** SHMT1, DHFR and TYMS are also decreased in A673 and UTES-14-01872 cells after EF knockdown. **C & D.** SurvExpress analysis of overall survival of patients correlated with expression of PHGDH, SHMT1 and SHMT2, demonstrating higher expression correlates with poorer overall survival in Ewing sarcoma patients. CI = confidence interval.

Figure 5.8 PHGDH is high in Ewing sarcoma tumors, and is important for cell viability. A. Immunohistochemistry of CD99 and PHGDH in Ewing sarcoma tumors from a Ewing sarcoma patient. Cell surface staining of CD99 is diagnostic for Ewing sarcoma. Cytosolic staining of PHGDH closely correlates with regions of tumor, indicating elevated PHGDH levels in tumor vs. adjacent tissue. **B & C.** PHGDH inibition in A673 cells by NCT502 and NCT503 causes decreased cell growth and eventual cell death. **D & E.** PHGDH inhibition also impaired cell growth of TTC466 cells. **F & G.** High-dose treatment of osteosarcoma cells (U2OS) and 293T cells show some growth defect, but not as much as in Ewing sarcoma cell lines. **H.** Diagramatic representation of serine/glycine synthesis and 1-carbon metabolism pathways that are decreased by EF knockdown. Enzymes are green text and metabolites are black text. Blue arrows indicate enzymes or metabolites that were observed as decreased in shEF vs. shLUC cells. Nucleotide and folate analogs were not measured. Co-factors and some intermediates are ommitted for clarity.

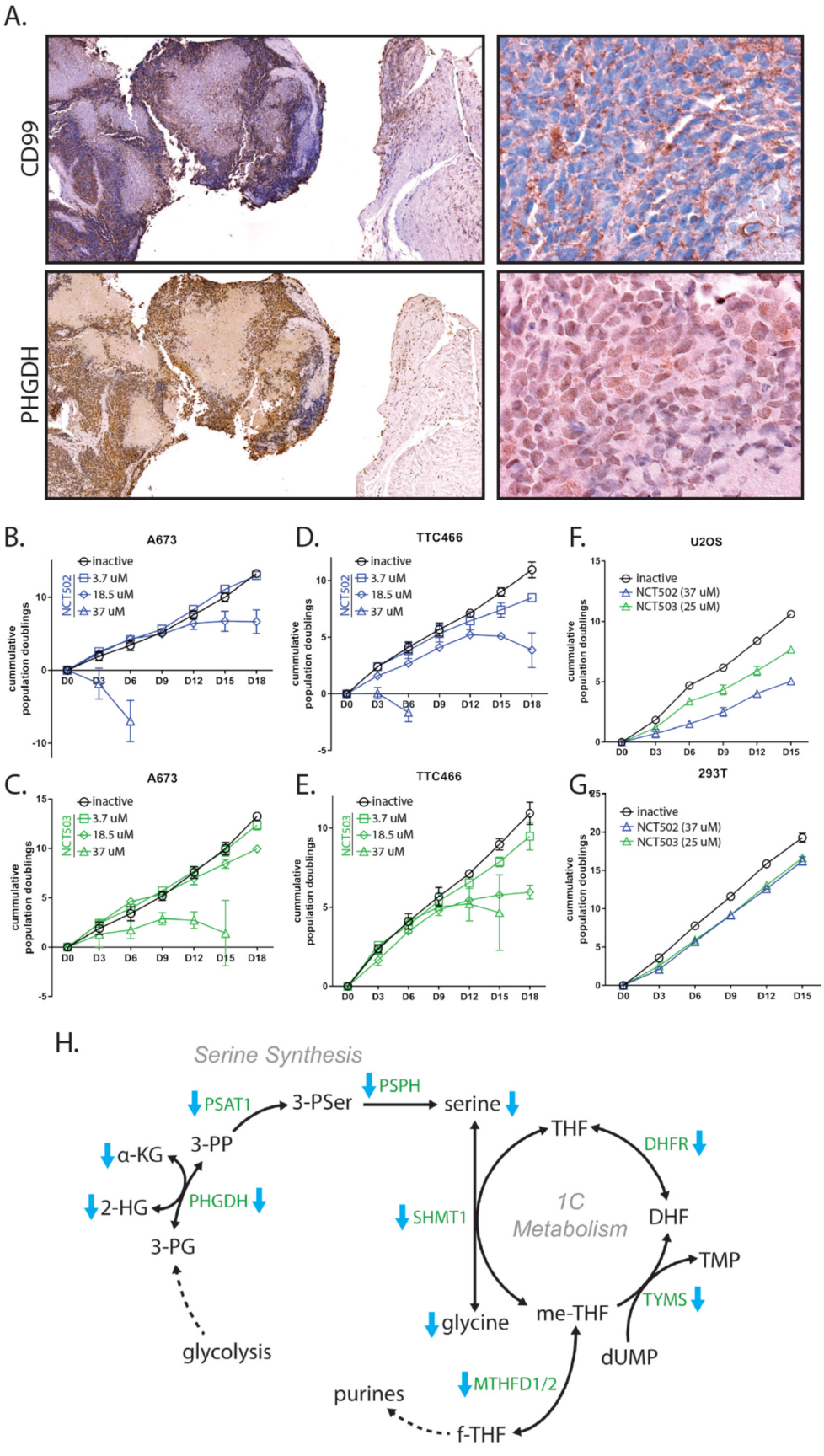
A.
CD99
PHGDH
B.
A673
inactive
NCT502
3.7 uM
18.5 uM
37 uM
cummulative population doublings
D.
TTC466
F.
U2OS
NCT502 (37 uM)
NCT503 (25 uM)
C.
NCT503
E.
G.
293T
H.
Serine Synthesis
PSAT1
3-PSer
PSPH
serine
3-PP
α-KG
2-HG
PHGDH
3-PG
glycolysis
THF
DHFR
SHMT1
1C Metabolism
DHF
TMP
TYMS
glycine
me-THF
dUMP
MTHFD1/2
purines
f-THF

Figure 5.9 Modulation PHGDH causes decreased 2-hydroxyglutarate, and altered expression and methylation of histones. A. Diagramatic representation of PHGDH enzyme function. PHGDH primarily catalyzes converion of 3-phospho-D-glycerate (3-PG) to 3-phosphoonoxypyruvate (3-PP), but also produces a minor product via conversion α-ketoglutarate (α-KG) to 2-hydroxyglutarate (2-HG). KEGG reaction numbers are indicated. **B & C.** 2-hydroxyglutarate abundance as measured by GC-MS is lower in shEF vs. shLUC A673 cells. Inhibition of PHGDH by NCT-502 also decreases levels of 2-HG in A673 cells. **D.** LINE-1 methylation, a surrogate of bulk DNA methylation, is not different in shEF, shPHGDH or shPSPH vs. shLUC cells. **E & F.** In UTES-14-01872 and TTC466 cells, knockdown of PHGDH results in increased levels of histone H3 and increased methylation of H3 histones at lysine 9 and 27. This was not seen in A673 cells. A673 and UTES-14-01872 cell lines express EWS/FLI; TTC466 cells express the EWS/ERG fusion protein. For H3K9me3 and H3K27me3, normalization to actin is shown in black beneath the respective bands; normalization to total H3 is shown in red text.

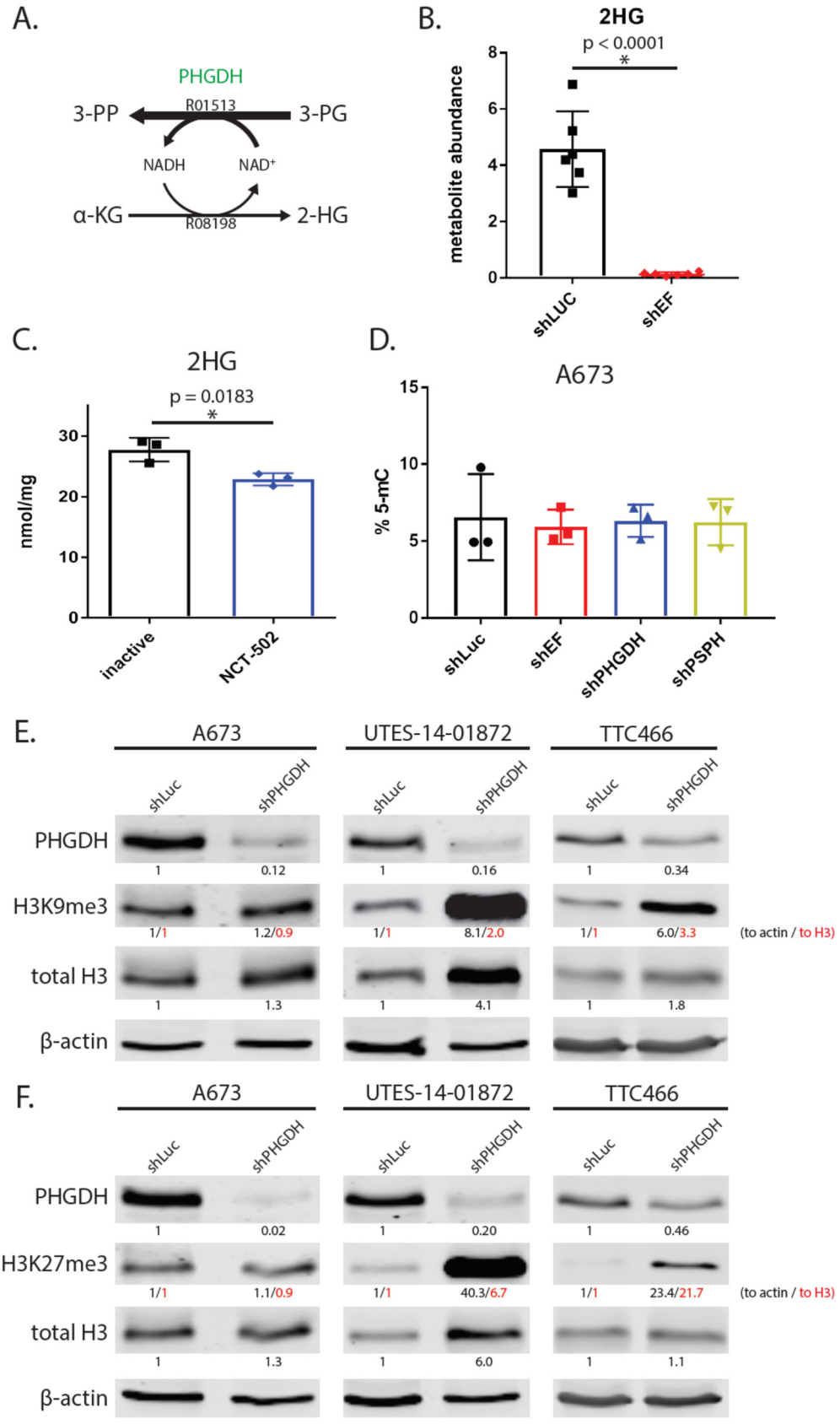
A.
PHGDH
3-PP
R01513
3-PG
NADH
NAD+
α-KG
R08198
2-HG
B.
2HG
p < 0.0001
*
metabolite abundance
shLUC
shEF
C.
2HG
p = 0.0183
*
nmol/mg
inactive
NCT-502
D.
A673
% 5-mC
shLuc
shEF
shPHGDH
shPSPH
E.
A673
UTES-14-01872
TTC466
shLuc
shPHGDH
PHGDH
H3K9me3
total H3
β-actin
1
0.12
1/1
1.2/0.9
1.3
0.16
8.1/2.0
4.1
0.34
6.0/3.3
1.8
(to actin / to H3)
F.
A673
UTES-14-01872
TTC466
shLuc
shPHGDH
PHGDH
H3K27me3
total H3
β-actin
1
0.02
1/1
1.1/0.9
1.3
0.20
40.3/6.7
6.0
0.46
23.4/21.7
1.1
(to actin / to H3)

CHAPTER 6

CONCLUSIONS AND OUTLOOK

The development of a targeted molecular therapy for Ewing sarcoma remains an elusive goal. Despite the fact that these tumors are driven by a single master regulator of oncogenesis, directly targeting EWS/FLI has been unsuccessful. Transcription factors are notoriously difficult to modulate pharmacologically, and delivery of RNA interference-based therapeutics has proven to be far from trivial. New technologies may provide new hope for targeting EWS/FLI directly, but compelling pre-clinical data have yet to be seen.

Amid such a dearth of methods capable of being directed against the principal driver of these tumors, researchers have looked downstream of EWS/FLI in search of targets that could be exploited therapeutically. While most of these efforts have focused on transcriptional regulation, epigenetic modification, and other nuclear processes, little attention has been focused on metabolic pathways. Indeed, metabolic systems that are co-opted or altered by the presence of EWS/FLI might include targetable enzymes that could be modulated by new therapies. An EWS/FLI-specific metabolic program could provide a targetable surrogate for EWS/FLI itself, providing a way to specifically destroy EWS/FLI-harboring cells through pharmacological modulation of metabolic or other enzymes.

The work presented herein represents some of the first steps toward understanding the metabolic derangements that occur as a result of the t(11;22) translocation. Further study of the alterations in carbon flux through various metabolic pathways will be a crucial next step in these investigations. More in-depth analysis of these processes using metabolic flux analysis and other techniques will provide crucial information and a higher-resolution understanding of these processes. Such research may reveal idiosyncratic metabolic programs unique to Ewing sarcoma, and provide novel treatment opportunities.

Further experiments such as these are currently being designed and carried out by several groups. As researchers push deeper into the realm of cellular metabolism in Ewing sarcoma, there is great potential for discovery. Future insights will not only provide a better view of the metabolic alterations that promote cancer formation, but they will provide hope to patients and their families that better therapies – and possibly even cures – might one day be found.